Université de Montréal

The biological importance of apurinic/apyrimidinic endonucleases in the maintenance of genetic stability

par

Ratsavarinh Vongsamphanh

Département de microbiologie et immunologie

Faculté de médecine

Thèse présentée à la Faculté des études supérieures

en vue de l'obtention du grade de philosophiae doctor (Ph.D.)

en microbiologie et immunologie

Octobre 2006

Université de Montréal

Faculté des études supérieures

Cette thèse intitulée:

The biological importance of apurinic/apyrimidinic endonucleases in the maintenance of genetic stability

présentée par:

RATSAVARINH VONGSAMPHANH

a été évaluée par un jury composé des personnes suivantes:

Dr. Elliot Drobetsky
président-rapporteur

Dr. Dindial Ramotar
directeur de recherche

Dr. Janos Filep
membre du jury

Dr. Daniel Durocher
examinateur externe

Dr. Jean-François Côté
représentant du doyen de la FES

RÉSUMÉ

Les dérivés réactifs de l'oxygène produisent de multiples lésions à l'ADN, notamment des sites abasiques (AP). Les dommages oxydatifs de l'ADN sont réparés principalement via la voie de réparation par excision de bases dans laquelle les AP endonucléases jouent un rôle crucial. Les cellules déficientes pour les AP endonucléases sont hypersensibles aux agents alkylants (e.g. MMS) et oxydants (e.g. H_2O_2). Nous sommes intéressés par l'étude moléculaire des AP endonucléases eucaryotiques afin de mieux comprendre leurs mécanismes enzymatiques. Notre première étude porte sur la structure et la fonction de la principale AP endonucléase de la levure *Saccharomyces cerevisiae*, Apn1. Nos résultats démontrent clairement l'importance des acides aminés Glu158 et Asp192 pour l'activité biologique d'Apn1, étant donné qu'une mutation d'un de ces résidus abolit significativement son activité enzymatique. Lors de notre deuxième étude, nous avons évalué le rôle de l'ADN glycosylase Ogg1 de la levure dans l'instabilité des séquences poly(GT) mitochondriales. Nous avons observé qu'une surproduction d'Apn1 cause une augmentation de l'instabilité des séquences poly(GT). Cet effet fût toutefois contrebalancé par la surexpression d'Ogg1. Nos résultats indiquent que la protéine Ogg1 compétionne avec Apn1 possiblement pour la liaison des sites AP afin d'empêcher la réparation incontrôlée par Apn1. Notre troisième étude avait comme but initial l'identification de l'homologue humain d'endo IV. Cependant, nous avons isolé l'enzyme glycolytique, GAPDH. Nos résultats démontrent que GAPDH interagit avec APE1 afin de stimuler son activité AP endonucléase en convertissant la forme oxydée d'APE1 en sa forme réduite. De plus, les résidus Cys152 et Cys156 de GAPDH sont importants pour la stimulation de APE1. Le rôle que joue GAPDH dans la résistance cellulaire face aux agents génotoxiques, tels le MMS et H_2O_2, fût également démontré par des tests de viabilité cellulaire. Collectivement, nos études confirment l'importance biologique des AP endonucléases dans la réparation des sites AP. De plus, elles ont permis de comprendre davantage les mécanismes par lesquels ces enzymes contribuent à la stabilité génétique dans la cellule.

Mots-clés : *dommage oxydatif à l'ADN, réparation par excision de bases, interaction protéique, modification posttranslationnelle.*

ABSTRACT

Living organisms are constantly exposed to reactive oxygen species which are known to cause a variety of DNA lesions, such as apurinic/apyrimidinic (AP) sites. The repair of oxidative DNA damage is primarily mediated by the base excision repair (BER) pathway. AP endonucleases are key enzymes in this process. Cells deficient in AP endonucleases are hypersensitive to alkylating (e.g. MMS) and oxidizing (e.g. H_2O_2) agents. We are interested in studying eukaryotic AP endonucleases at the molecular level to gain insights into their mechanisms of DNA binding and cleavage at AP sites. In our first study, we carried out the first structure/function analysis of Apn1, the major AP endonuclease in yeast *Saccharomyces cerevisiae*. Our data indicate that two conserved amino acids residues of Apn1, Glu158 and Asp192, are critical for its biological function, since glycine substitutions at these positions abolished its DNA repair activities. In our second study, where we evaluated the role of yeast Ogg1 DNA glycosylase in the maintenance of a mitochondrial poly(GT) tract reporter system, we discovered that overproduction of Apn1 causes instability of the poly(GT) tracts. Interestingly, this effect was counteracted by overexpression of Ogg1. Our results clearly suggest that uncontrolled DNA cleavage by Apn1 is prevented by Ogg1 which most likely competes with Apn1 for binding to AP sites. In our final study, we set out to identify the endo IV homolog in human cells, but we unexpectedly re-isolated GAPDH, a classical glycolytic enzyme. We demonstrated that GAPDH interacts with APE1 to stimulate the AP endonuclease activity by converting the oxidized forms of APE1 to the reduced forms. Futhermore, we also showed that Cys152 and Cys156 of GAPDH are important for APE1 reactivation. Consistent with this notion, we demonstrated that GAPDH plays an important role in the cellular resistance against genotoxic agents such as MMS and H_2O_2 by cell survival assays. Taken together, our studies reinforce the biological significance of eukaryotic AP endonucleases in the repair of AP sites, but more importantly, they provide valuable insights into the mechanisms by which AP endonucleases maintain genomic stability in the cell.

Keywords: *oxidative DNA damage, base excision repair, protein interaction, posttranslational modification.*

Table of Contents

List of Figures

List of Tables

List of Abbreviations

AP	apurinic/apyrimidinic
AP-1	activator protein-1
APE1	apurinic/apyrimidinic endonuclease 1 (human)
Apn1	apurinic/apyrimidinic endonuclease 1 (yeast)
ATP	adenosine triphosphate
BER	base excision repair
bp	base pair
BRCT	BRCA1 C-terminus
Can^R	Canamycin resistance
cDNA	complimentary deoxyribonucleic acid
C. elegans	*Caenorhabditis elegans*
CHO	Chinese hamster ovary
CKI/II	casein kinase I/II
DHT	5,6-dihydrothymine
DHU	5,6-dihydrouracil
dNTP	deoxynucleotide triphosphate
dRP	5'-deoxyribose-5-phosphate
dRpase	5'-deoxyribose-5-phosphodiesterase
DTT	dithiothreitol
E. coli	*Escherichia coli*
EDTA	ethylenediaminetetraacetic acid
EMSA	electrophoretic mobility shift assay
Endo III	endonuclease III
Endo IV	endonuclease IV
Ery^R	erythromycin resistance
Exo III	exonuclease III
FapyA	4,6-diamino-5-formamidopyrimidine
FapyG	2,6-diamino-4-hydroxy-5-formamidopyrimidine
FEN1	flap endonuclease 1

GAL1	galactose 1
GAPDH	glyceraldehyde-3-phosphate dehydrogenase
Gfp	green fluorescent protein
Gst	glutathione-*S*-transferase
H-Bond	hydrogen bond
HIF-1α	hypoxia-inducible factor-1α
H_2O_2	hydrogen peroxide
HPLC	high performance liquid chromatography
HSP70	heat-shock protein 70
IPTG	isopropyl thio-β-D-galactoside
kb	kilobase
kDa	kiloDalton
LB	Luria broth
MMR	mistmatch repair
MMS	methyl methane sulfonate
MSI	microsatellite instability
mtDNA	mitochondrial DNA
MWCO	molecular weight cut-off
NAC	N-acetylcysteine
NAD+	nicotinamide adenine dinucleotide
NER	nucleotide excision repair
NF-κB	nuclear factor-κB
NLS	nuclear localization signal
Ogg1	8-oxo-deoxyguanosine DNA glycosylase
$\cdot O_2^-$	superoxide anion
·OH	hydroxyl radical
8-oxo-dGuo	8-oxo-deoxyguanosine/8-oxo-7,8-dihydro-2'-deoxyguanosine
PARP	Poly(ADP-ribose) polymerase 1
PCNA	proliferating cell nuclear antigen
PCR	polymerase chain reaction
Pde1	3'-phosphodiesterase 1

Pir1	Protein with internal repeats
PKC	protein kinase C
Pol β, δ, ε	polymerase beta, delta, epsilon
Ref-1	redox effector factor-1
RF-C	replication factor-C
RNAi	RNA interference
ROS	reactive oxygen species
rRNA	ribosomal ribonucleic acid
Rrp1	Recombination repair protein 1
S. cerevisiae	*Saccharomyces cerevisiae*
Siah1	Seven in absentia homolog 1
SDS-PAGE	sodium dodecyl sulfate polyacrylamide gel electrophoresis
siRNA	small interfering RNA
S. pombe	*Schizosaccharomyces pombe*
ssb	single-strand break
Tg	thymine glycol
THF	tetrahydrofuran
TRX	thioredoxin
UDG	uracil DNA glycosylase
UV	ultraviolet
WRN	Werner protein
YPD	yeast peptone dextrose
XPG	xeroderma pigmentosum complementation group G
XRCC1	x-ray cross-species complementing 1

Acknowledgements

In 1998, I carried out my first research project as a Master student in microbiology and immunology at the University of Montreal. I chose as subject DNA Repair. I came in an amazing world of researchers, scientists, and congresses that fascinated me. After obtaining my Master degree in 2001, I had the possibility to pursue my graduate studies in the amazing field of DNA Repair as a Ph.D. student. Now, a little more than five years later, that opportunity has resulted in this thesis.

I would like to thank the Terry Fox Foundation of the National Cancer Institute of Canada (NCIC) for providing funding for my research studentship from July 2002 to July 2005.

Writing a thesis is not something you just do by yourself at an unimpeded moment. During the period of five years, many people have been a great support. Colleagues at the Guy-Bernier Research Center, friends, and family have helped me in accomplishing this work. Therefore, I would like to take this opportunity to thank a number of them in particular.

First and foremost, my supervisor, Dr. Dindial Ramotar, whose enthusiastic cry of 'Any Results!?' will haunt me for the rest of my days. His unquenchable curiosity and love for the subject are probably the most valuable lessons I have learned from this Ph.D., and his continual support and encouragement have kept me going over the last eight or so years!!!

Furthermore, I would like to express my deepest gratitude and thanks to my colleagues at the Guy-Bernier Research Center, especially Géraldine M., Marie-Ève B, Julie R., and Isabelle L., and all past and present members of Dr. Ramotar's group, particularly Xiaoming Y., Anick L., Arshad J., Andrea S., and Sonish A., for contributing to such an inspiring and pleasant atmosphere.

Obviously, the mentioned time period of five years was not spent twenty-four hours a day, seven days a week on research and writing. Fortunately, I am in the wealthy position of being surrounded by a lot of friends with whom I spent many holidays. Their presence gave me the very much-needed distraction to my research.

Last but not least, I want to thank my family. The warm relationship I have with my brother, Prattana, is absolutely a pleasant environment in which to write a thesis.

I would like to thank my father, Bounpheng, for his encouragement and kind support which were felt even from being miles a part.

Finally, my heartily profound thanks, gratitude, and appreciation are addressed to my mother, Thongnhoune, who has undoubtedly been my strongest motivator. While raising two children by herself, she must have had her hands full and presumably has gone through not always easy time. I hope this thesis shows that things turned out fine.

Once again, thank you all!!!

Contributions of Authors

The following describes the contribution of each co-author for these manuscripts:

(1) Jilani, A., Vongsamphanh, R., Leduc, A., Gros, L., Saparbaev, M., and Ramotar, D. (2003) **Characterization of Two Independent Amino Acid Substitutions that Disrupt the DNA Repair Functions of the Yeast Apn1**. *Biochemistry*, Vol. 42, No. 21, pp. 6436-6445 (Chapter 2).

Ratsavarinh Vongsamphanh made the following constructs which were all used in this study: pGFP-APN1, pGFP-APN1(E158G), and pGFP-APN1(D192G). She determined that the pGFP-APN1 plasmid expressed a functionally active Gfp-Apn1 fusion protein by drug complementation assay in *apn1Δapn2Δ* (YW781) double mutant strain (Figure 2-1). Miss Vongsamphanh also demonstrated that neither pGFP-APN1(E158G) nor pGFP-APN1(D192G) mutant plasmid conferred resistance to MMS (Figure 2-1), suggesting that the mutant proteins are inactive.

Ratsavarinh Vongsamphanh compared the expression levels of native Apn1 and its mutant forms fused to Gfp in yeast strains YW465 (parent) and YW781 (*apn1Δapn2Δ*) by Western blot (Figure 2-2) using monoclonal anti-Gfp antibodies to exclude the possibility that the lack of drug complementation is due to a reduction in the expression level of the mutant proteins.

Anick Leduc examined the cellular location of Gfp-Apn1 and its mutant forms by immunofluorescent microscopy (Figure 2-3). She showed that the native Gfp-Apn1 and the mutants Gfp-Apn1 E158G and Gfp-Apn1 D192G fusion proteins are localized to the nucleus, thus excluding the possibility that the mutant proteins harbor a defect in nuclear translocation.

Arshad Jilani made the pGST-APN1 construct. Anick Leduc then used this plasmid as the template for glycine substitution at positions E158 and D192 which produce the plasmids pGST-APN1(E158G) and pGST-APN1(D192), respectively. Dr. Jilani evaluated the expression of all three GST constructs in bacteria BW528 (*xthΔnfoΔ*) by Coomassie blue-stained SDS-PAGE gel (Figure 2-4A) and purified the

fusion proteins on a glutathione-*S*-transferase affinity column (Figure 2-4B) followed by ion-exchange chromatography on monoS (Figure 2-4C).

Miss Leduc tested if the native fusion protein, Gfp-Apn1, and the mutant fusion proteins Gst-Apn1 E158G and Gst-Apn1 D192G complemented the drug sensitivity of bacteria BW528 (Figure 2-5). The Gst-Apn1 fusion protein was able to restore parental resistance to both MMS (Figure 2-5A) and H_2O_2 (Figure 2-5B) but not the mutant proteins, suggesting that these mutant proteins are unable to act on the damaged DNA.

Arshad Jilani and Laurent Gros compared the ability of purified Gst-Apn1 fusion protein and the mutant forms to process DNA damage *in vitro*. Mr. Jilani assessed the AP endonuclease and the 3'-diesterase activities (Figure 2-6A and B, respectively) and Mr. Gros analyzed the nucleotide incision repair activity (Figure 2-6C).

Dr. Jilani monitored the ability of a fixed amount of purified Gst, Gst-Apn1, Gst-Apn1 E158G, and Gst-Apn1 D192G to bind to DNA using an electrophoretic mobility shift assay (Figure 2-7A). Ratsavarinh Vongsamphanh analyzed the binding of increasing amounts of the purified proteins to the 42-mer labeled (U•G) oligonucleotide by mobility shift analysis (Figure 2-7B).

(2) Vongsamphanh, R., Wagner, J.R., and Ramotar, D. (2006) ***Saccharomyces cerevisiae* Ogg1 prevents poly(GT) tract instability in the mitochondrial genome.** *DNA Repair*, Vol. 5, No. 2, pp. 235-247 (Chapter 3).

Ratsavarinh Vongamphanh generated the following mutants by one-step gene targeting approach: RVY6 (*ogg1Δ*), RVY7 (*apn1Δ*), RVY8 (*ntg1Δ*), RVY9 (*ogg1Δ ntg1Δ*), and RVY10 (*ogg1Δ apn1Δ*). All of these strains were used in this study.

Miss Vongsamphanh made the pOGG1-GFP construct which was subsequently used to subclone the *OGG1-GFP* fragment into the multicopy vector pYES2.0 to create the plasmid pYES-OGG1-GFP. This later construct produces a higher expression level of the Ogg1-Gfp fusion protein.

Ratsavarinh Vongsamphanh prepared the mitochondrial extracts from the parent (CAB193) (kindly provided by Dr. E.A. Sia, University of Rochester, New

York, USA) and the *ogg1Δ* mutant strain. She found that Ogg1 is functionally active in the mitochondria by an enzymatic assay for Ogg1 activity (Figure 3-1).

Miss Vongsamphanh determined the rate of mutation to Arg^+ in the parent strain CAB193, the *ogg1Δ* null mutant, the parent with the plasmid pOGG1 (kindly provided by Dr. S. Boiteux, CNRS-CEA, Fontenay aux Roses, France), and the *ogg1Δ* null mutant with pOGG1 under aerobic conditions (Figure 3-2) and under anaerobic conditions (Figure 3-4).

Dr. Richard Wagner isolated mitochondrial DNA from both the parent and the *ogg1Δ* null mutant strains and compared the level of 8-oxo-Guo lesions present in the the mitochondrial poly(GT) tract using HPLC (data not shown). However, this quantative approach failed to reveal any significant difference between the *ogg1Δ* mutant and the parent strain.

Ratavarinh Vongsamphanh extracted mitochondrial DNA from the parent CAB193, the *ogg1Δ* null mutant, fifteen Arg^+ derivatives of the parent, and fifteen Arg^+ revertants of the *ogg1Δ* null mutant strains. She examined the types of alterations present on the poly(GT) tract by PCR analysis (Figure 3-3).

Miss Vongsamphanh evaluated the effect of DNA repair proteins on the rate of the poly(GT) tract instability in the mitochondrial genome by calculating the rate of the Arg^+ revertants in various strains containing certain vector or plasmid (Table III-I).

(3) Jilani, A., Vongsamphanh, R., Azam, S., and Ramotar, D. (2006) **Human GAPDH functions as a redox factor to reactivate the oxidized form of the DNA repair enzyme APE1**. In preparation (Chapter 4).

Arshad Jilani made the following constructs which were used in this study: pHIS-APE1 and pGST-GAPDH. He then used the latter plasmid as the template for glycine substitution at positions C152, C156, and C247 by site-directed mutagenesis to produce the plasmids pGST-GAPDH C152G, pGST-GAPDH C156G, pGST-GAPDH C247G, respectively.

Dr. Jilani cultured LF1 human lung fibroblasts. He prepared the cell extracts and subjected them to a six-step column chromatography purification to enrich for a

Mg^{2+}-independent AP endonuclease activity. He analyzed the six eluted fractions from the final step of purification by SDS-PAGE gel stained with Coomassie blue (Figure 4-1A) and by AP endonuclease assay (Figure 4-1B). Ratsavarinh Vongsamphanh measured the AP endonuclease activity of the purified polypeptide (Figure 4-1C). Protein sequencing by LC-MS, which was done by Harvard's Microchemistry Facility, revealed that the purified protein is GAPDH.

Both Mr. Jilani and Miss Vongsamphanh purified the following fusion proteins: GST-GAPDH, GST-GAPDH C152G, GST-GAPDH C156G, GST-GAPDH C247G, and HIS-APE1. All the purified fusion proteins were used in our *in vitro* studies. Ratsavarinh Vongsamphanh measured GAPDH glycolytic activity of the purified polypeptide, the various purified GST-GAPDH fusion proteins as well as the the commercial preparations of GAPDH (Figure 4-2A). Dr. Jilani analyzed the expression level of the purified GST-GAPDH by Coomassie blue stained SDS-PAGE gel (Figure 4-2B).

The interaction between GAPDH and APE1 was detected by HIS-APE1 affinity columns (done by Arshad Jilani; Figure 4-3A), and by GST pull-down assays and by immunoprecipitation experiments (both done by Ratsavarinh Vongsamphanh; Figure 4-3B and C, respectively). Arshad and Ratsavarinh performed an AP endonuclease assay on commercial preparations of GAPDH from various organisms (Figure 4-3D).

Both Dr. Jilani and Miss Vongsamphanh measured the effect of increasing concentrations of purified GST-GAPDH on a fixed amount of purified HIS-APE1. They found that GAPDH stimulated APE1 AP endonuclease activity in a dose-dependent manner (Figure 4-4).

Mr. Jilani and Ratsavarinh analyzed the effect of GST-GAPDH on the redox status of the reduced and oxidized HIS-APE1 by SDS-PAGE gel stained with silver stain (Figure 4-5A and data not shown). Both Arshad and Ratsavarinh verify the effect of GAPDH on the AP endonuclease activity of oxidized APE1 (Figure 4-5B). Ratsavarinh tested if other reducing agents (e.g. DTT, glutathione, and NAC), magnesium, or DTT pre-soaked APE1 can also stimulate oxidized APE1 (data not shown).

Dr. Jilani did the AP endonuclease assay with the various GAPDH mutants (Figure 4-6). The mutants GAPDH C152G and GAPDH C156G are unable to stimulate APE1 AP endonuclease activity. Miss Vongsamphanh demonstrated by an AP endonuclease assay that only reduced GAPDH can stimulated oxidized APE1 (data not shown).

Miss Vongsamphanh cultured the DLD-1 cell line stably transfected with either pGFP or pGFP-GAPDH plasmid. She measured cell survival by clonogenic assay following MMS, H_2O_2, and UVC treatment (Figure 4-7A).

Sonish Azam did the siRNA knockdown of GAPDH in HCT116 by tranfection. Dr Azam analyzed the effectiveness of the siRNA treatment by Western blot (Figure 4-7B) and she performed the clonogenic assay after MMS and UVC treatments (Figure 4-7C).

CHAPTER 1

GENERAL INTRODUCTION

OXIDATIVE DNA DAMAGE

Living organisms are constantly exposed to potentially harmful reactive oxygen species (ROS). One of the cellular targets for oxidative damage by ROS is DNA [1]. Failure to repair oxidative DNA lesions may lead to mutagenesis, carcinogenesis, and aging [2].

Generation and detoxification of reactive oxygen species

ROS such as hydrogen peroxide (H_2O_2), superoxide anions ($\cdot O_2^-$) and hydroxyl radicals ($\cdot$OH) are generated through both endogenous and exogenous sources including oxidative electron transport chain in the mitochondria, pathological processes such as infection and inflammation, metabolism of exogenous compounds (e.g. paraquat), cigarette smoke, ultraviolet (UV) light, and ionizing radiation [3-5]. Amongst all the oxygen radicals, the $\cdot$OH is the most reactive towards biological molecules [6].

To prevent the negative effects of ROS, aerobic organisms have evolved numerous defense mechanisms which scavenge and inactivate ROS. The simplest defense mechanism consists of several low molecular weight nonenzymatic antioxidants that include vitamins C and E, glutathione, and thioredoxin [7]. The other, more complex, defense mechanism implicates the activation of enzymes, such as glutathione peroxidase, superoxide dismutase, and catalase [8,9]. Low levels of ROS can escape these natural cellular defense systems, thus, resulting in a tolerable background level of damage. If the production of ROS however overwhelms the cellular detoxification mechanisms, oxidative stress is the result [10]. This condition causes an accumulation of oxidative damage to biomolecules such as lipids, proteins, and DNA [5]. Since proteins and lipids are readily degraded and resynthesized, the most significant consequence of oxidative stress is thought to be DNA damage, specifically, to its base and sugar moieties [11,12].

Types of oxidative DNA lesions

Base damage

More than 70 different types of base damage have been identified in DNA following exposure to oxidative stress, thus forming the major class of ROS-induced DNA lesions [7]. The chemical structures of the major oxidative DNA base damages are shown in Figure 1-1. The C_5=C_6 double bond of pyrimidines is particularly sensitive to an attack by •OH, generating a variety of oxidative pyrimidine lesions, including thymine glycol (Tg), uracil glycol, 5-hydroxy-dU, and 5-hydroxy-dC [13-15]. Similarly, the C_4-, C_5- and C_8-position of purines are highly susceptible to an addition of •OH, producing mainly 8-oxo-dGuo, 8-oxo-dA, and formamidopyrimidines [7]. Tg and 8-oxo-dGuo are representative of oxidized pyrimidines and purines, respectively (insets in Figure 1-1). The biological consequences of many oxidative base lesions have been studied extensively. For example, unrepaired Tg is cytotoxic as it block DNA replication, whereas 8-oxo-dGuo is highly mutagenic since it readily bypassed by DNA polymerases [1,16-18]. Unrepaired 8-oxo-dGuo frequently mispairs with adenine during DNA replication, thereby generating G•C to T•A transversion mutations [17,18].

Sugar damage

In addition to the base residue, •OH also targets the sugar moiety of DNA, resulting in the abstraction of hydrogen atoms from carbon atoms of the deoxyribose residue [7]. The oxidized carbon can undergo additional reactions, depending on the availability of molecular O_2, thus producing several sugar modifications, including single-strand breaks (ssb) and a variety of apurinic/apyrimidinic (AP) sites (Figure 1-2) [7]. AP sites are also formed spontaneously at a substantial rate due to the lost of purine bases. [19] It has been estimated that at least 10 000 depurination events occur in a single mammalian cell per day, thus making AP sites one of the most frequent lesions in DNA [20]. Sugar modifications, such as ssb, may act as an

Figure 1-1. Chemical structures of the major oxidative DNA base lesions.
The representative of oxidized pyrimidines and purines: thymine glycol (Tg) and 8-oxo-deoxyguanosine (8-oxo-dGuo), respectively, are shown in the insets.

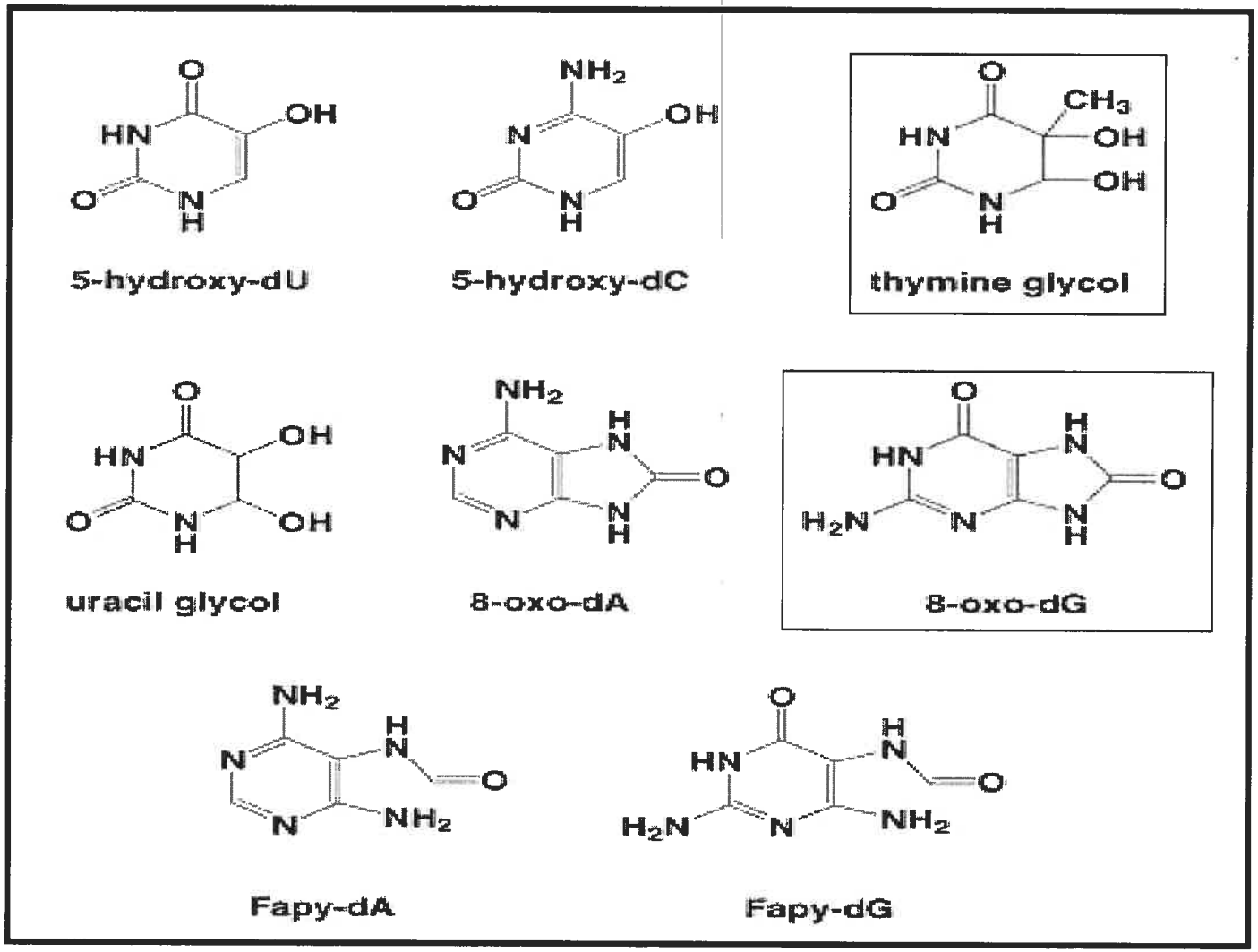
5-hydroxy-dU
5-hydroxy-dC
thymine glycol
uracil glycol
8-oxo-dA
8-oxo-dG
Fapy-dA
Fapy-dG

FIGURE 1-1

Figure 1-2. Chemical structures of commons forms of abasic (AP) DNA damage. Structure of AP lesions: natural AP site (top), C4'-oxidized AP site (middle), and C1'-oxidized AP site, 2-deoxyribonolactone (bottom).

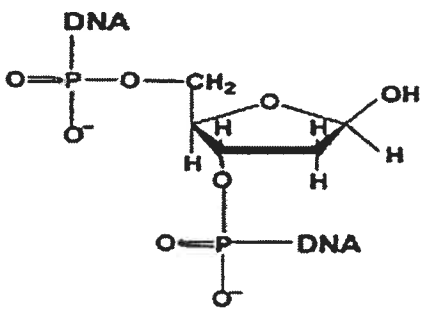

hydrolytic (natural) AP site

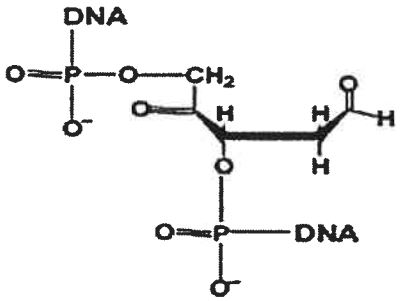

2-deoxypentose-4-ulose
(4'-oxidation)

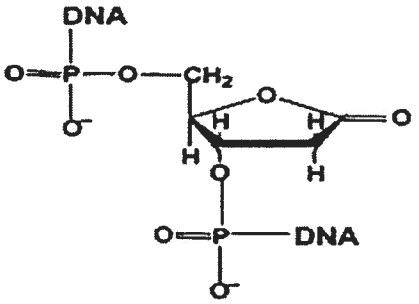

2-deoxypentonic acid lactone
(1'-oxidation)

FIGURE 1-2

inhibitor of DNA replication, and are thus toxic to cells [7]. On the other hand, unrepaired AP sites can result in a block to DNA replication, cytotoxicity, and mutations [20].

Thus, to prevent such harmful outcomes of the numerous DNA base and sugar lesions, all organisms have evolved several DNA repair mechanisms to ensure proper removal of oxidative DNA damages.

REPAIR OF OXIDATIVE DNA DAMAGE

The highly conserved base excision repair (BER) pathway is believed to be the primary defense mechanism against oxidative DNA base damage induced by ROS or simple alkylating agents, such as methyl methane sulfonate (MMS) [21].

Base excision repair

The multi-step BER process involves the concerted action of several proteins that recognize, excise, and repair an oxidative DNA base lesion, ultimately replacing the damaged moiety with the correct nucleotide (Figure 1-3 and Table I-I) [22,23]. BER is initiated by a DNA glycosylase that cleaves the *N*-glycosilic bond between the damaged base and DNA sugar phosphate backbone [24,25]. DNA glycosylases are divided into two groups: monofunctional and bifunctional DNA glycosylases [26,27]. Monofunctional glycosylases possess only base excision activity (Figure 1-3, depicted to the left), whereas bifunctional glycosylases act both to excise a damaged base and to incise 3' at the resulting AP site with their associated AP lyase activity, yielding a strand break with a 3'-blocking group and a normal 5'-phosphate residue (Figure 1-3, depicted to the right) [26,27]. For monofunctional glycosylases, the resulting AP site is cleaved at its 5' by an AP endonuclease, leaving behind a strand break with a normal 3'-OH group and an abnormal 5'-deoxyribose-5-phosphate (dRP) fragment (Figure 1-3, middle). In either case, the abnormal 3'-blocking group and 5'-dRP residue, produced by an AP lyase and AP endonuclease activity, respectively, must be processed prior to repair completion. The 3'-blocking group is excised by an AP endonuclease-associated 3'-phosphodiesterase activity, while the

Figure 1-3. Schematic representation of the base excision repair (BER) pathway. Shown is a general model of the short-patch (right) and the long-patch (left) BER pathways, and the enzymes to be involved in the individual steps. See main text for additional details.

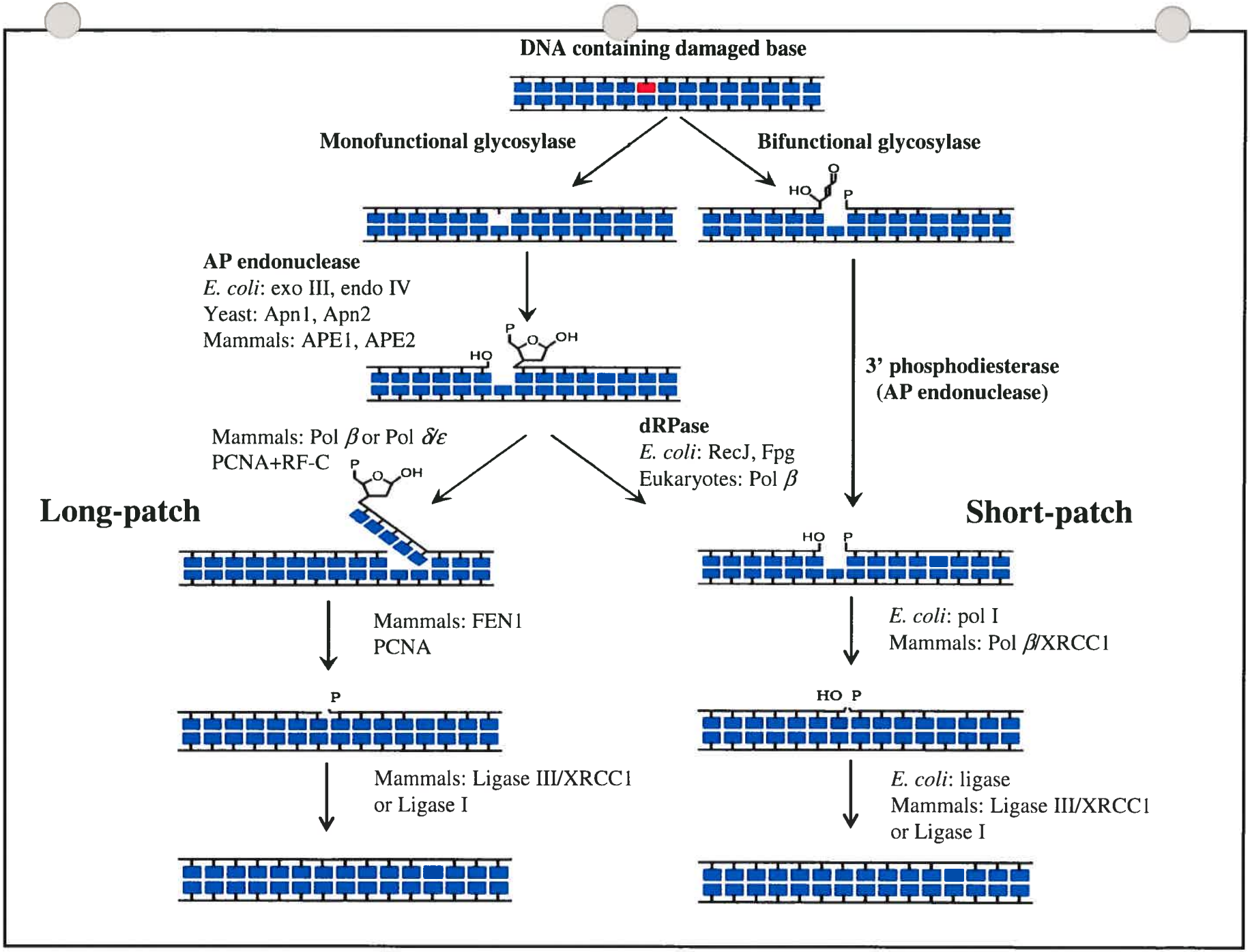
DNA containing damaged base
Monofunctional glycosylase
Bifunctional glycosylase
AP endonuclease
E. coli: exo III, endo IV
Yeast: Apn1, Apn2
Mammals: APE1, APE2
3' phosphodiesterase
(AP endonuclease)
Mammals: Pol β or Pol δ/ε
PCNA+RF-C
dRPase
E. coli: RecJ, Fpg
Eukaryotes: Pol β
Long-patch
Short-patch
Mammals: FEN1
PCNA
E. coli: pol I
Mammals: Pol β/XRCC1
Mammals: Ligase III/XRCC1
or Ligase I
E. coli: ligase
Mammals: Ligase III/XRCC1
or Ligase I

FIGURE 1-3

Table I-I. Summary of the principal BER enzymes in *Escherichia coli*, *Saccharomyces cerevisiae*, and human.

E. coli	*S. cerevisiae*	Human	Repair activity
ung	*UNG*	*UDG*	Uracil DNA glycosylase
alkA	*MAG*	*MPG/AAG*	Methylpurine DNA glycosylase
-	-	*TDG*	Thymine DNA glycosylase; excises T opposite G
nth	*NTG1, 2*	*NTH1*	Oxidized pyrimidine (Tg) DNA glycosylase; AP lyase
nei	-	*NEIL1, 2*	Oxidized pyrimidine DNA glycosylase; AP β,δ lyase
fpg	*OGG1, 2*	*OGG1*	8-oxo-dGuo DNA glycosylase; AP lyase
mutY	-	*MYH*	Adenine DNA glycosylase; excises A opposite 8-oxo-dGuo
mutT	-	*MTH*	8-oxo-dGuo triphosphatase
xth	-	*APE1*	AP endonuclease; 3'-repair diesterase; 3'-exonuclease
	APN2	*APE2*	3'-5' exonuclease; 3'-repair diesterase; AP endonuclease
nfo	*APN1*	**Absent to date**	AP endonuclease; 3'-repair diesterase
polI	*RAD27*	*FEN1*	Flap endonuclease; functions in long-patch BER
-	*POLX*	*POLβ*	Gap-filling DNA polymerase (in the nucleus); dRP lyase
	POL2, 3	*POLδ/ε*	Replicative DNA polymerases
-	*MIP1*	*POLG*	Gap-filling DNA polymerase (in the mitonchondria); dRP lyase
polIII (β-subunit	*POL30*	*PCNA*	Sliding clamp for DNA polymerase *β* and *δ/ε*; stimulates FEN activity, as well as other long-patch BER activities
polIII (γ-complex)	*CDC44*	*RFC*	PCNA loading factor
ligA	*CDC9*	*LIG1, 3*	Nick ligase; LIG1 functions in short- and long-patch BER, whereas LIG3 acts mainly in short-patch BER
-	-	*XRCC1*	Scaffold protein (no known enzymatic activity)

transient 5'-dRP residue is removed by DNA polymerase β (Pol β)-associated 5'-deoxyribose-5-phosphodiesterase (dRPase) activity. Then, Pol β inserts the correct nucleotide, and a DNA ligase seals the nick, thereby, repairing the damage [28]. The repair pathway described above is named short-patch BER (Figure 1-3, pathway on the right).

An alternative BER pathway

In mammals, an alternative BER pathway exists, termed the long-patch pathway which involves the replacement of approximately 2 to 10 nucleotides, including the damaged base (Figure 1-3, pathway on the left) [29]. In addition to the protein described for the short-patch pathway, the long-patch BER involves the replicative enzymes Pol δ and ε, the accessory factors PCNA (proliferating cell nuclear antigen) and RF-C (replication factor-C), as well as the endonuclease FEN1 (flap endonuclease 1) [30,31]. Either Pol β or Pol δ/ε, with the assistance of PCNA and RF-C, carries out strand-displacement synthesis to replace the missing nucleotides [30,31]. The resulting flap structure containing the 5'-dRP residue is subsequently removed by the flap endonuclease activity of FEN1, and the remaining nick is then sealed by DNA ligase I [30,31]. Studies have shown that both the fission yeast *Schizosaccharomyces pombe* (*S. pombe*) [32] and the budding yeast *Saccharomyces cerevisiae* (*S. cerevisiae*) have homologues to mammalian FEN1, PCNA, and RF-C [26]. However, the existence of the long-patch repair pathway has been confirmed only in *S. pombe* [32].

Potential mechanisms of switching between BER subpathways

The short-patch BER predominates over the long-patch pathway in mammals, yet the precise mechanism that controls the switching between these two pathways remains undetermined [33,34]. Previous reports have postulated that the type of DNA lesions and the nature of DNA glycosylases involved constituted the major determinants in the choice of the BER subpathway. Base lesions (e.g. 8-oxo-dGuo and Tg) that are excised by bifunctional glysosylases (e.g. OGG1 and NTH1) were shown to trigger mainly the short-patch repair since the 5'-phosphate residue

produced after AP lyase incision prevents strand displacement by Pol β (Figure 1-3, pathway on the right) [35]. In contrast, both the short- and long-patch BER subpathways are activated when monofunctional glycosyalses (e.g. UDG) initiate repair of damaged bases, such as uracil [35]. Recently, Petermann *et al.* however provided strong evidence for a key role of the Ligase III/XRCC1 complex in regulating the switching between the BER subpathways [36]. They demonstrated that the short-patch subpathway predominates when ATP-dependent ligation of the nick containing 5'-dRP residue takes place. Conversely, when ligation is inhibited due to ATP shortage and/or mutations in Lig III, XRCC1 stimulates Pol β-dependent DNA synthesis of a multi-nucleotide patch, thus resulting in the activation of the long-patch BER subpathway. Consistent with this notion, the authors showed that the long-patch repair prevails over the short-patch subpathway in HeLa cells knockdowned for the Lig III/XRCC1 complex [36].

Association between BER defects and human cancer

Genetic polymorphisms

Many highly prevalent single-nucleotide polymorphisms have been found in several BER genes, such as OGG1, APE1, Pol β and XRCC1 [37]. However, to date, no human diseases have been directly connected to their defects. Various case-control studies have investigated the association between the genetic variants of OGG1 (Ser326Cys), APE1 (Asp148Glu), Pol β (Lys289Met and Ile260Met), and XRCC1 (Arg194Trp, Arg280His, and Arg399Gln) and cancer risk [37]. However, these epidemiological investigations have yet to clearly demonstrate a direct effect of these polymorphisms on cancer susceptibility. For example, the Ser326Cys polymorphism of OGG1 has inconsistently been associated with risk of lung cancer [37]. Out of five studies which analyzed the homozygous mutant alleles, two were statistically significant whereas two studies showed no interaction [37]. Similarly, results of functional studies on the Ser326Cys OGG1 variant are also inconclusive. Some studies suggest reduced repair activity with the Ser326Cys variant, whereas others did not find an association between the Ser326Cys polymorphism in cancer and DNA repair capacity [37]. Thus, larger epidemiologic and functional studies are needed to

clearly establish a relationship between cancer and these genetic variants of BER genes.

However, Al-Tassan and colleagues have demonstrated that inherited defects of the adenine DNA glycosylase MYH is associated with somatic GC to TA tranversion mutations in the adenomatous polyposis coli (APC) gene, which is normally linked to familial adenomatous polyposis, a type of hereditary colon cancer [38]. MYH is thus the first BER gene associated with a human cancer syndrome.

Mouse models

Over the last decade, several BER-deficient mouse models have been generated to study the relationship between BER dysfunction and carcinogenesis [39]. A summary of the BER mouse models, and their related phenotypes, is delineated in Table I-II. At first glance, it is evident that the next generation of mouse models should comprised of combined deficiencies of DNA glycosylases which initiate the BER pathway as well as of conditional models of the intermediate and late steps of BER before a direct link can be established between BER deficiency and cancer.

AP ENDONUCLEASES

In addition to being central damage intermediates in BER, AP sites are considered to be one of the most frequent endogenous lesions in DNA [19,40]. Due to their mutagenic and cytotoxic properties, the repair of AP sites is essential to ensure genome stability and cell survival [41]. AP sites can be processed either by AP endonucleases or glycosylases/AP lyases (Figure 1-3). Still, The 3'-blocking groups produced following incision by glycosylases/AP lyases must be further processed to produce an accessible 3'-OH termini required for repair synthesis by DNA polymerases [1]. The majority of the cellular 3'-phosphodiesterase activity is provided by AP endonucleases (Figure 1-3, pathway on the right) [1]. Thus, this class of enzymes is considered to be far more efficient in repairing AP sites than glycosylases/AP lyases.

Table I-II. Summary of BER mouse models.

Mouse model	Relevant phenotype	Reference
Ogg1	Mice are viable Increased 8-oxoG level and G to T transversions	[42]
Myh	Mice viable Two-fold increased spontaneous mutation frequency in null ES cells	[43]
Ogg1/Myh	Mice viable Significantly enhanced tumor incidence	[44]
Nth1	Mice are viable and exhibit no abnormalities Increased levels of Tg	[45]
Ogg1/Nth1	Cells are defective in the repair of oxidized pyrimidines in mtDNA	[46]
Ung	Mice are viable and develop normally Increased incidence of B-cell lymphomas at old age	[47]
Aag	Mice are viable and develop normally Cells exhibit increased sensitivity to DNA-alkylating agents	[48,49]
Apex1	Embryonic lethal at E7.5 Cells from heterozygous mutants are sensitive to oxidizing agents	[50,51]
Pol β	Embryonic lethal at E18.5	[52]
Fen1	Embryonic lethality at E4.5 $Fen^{+/-}$ mice are normal	[53,54]
XRCC1	Embryonic lethal at E8.5	[55]
Lig I	Embryonic lethal at E15.5-16.5	[56]

Sequence and structural conservation of AP endonucleases

AP endonucleases are evolutionary highly conserved DNA repair enzymes which are grouped into two distinct families, the exonuclease (exo) III and the endonuclease (endo) IV families, named after the *Escherichia coli* (*E. coli*) members [1,57-59]. The exo III family includes *E. coli* exo III, *S. cerevisiae* Apn2, *Caenorhabditis elegans* (*C. elegans*) EXO-3, human APE1 and APE2. The exo III members are small, monomeric, divalent metal ion-dependent enzymes that are sensitive to metal-chelating agents, such as EDTA [60-62]. On the other hand, AP endonucleases of the endo IV family, comprising *E. coli* endo IV, *S. cerevisiae* Apn1, and *C. elegans* APN-1, are resistant to inactivation by EDTA since they are metal ion-independent enzymes [60,63]. Although no homolog of the endo IV family has yet been identified in human cells, such activity is likely to be present in there as well (See Table I-III for a summary of the AP endonuclease enzymes).

In addition to their sequence similarity, related AP endonucleases also share structural homology, as suggested by high-resolution crystal structures for their representative members. Both *E. coli* exo III and human APE1 possess a characteristic four-layered α,β-sandwich fold which is also found in the digestive enzyme DNase I [64,65]. However, their DNA-binding domain loops adopts an extrahelical conformation that is not observed for DNase I. These protruding loops are proposed to be involved in damage recognition and bond cleavage at AP sites [65]. Recently, Kaneda and colleagues demonstrated by site-directed mutagenesis that the amino acid residues, Trp-212 and Trp-280, near the catalytic site of exo III and APE1, respectively, are critical for AP site recognition as well as AP endonuclease activity [66]. They propose a model whereby the tryptophan residue of exo III-related enzymes acts as an AP site 'recognizer' by intercalating its aromatic side chain into the AP site pocket, followed by flipping out of the AP site from the duplex into the enzyme catalytic pocket with DNA kinking at the AP site [66]. For

Table I-III. Comparison of AP endonucleases in bacteria, yeast, and human.

	E. coli		*S. cerevisiae*		Human	
Gene name	***xth***	***nfo***	***APN1***	***APN2***	***APE1***	**APE2**
Protein name	exo III	endo IV	Apn1	Apn2	APE1	APE2
Family name	Exo III	Endo IV	Endo IV	Exo III	Exo III	Exo III
Cofactors	Mg^{2+}	no	no	Mg^{2+}	Mg^{2+}	Mg^{2+}
Inhibitors	EDTA	no	no	EDTA	EDTA	EDTA
Length	268 aa	285 aa	367 aa	520 aa	317 aa	518 aa
Molecular weight	30.97 kDa	31.48 kDa	41.44 kDa	59.45 kDa	35.42 kDa	57.4 kDa
AP endonuclease activity	90%	10% *20-fold induction by paraquat	97%	3%	95%	Weak
3'-phosphodiestease activity	90%	10% *20-fold induction by paraquat	97%	30- to 40-fold more efficient than AP endonuclease	100- to 200-fold less efficient than AP endonuclease	Strong
3'-5' exonuclease activity	Robust Specific for 3' recessed ends of DNA	High Preference for 3' recessed substrate	Robust Preference for 3' recessed DNA	30- to 40-fold more efficient than AP endonuclease	100- to 200-fold less efficient than AP endonuclease	Robust
Nucleotide incision activity	Absent	Present	Present	Absent	Present	Absent
Relevant mutant phenotype	Hypersensitive to oxidizing agents	Hypersensitive to oxidizing agents	Hypersensitive to alkylating and oxidizing agents	Sensitive to alkylating agents	Embryonic lethal in null mice	Growth retardation in null mice

the endo IV family, the high-resolution structure of *E. coli* endo IV suggests that this AP endonuclease and its homologues may use the classic $\alpha_8\beta_8$ TIM barrel fold to promote flipping of both the AP site and its orphan nucleotide out of the duplex with a 90° bend in the DNA, but allowing only the damaged nucleotide in the enzyme active site pocket [67]. The conformational changes induced in endo IV upon DNA binding would allow the AP site to directly make contact with the three Zn^{2+} ions, which are essential for the catalytic activities of all endo IV-related AP endonucleases [67]. Thus, solving the crystal structures of representative AP endonucleases has provided the structural basis for understanding the catalytic mechanism of the exo III and endo IV family members [60].

E. coli AP endonucleases

Exo III

The exo III enzyme, encoded by the *xth* gene, was initially identified as a phosphatase-exonuclease, but subsequently was discovered to be the major constitutive AP endonuclease in *E. coli* extracts. Exo III is a 268 amino acid enzyme with a molecular mass of 31 kDa and accounts for approximatively 90% of the cellular AP endonuclease activity [59,68,69]. Exo III is also endowed with a strong 3'-phosphodiesterase activity, an efficient 3'-5' exonuclease activity, and an endonuclease activity at urea residues in oxidized DNA [70]. *E. coli* mutants lacking exo III (*xthΔ*) are sensitive to oxidizing agents such as H_2O_2 and are hypersensitive to UVB light [71-74]. A recent study clearly suggests that exo III plays a crucial role in the repair of UVB-induced toxic lesions, as pre-treatment with dipyridyl (an iron chelator) completely restores wild-type resistance in the *xthΔ* strain [74]. Dipyridyl prevents the Fenton reaction ($Fe^{2+} + H_2O_2 \rightarrow Fe^{3+} + {\cdot}OH + OH^-$) to occur via the chelation of a ferrous iron (Fe^{2+}), thus protecting cells from ROS-induced DNA lesions [74]. In fact, several studies have demonstrated that *xthΔ* strains accumulate large amounts of unrepaired ssb with blocked 3' termini which are genotoxic damages [73,75].

Endo IV

The *xth* mutants possess a residual (10%) AP endonuclease activity that displays no requirement for metal ions. A large-scale screening of clones overexpressing a Mg^{2+}-independent AP endonuclease activity led to the isolation of the *nfo* gene which encodes the endo IV protein. The *nfoΔ* mutant is less sensitive to oxidative and alkylating agents (e.g. H_2O_2 and MMS, respectively) as compared to the *xthΔ* strain, indicating that endo IV serves as an back-up enzyme in the repair of AP sites [75]. However, recently, endo IV was demonstrated to play a determinant role in the avoidance of UVB-induced mutagenic lesions [74]. Moreover, the protein expression levels of endo IV can be induced more than 20-fold by paraquat, a superoxide-producing agent. The up-regulation of endo IV may be important during oxidative stress or when certain DNA lesions are refractory to repair by exo III [76].

S. cerevisiae AP endonucleases

Apn1

In the budding yeast *S. cerevisiae,* Apn1 is the predominant AP endonuclease representing more than 90% of the total AP endonuclease activity [77]. Apn1 was first described as a 3'-phosphodiesterase since the purified Apn1 cleaved synthetic DNA substrates containing 3'-phosphoglycolaldehyde esters [77]. Both the AP endonuclease and 3'-phosphodiesterase activities of yeast Apn1 showed no metal requirement similarly to bacteria endo IV [77-79]. Screening a yeast λgt11 expression cDNA library in *E. coli* using a polyclonal antibody produced from the purified Apn1 lead to the successful identification of the *APN1* gene [80]. Comparison of the primary structure of Apn1 with that of *E. coli* endo IV revealed that the yeast protein is indeed homologous to endo IV and bears an extra 82 amino acid residues at the C-terminus [80,81]. This additional C-teminal region of *APN1* contains a bipartite nuclear localization signal (NLS) which when deleted causes cytoplasmic accumulation of Apn1 [81]. Moreover, we have previously demonstrated that Pir1, a cell wall constituent, interacts with Apn1 bipartite NLS, causing Apn1 to translocate

into the mitochondria [82]. We observed in *pir1Δ* mutants a striking nuclear accumulation (~3-fold) of Apn1, which coincided with drastically reduced levels in the mitochondria [82]. Apn1 encompasses several enzymatic activities: (i) an AP endonuclease activity, that hydrolyses the phosphodiester backbone 5' to an AP site [1], (ii) a 3'-phosphodiesterase activity, that removes 3' DNA-blocking groups such as 3'-phosphates, 3'-phosphoglycolates, and 3'-α,β-unsaturated aldehydes [1], (iii) a 3'-tyrosyl-DNA phosphodiesterase activity, that hydrolyzes the tyrosine residue of topoisomerase 1 linked to a 3' DNA end [83], (iv) an endonuclease activity, that nicks 5'-side of oxidatively damaged DNA bases such as FapyA and FapyG [84], and (v) a 3'→5' exonuclease activity, that removes either a 3'-terminal nucleotide at a nick or a misincorporated 8-oxo-dGuo [85,86].

Apn1-deficient strains of *S. cereviasiae* display hypersensitivity to H_2O_2 and MMS which produces ssb with blocked 3'-termini and abasic sites, respectively [40]. Interestingly, *apn1Δ* null mutants are not sensitive to bleomycin, suggesting the presence of another enzyme more proficient at removing bleomycin-induced 3'-blocking groups. Loss of Apn1 results in a 10- to 15- fold increase in the nuclear spontaneous mutation rate [40]. The mutations correspond mainly to AT to CG transversions [87]. The high frequency of spontaneous mutations in the *apn1Δ* null mutants is primarily due to unrepaired AP sites [88]. Deletion of Apn1 has no effect on the rates of spontaneous mitochondrial mutations. However, when Apn1-deficient cells are exposed to MMS, they display approximately 6-fold increase in mitochondrial spontaneous mutation rates, suggesting an important role of Apn1 in the repair of damaged mitochondrial DNA [82,89].

Apn2

A residual (5%) AP endonuclease activity was partially purified initially by Sander and Ramotar [90] and termed Pde (3'-phosphodiesterase). Later, Johnson *et al.* independently characterized the Pde protein and renamed it Apn2 [89]. Apn2 shares 36% and 33% sequence homology with *E. coli* exo III and human APE1, respectively [89,91]. In addition to its AP endonuclease activity, Apn2 also contains 3'-phosphodiesterase and 3'→5' exonuclease activities [92]. These two latter

activities of Apn2 were estimated to be 30- to 40-fold higher than its AP endonuclease activity [92]. Furthermore, a direct interaction of Apn2 with PCNA strongly stimulates its 3'-phosphodiesterase and the 3'→5' exonuclease activities [93].

Cells deficient in Apn2 are less sensitivity to MMS than the *apn1Δ* strains. However, *apn1Δapn2Δ* double mutants are 15-fold more sensitive to MMS and 2- to 3-fold more sensitive to H_2O_2 and bleomycin than *apn1Δ* single mutants [91,94]. The *apn1Δapn2Δ* mutant strains show both enhanced spontaneous and MMS-induced mutation rates in comparison to the wild type [89,91]. The expression of Apn2 in *apn1Δapn2Δ* mutants restores some resistance to MMS and partially decreases the rate of spontaneous mutations [91]. Together, these observations indicate that Apn2 provides important back-up DNA repair activities for Apn1.

Human AP endonucleases

APE1

In humans, the exo III-related protein APE1 (also called Ref-1, HAP1, and APEX1) is considered the major AP endonuclease, representing approximately 95% of the total cellular AP endonuclease activity [95-98]. APE1 harbors its own bipartite NLS, located within its N-terminal 20 amino acid residues, which allows for its nuclear import but also localization to the mitochondria following cleavage by an unknown specific mitochondria-associated peptidase [99,100]. APE1 is also endowed with a 3'-phosphodiesterase as well as a 3'→5'-exonuclease activity, which are much weaker than its AP endonuclease activity [1]. Moreover, Gros *et al.* demonstrated that APE1 is also capable of incising directly 5' of oxidative base lesions, such as 5,6-dihydro-2-deoxyuridine, in a DNA glycosylase-independent manner [101].

The biological importance of APE1 is underlined by the embryonic lethality in knock-out mice and the lack of stable APE1-deficient cell lines [102]. Recently, Fung and Demple addressed the cellular role of APE1 by using RNAi technology [103]. They showed that APE1 downregulation blocked cell proliferation and

stimulated apoptosis, which was correlated with accumulation of AP sites [103]. These effects were reversed by expression of *S. cerevisiae* Apn1, a protein that is structurally unrelated to APE1 but shares several enzymatic activities in the repair of AP sites [103] [104]. Their results clearly establish that APE1 plays a vital role in the repair of endogenous DNA damage that, when left unrepaired triggers apoptotic cell death.

APE2

To date, no endo IV homologs have been identified in human cells. In their own search for novel human AP endonuclease/3'-phosphodiesterase enzymes, Hadi and Wilson have however identified a second exo III-like protein termed APE2 [105]. The ubiquitously expressed APE2 enzyme is composed of 518 amino acids with a predicted molecular mass of 62 kDa and shares significant amino acid sequence similarity to the core nuclease domain of APE1 and exo III (29% and 27% sequence identity, respectively) [105]. Peptide sequence comparison revealed that APE2 lacks the extended N-terminal domain present in APE1 but possesses a longer C-terminal region, which is absent in APE1 and exo III, thus indicating the existence of a second exoIII-like subfamily. This new exo III-like subgroup comprises also of *S. cerevisiae* Apn2 and *S. pombe* Apn2 [106].

An initial insight into the biological significance of APE2 was provided by homozygous APE2-null mice which exhibited growth retardation and dyshematopoiesis accompanied by G_2/M arrest [107]. To shed more light on the role of human APE2, Burkovic *et al.* expressed recombinant APE2 in yeast and showed that recombinant enzyme exhibits a weak AP endonuclease activity, but shows strong 3'→5' exonuclease and 3'-phosphodiesterase activities that act preferentially on mistmatched 3'-nucleotides from DNA [108]. Moreover, mutational analysis revealed that Asp177 is an active site residue of APE2 [108]. This study strongly suggests that the intrinsic activities of APE2 are determinant in the removal of 3'-blocking termini, as well as in the proofreading of errors incorporated by DNA polymerases [108].

APE1 more than a DNA repair enzyme

APE1 is also known as Ref-1 (redox effector factor-1) due to its redox activity that acts on redox-sensitive transcription factors [109]. APE1/Ref-1 was first found to copurify with the transcription factor AP-1 during column chromatography [110]. Subsequently, APE1/Ref-1 was demonstrated to reduce the conserved cysteine residues in the DNA binding domains of c-Fos and c-Jun, the two subunits of AP-1, thus promoting the binding to their DNA cognate sequences [97]. Since then, APE1/Ref-1 has been shown to modulate the DNA binding activities, and thus the transcriptional regulatory potential of proteins such as NF-κB (nuclear factor-κB), Myb, HIF-1α (hypoxia inducible factor-1α) and p53 via a redox mechanism [111].

The redox function of APE1/Ref-1 is located in the N-terminal 127 amino acids, whereas its nuclease activity resides in the C-terminal 157 amino acids [112]. The nuclease region of APE1/REF-1 shares a high degree of sequence homology with other functionally related repair proteins such as bacteria exo III and fruit fly Rrp1, but the redox domain is present only in mammals [112]. The redox activity of APE1/Ref-1 may have evolved to sustain embryonic development, since deletion of an exo III-like protein does not cause lethality in lower organisms [112]. However, at the cellular level, APE1/Ref-1 nuclease function is more important for the repair of spontaneous DNA damage that, when accumulated, can induce cell death [102,112,113]

Regulation of APE1 activities

Considering the key roles of APE1 in DNA repair and gene regulation, the cell has developed several strategies to regulate the APE1 enzyme at both the transcriptional and posttranslational levels [111]. In terms of transcriptional regulation, it has been shown that ROS, such as H_2O_2, induce APE1 mRNA, which correlates with an increase in APE1 protein levels and activity [114]. APE1 cellular functions are further modulated through two non-mutally exclusive posttranslational mechanisms, namely subcellular localizations and posttranslational modification [115]. Upon exposure to ROS, APE1 accumulates in the nucleus as a result of both an

increased in nuclear translocation and a decreased in nuclear export via the binding of its bipartite NLS with nuclear importins α1 and α2 and the inhibition of its nuclear export signal, respectively [99]. Several posttranslational modifications, such as acetylation, phosphorylation and oxidation/reduction have been reported to influence APE1 functions [111,115]. Acetylation of APE1 by p300 was shown to affect the transcriptional regulatory function of APE1 [115]. However, the reports on the impact of phosphorylation by PKC (protein kinase C), CKI and CKII (casein kinase I and II, repectively) on APE1 activities remain inconsistent [115]. Some studies suggest that phosphorylation of APE1 might abolish its AP endonuclease activity [115].

The redox status of APE1 is another important regulatory factor determining its cellular activities [111,115]. Hirota *et al.* demonstrated that thioredoxin (TRX), an endogenous dithiol-reducing molecule, acts as a hydrogen donor for APE1. Reduced APE1, in turn, potentiates the DNA-binding and transactivation abilites of AP-1 [116]. In a similar manner, TRX and APE1 cooperate in the control of basal p53 stability and activity [117]. While reduction of APE1, on the one hand, appears to be a positive regulatory mechanism for its transcriptional functions, oxidation, on the other, has a negative impact on APE1 AP endonuclease activity [118]. Treatment of APE1 with oxidizing agents, such as H_2O_2 and diamide, causes a significant decrease in AP endonuclease activity, which was neutralized by the addition of certain amounts of DTT, suggesting a direct effect of oxidation [118]. Furthermore, site-directed mutagenesis studies revealed that Cys310 residue of APE1 is likely to be oxidized, whereas Cys63 and Cys95 are most susceptible to a reduction reaction [115] [118].

Protein-protein interactions involving APE1

APE1 has been demonstrated to be an important modulator of the multi-step BER pathway. APE1 accomplishes this regulatory role mainly through physical and/or functional protein-protein interactions with both up- and down-stream BER enzymes (Table I-IV) [115]. BER is initiated by DNA glycosylases which recognize and excise a damaged base leaving behind an AP site. The activity of several

glycosylases, such as OGG1 [119], UNG [120], TDG [121] and NTH1 [122], is stimulated by an association with APE1. However, only TDG and MYH interact physically and form stable complexes with APE1 [121,123]. Since most of the glycosylases display a high affinity for base lesions and AP sites, APE1 is thought to stimulate the displacement of the glycosylases from their DNA products via protein interactions, thus facilitating glycosylase turnover. APE1 was shown to interact also with downstream BER proteins, such as FEN1 [124], Pol β [125], PCNA [124], XRCC1 [126] and LIG1 [127]. In these interactions, the AP endonuclease modulates its patner's activity, with the exception of XRCC1, which alters the functions of APE1 (see Table I-IV).

Adding to its complex network of protein interactions with BER proteins, APE1 also interacts with proteins participating in other cellular processes, such as transcription and replication. APE1 was demonstrated to interact with WRN (Werner syndrome protein), PARP (Poly(ADP-ribose) polymerase 1), HSP70 (heat-shock protein 70), and the tumor-suppressor protein p53 [128-132]. The effects of these various interactions are summarized in Table I-IV.

Table I-IV. Effects of the various proteins interactions involving APE1 on the BER pathway.

Interacting patner	Consequence of the interaction	Reference
BER proteins		
UDG	Stimulates displacement of UDG from AP sites	[120]
TDG	Stimulates the turnover o f TDG at AP sites	[121]
MYH	Facilitates the release of MYH from its DNA products	[123]
FEN1	Enhances both the exo- and endonuclease activities of FEN1 Stimulates LP-BER	[124,127]
Pol β	Stimulates the 5'-dRP lyase activity of Pol β	[125]
PCNA	Coordinates LP-BER	[124]
XRCC1	Increases APE1 AP endonuclease and 3'-phosphodiesterase activity Promotes SP-BER	[126]
LIG1	Stimulates DNA ligase 1 activity	[127]
Other proteins		
WRN	Inhibits WRN helicase activity on BER intermediates	[128]
PARP	Blocks APE1 stimulation of strand-displacement DNA synthesis by Pol β Inhibits the exonuclease activity of APE1	[129]
HSP70	Stimulates APE1 AP endonuclease activity	[130]
p53	Stimulates p53 DNA binding by promoting its tetramerization Induces p53 transactivation and pro-apoptotic activities	[132]

HYPOTHESIS AND OBJECTIVES

AP endonuclease enzymes are crucial players in the BER pathway. They are grouped into two distinct families, the exo III family and endo IV family. Cells lacking AP endonuclease activity are hypersensitive to oxidizing and alkylating agents, such as H_2O_2 and MMS, which induce ssb with blocked 3'-termini and AP sites, respectively. We were particularly interested in understanding the molecular mechanisms by which eukaryotic AP endonucleases maintain genomic integrity in the nucleus as well as in the mitochondria. We set out to study the structure/function and/or protein interactions of AP endonucleases, which could provide us with valuable insights into their mechanisms of binding and cleavage of oxidative DNA lesions as well as their regulation inside the cell. In our first study (Chapter 2) which aimed at identifying the critical amino acid residues of *S. cerevisiae* Apn1 for its biological function, we showed by mutational analysis that Glu158 and Asp192 are crucial for the DNA repair functions of Apn1. In our second study (Chapter 3), we set out to evaluate the role of yeast Ogg1 DNA glycosylase in the maintenance of a mitochondrial poly(GT) tract reporter system. Interestingly, we discovered that overproduction of Apn1 triggers instability of the poly(GT) tract, but which was counteracted by the simultaneous overexpression of Ogg1. In our third study (Chapter 4), we initially aimed at purifying an endo IV homolog in human cells. However, the goal of this project changed when we unexpectedly re-isolated GAPDH, a well-established glycolytic enzyme, during our purification of a Mg^{2+}-independent AP endonuclease. We demonstrated that GAPDH physically interacts with APE1 to reduce the oxidized forms of APE1, which resulted in the reactivation of the AP endonuclease activity. In addition, we demonstrated the importance of Cys152 and Cys156 residues of GAPDH in the reactivation of APE1 by site-directed mutagenesis. The biological importance of GAPDH in the cellular protection against genotoxic agents, which induce APE1-repairable lesions, was further supported by clonogenic assays using human colon carcinoma cells overexpressing GAPDH or knockdowned for GAPDH.

CHAPTER 2

Characterization of two independent amino acid substitutions that disrupt the DNA repair functions of the yeast Apn1

Published in *Biochemistry* **2003**, Vol. 42, No. 21, pp. 6436-6445.

Characterization of two independent amino acid substitutions that disrupt the DNA repair functions of the yeast Apn1[Ψ]

ARSHAD JILANI[1], RATSAVARINH VONGSAMPHANH[1], ANICK LEDUC[1], LAURENT GROS[2], MURAT SAPARBAEV[2], AND DINDIAL RAMOTAR [1‡]

Running title: Two variants of Apn1 lacking DNA repair functions

[‡]Corresponding author:

[1]Guy-Bernier Research Centre, University of Montreal, 5415 de l'Assomption, Montreal, Quebec, Canada H1T 2M4. Telephone: (514) 252-3400 ext 4684. Fax: (514) 252-3430.

E-mail: [redacted]

[2]Groupe Réparation de l'ADN, Unité Mixte de Recherche 8532 CNRS, Laboratoire de Biotechnologies et Pharmacologie Génétique Appliquée-École Normale Supérieure Cachan, Institut Gustave-Roussy, 94805 Villejuif Cedex, France. Telephone: 33 1 42115404. Fax: 33 1 42115276.

E-mail: [redacted]

[Ψ]This work was partially funded by the National Cancer Institute of Canada (NCIC) with funds from the Canadian Cancer Society and the Natural Sciences and Engineering Research Council of Canada (D.R.), and by European Community Grant QLK4-2000-00286 and Association pour la Recherche sur le Cancer (M.S.). D.R. is supported by a senior fellowship from the Fonds de la Recherche en Santé du Québec, and L.G. is supported by a postdoctoral fellowship from European Community.

ABSTRACT

The members of the Endo IV family of DNA repair enzymes, including *Saccharomyces cerevisiae* Apn1 and *Escherichia coli* endonuclease IV, possess the capacity to cleave abasic sites and to remove 3'-blocking groups at single-strand breaks *via* apurinic/apyrimidinic (AP) endonuclease and 3'-diesterase activities, respectively. In addition, Endo IV family members are able to recognize and incise oxidative base damages on the 5'-side of such lesions. We previously identified eight amino acid substitutions that prevent *E. coli* endonuclease IV from repairing damaged DNA *in vivo*. Two of these substitutions were glycine replacements of Glu145 and Asp179. Both Glu145 and Asp179 are among nine amino acid residues within the active site pocket of endonuclease IV that coordinate the position of a trinuclear Zn cluster required for efficient phosphodiester bond cleavage. We now report the first structure-function analysis of the eukaryotic counterpart of endonuclease IV, yeast Apn1. We show that glycine substitutions at the corresponding conserved amino acid residues of yeast Apn1, i.e., Glu158 and Asp192, abolish the biological function of this enzyme. However, these Apn1 variants do not exhibit the same characteristics as the corresponding *E. coli* mutants. Indeed, the Apn1 Glu158Gly mutant, but not the *E. coli* endonuclease IV Glu145Gly mutant, is able to bind DNA. Moreover, Apn1 Asp192Gly completely lacks enzymatic activity, while the activity of the *E. coli* counterpart Asp179Gly is reduced by ~40-fold. The data suggest that although yeast Apn1 and *E. coli* endonuclease IV exhibit a high degree of structural and functional similarity, differences exist within the active site pockets of these two enzymes.

INTRODUCTION

Apurinic/apyrimidinic (AP) sites, produced in cellular DNA both spontaneously and by many chemical mutagens (*e.g.*, oxidative and alkylating agents), are highly genotoxic and must be repaired by AP endonucleases to prevent genetic mutations [1,133]. The yeast *Saccharomyces cerevisiae* possesses a 40.5 kDa DNA repair enzyme, Apn1, which is localized to the nucleus as well as to the mitochondria [40,81,82]. Apn1 is a key component of the base excision repair pathway, and functions to hydrolyze AP sites by cleaving the DNA backbone 5' to the AP site to produce a 3'-hydroxyl group and a 5'-deoxyribose phosphate [40,78,133]. The 5'-deoxyribose phosphate is then removed by a 5'-deoxyribose phosphodiesterase, such as yeast Rad27, to create a gap which is then filled in and sealed by the sequential action of DNA polymerases and DNA ligase [134,135]. Apn1 also possesses a 3'-diesterase activity, which removes a multitude of 3'-blocking groups (e.g., 3'-phosphoglycolate and 3'-phosphate) at DNA single-strand breaks induced by oxidative agents, including the antitumor drug bleomycin and hydrogen peroxide (H_2O_2) [77,78]. More recently, we have shown that Apn1 recognizes and cleaves oxidized bases immediately 5' to the lesion to create a 3'-hydroxyl group [84]. This enzyme is also able to act on nicked DNA to remove the 3'-nucleotide, thereby generating a single-nucleotide gap [84]. Thus, Apn1 can be viewed as having multiple enzymatic activities.

Mutants lacking Apn1 (*apn1Δ*) are hypersensitive to the alkylating agent methyl methane sulfonate (MMS) due to defective repair of MMS-induced AP sites [136], and also display a 10- to 15-fold increase in the rate of spontaneous AP site-induced single base-pair mutations [87,88,137]. *apn1Δ* mutants are not sensitive to agents that generate DNA strand breaks with blocked 3'-termini due to the presence of another compensating AP endonuclease/3'-diesterase activity, i.e., Apn2 (also called Pde1 and Eth1) [89,91]. When both *APN1* and *APN2* genes are deleted, the resulting *apn1Δapn2Δ* double mutant is exquisitely sensitive to MMS, and displays hypersensitivity to agents such as H_2O_2 that creates strand breaks terminated with 3'-blocking groups [89].

Apn1 belongs to the Endo IV family of DNA repair enzymes, which is exemplified by *Escherichia coli* endonuclease IV (endo IV) [133]. Recent studies have shown that Apn1/endo IV homologues also exist in the fission yeast *Schizosaccharomyces pombe*, as well as in the nematode *Caenorhabditis elegans*, underscoring the importance of Endo IV family members in the repair of damaged DNA [133]. These members share five highly conserved regions (RI-RV) that are distributed along the entire length of the proteins [133]. For example, the RIII region contains a stretch of amino acid residues (KSRxGVCIDTCHxFAxGYD) that are identical in all members [133]. Consistent with this substantial degree of amino acid sequence homology, cross-species complementation revealed that Endo IV family members are also highly functionally conserved. For example, yeast Apn1 can substitute for *E. coli* endo IV and *vice versa* [138]. However, despite the high degree of evolutionary conservation among Endo IV family members, no corresponding homologue has yet been found in human cells [133].

We have been interested in elucidating the mechanism by which *E. coli* endo IV recognizes and cleaves phosphodiester bonds at sites of DNA damage. Using chemical mutagenesis, we previously identified eight essential amino acid substitutions that alter endo IV function with respect to both AP site cleavage and removal of blocked 3'-termini [139]. Indeed, mutants bearing these substitutions showed parallel reductions of AP endonuclease/3'-diesterase activities, ranging from 10- to 150-fold [139]. One of the mutants, bearing the substitution E145G located in the conserved region RII, actually prevented endo IV from binding to DNA [139]. Other substitutions destabilized the protein and were deemed essential for the proper maintenance of the tertiary structure [139]. Concurrent with our reported findings, the high resolution atomic structure of endo IV was published and assigned the side chain of nine amino acid residues as coordinating a trinuclear Zn cluster within the active site pocket of the enzyme. Among our own panel of endo IV mutants are variants in which two of these nine amino acid residues (*i.e.*, either Glu145 or Asp179) have been replaced with glycine [139]. We therefore set out to investigate if the corresponding conserved amino acid residues of Apn1 (i.e., Glu158 and Asp192) are also essential for biological function. Our data clearly reveal that glycine substitution

at either Glu158 or Asp192 of Apn1 prevents the mutant protein from repairing damaged DNA *in vivo*, although these mutants differ substantially from their endo IV mutant counterparts. We suggest that Apn1 and endo IV use slightly different mechanisms to catalyze the processing of damaged DNA.

MATERIALS AND METHODS

Strains, media, genetic analysis, and transformation

The bacterial strains used in this study were the parent AB1157 and the mutant BW528 [*Δ(xth-pnc)*, *nfo1::kan*)] (kindly provided by Dr. B. Weiss, Emory University, Atlanta, GA). The bacteria were transformed with the indicated vector or plasmid (see below) by the $CaCl_2$ method. The *E. coli* strain used for plasmid maintenance was DH5α. The *S. cerevisiae* strains used in this work were YW465 (*MATα;ade2Δ0 his3Δ-200 leu2Δ-1 met15Δ0 trp1Δ-63 ura3Δ0*), YW605 (isogenic to YW465, except *apn1Δ::HIS3*), and YW781 (isogenic to YW465, except *apn1Δ::HIS3 apn2Δ::KanMX4*) and were generously provided by T. Wilson (Ann Arbor, MI). Yeast cells were grown in either complete yeast peptone dextrose (YPD) or minimal synthetic (SD) medium, to which standard nutritional supplements had been added at 20 μg/mL. Transformation were carried out as described previously [140].

Construction of the plasmids GFP-APN1 and GST-APN1

The *APN1* gene (bp −13 to +1383) was amplified by polymerase chain reaction (PCR) from the plasmid *YepApn1* using the primers APN1-F1-*Eco*R1 (5'-$^{-13}$CGGAACCATCGAATTCCCTTCGACACCTAGCTTTG^{21}-3') and DR-2B (5'-^{1383}CCATAAGAGGATGGTCGACCGCCTTCCTTAG^{1353}-3') bearing the restriction sites (underlined) for *Eco*RI and *Sal*I, respectively. The amplified 1.4 kb DNA fragment was digested with *Eco*RI and *Sal*I and subcloned downstream of the green fluorescent protein (*Gfp)* gene, which is under the control of the *GAL1* promoter in the yeast expression vector pYES2.0, to produce the plasmid p*GFP-APN1*. In a similar fashion, the fragment was cloned downstream of the glutathione *S*-transferase (*Gst*) gene and placed under the control of the *lac* promoter in the *E. coli* expression vector pGEX-4T-1 (Amersham Pharmacia Biotech) to produce the plasmid p*GST-APN1*.

plates were inverted, uncovered, and dried in a 37°C incubator for 1 h. Then bacterial or yeast cells were replicated as a thin line along the drug gradient, and photographed after 24 h of growth at 37°C. Growth along the gradient (~82 mm) is considered to be 100%.

Immunodetection

The proteins were separated on 10% SDS-PAGE gel and transferred onto a nitrocellulose membrane (8 cm x 10 cm) (Amersham Life Science) which was then blocked with TSE buffer [10 mM Tris-HCl (pH 7.45), 150 mM NaCl, 0.1% Tween, and 1 mM EDTA] containing 5% powdered milk for 1 h. The membrane was probed for 16 h at 4°C with 10 mL of TSE containing anti-Gfp monoclonal antibodies (Clonetech) at a dilution of 1:5000. Following the probing, the membrane was washed three times for 15 min each time with TSE before addition of 10 mL of the anti-mouse IgG conjugated to horseradish peroxidase at a dilution of 1:2500 (BIO/CAN Scientific, Inc.) for 1 h at room temperature. Finally, the membrane was washed again three times for 15 min each time with TSE, and immunoreactive polypeptides were detected by chemiluminescence (Dupont-NEN).

Purification of Apn1, Gst-Apn1 and the mutant forms

BW528 cells bearing the plasmids p*GST-APN1*, p*GST-APN1(E158G)*, and p*GST-APN1(D192G)* were grown overnight at 30°C in 8 mL of LB containing 100 μg/mL ampicillin, and then subcultured into 250 mL LB medium containing 100 μg/mL ampicillin to an OD of 0.6 at 600 nm. IPTG (Sigma) was then added to a final concentration of 1 mM, and the culture was grown for an additional 140 min. Cell pellets were resuspended in 2.5 mL of buffer A which consisted of 50 mM Tris-HCl (pH 7.5), 100 mM NaCl, 0.5 mM EDTA, 0.5 mM DTT, and the protease inhibitor cocktail (Complete Mini, EDTA-free, Roche Diagnostics GmbH). Cell extracts were prepared as previously described [141] with the slight modification of using three freeze-thaw cycles (freezing in ethanol/dry ice freezing bath and thawing

at 37°C). Extracts were then sonicated 2 x 5 s (at 50% power), centrifuged at 12 000 rpm at 4°C, and the supernatants were loaded onto a 0.25 mL glutathione-Sepharose 4B mini column (Amersham Pharmacia Biotech) pre-equilibrated with buffer A. The column was washed three times with buffer A and eluted with 500 µL of 50 mM Tris-HCl (pH 8.0) containing 10 mM reduced glutathione. The eluted proteins were dialysed in a Spectra/Por 1 dialysis tube (MWCO 6K-8K, Spectrum) against 500 mL of buffer A for 3 h with three intervening changes. The dialyzed proteins were loaded onto a 50 µL Macro-Prep 50S (Bio-Rad) mini column pre-equilibrated in buffer A, and the flow-through fractions containing the Gst-Apn1 or the Gst-Apn1 mutants were collected and concentrated in a 4.0 mL capacity 10K cut off Ultrafree Biomax concentrator (Millipore Corp.) to 150 µL. The concentrations of the proteins were determined according to the method of Bradford [142].

The open reading frame DNA encoding *Apn1* was cloned into pET11a (Novagen, Madison, WI) and the protein overexpressed in *E. coli* BL21 Star cells (Invitrogen SARL, Gergy Pontoise, France). Purification of the protein was achieved using three chromatographic steps: DEAE-sepharose (Waters), sulfopropyl Sepharose cation exchange (Amersham Biosciences, Little Chalfont, UK) and AcA54 gel filtration (IBF, Villeneuve-la-Garenne, France).

AP endonuclease and 3'-diesterase assays

For the AP endonuclease assay, a 42-mer U21•G oligo (5'-GCTGCATGCCTGCAGGTCGA**U**TCTAGAGGATCCCGGGTACCT-3') containing a single uracil at position 21 was labelled at the 5'-end by T4 polynucleotide kinase (PNK) (Gibco) using [γ-^{32}P]ATP (Pharmacia), and annealed to the complementary 42-mer oligo (3'-CGACGTACGGACGTCCAGCT**G**AGATCTCCTAGGGCC-CATGGA-5') to generate the U•G mismatch [143]. To create the AP site substrate, this labelled double-stranded oligonucleotide was treated with uracil DNA glycosylase (UDG) (New England Biolabs) for 30 min at 37°C. The AP endonuclease assay and product resolution by urea-PAGE were performed as previously described [139]. To generate the 3'-blocked termini, the labelled double-

stranded oligonucleotide was treated with endonuclease III (kindly provided by Dr. Melamede, University of Vermont, Burlington, VT) at 37°C for 1 h to convert all the AP sites into 3'-blocked ends. The 3'-diesterase assay and analysis of the reaction product by urea-PAGE were performed as previously described [139].

DNA glycosylase-independent incision of oxidatively damaged DNA

Oligodeoxyribonucleotides were purchased from Eurogentec (Seraing, Belgium), including modified oligonucleotides containing either 5,6-dihydrouracil (DHU), 5,6-dihydrothymine (DHT), or tetrahydrofuran (THF) residues: 5'-TGACTGCATA**X**GCATGTAGACGATGTGCAT-3' (30-mer), where X is the position of the modified base, DHU or DHT. The complementary oligonucleotides contained either dG or dA opposite the modified base. The resulting duplex oligonucleotides were termed dHU/G and dHT/A, respectively. This sequence context was previously used to study the repair of a thymine fragmentation product [144]. Oligonucleotides were 5′-end labeled by T4 polynucleotide kinase (New England Biolabs, Beverly, MA) in the presence of [γ-^{32}P]ATP (6000 Ci/mmol, ICN Pharmaceuticals, Inc., Costa Mesa, CA) or 3′-end labeled by terminal transferase (New England Biolabs) in the presence of [α-^{32}P]dCTP (3000 Ci/mmol, Amersham Biosciences, Piscataway, NJ) as recommended by the manufacturers. The oligonucleotides were then annealed to the appropriate complements in buffer containing 0.5x SSC [75 mM NaCl and 7.5 mM citric acid trisodium salt (pH 7.0)] at 65°C for 5 min as previously described [145]. For determination of nucleotide incision activity, 0.4 pmol (or 0.2 pmol for THF/G oligonucleotide) of 5'-[^{32}P]- or 3'-[^{32}P]-dCMP-labeled oligonucleotide duplex was incubated with 10 ng (or 5 ng for THF/G oligonucleotide) of the given repair protein(s) for 30 min (or 10 min for THF/G oligonucleotide) at 37°C in reaction buffer (20 μL) containing 50 mM HEPES (pH 7.5), 50 mM KCl, 0.1 mM EDTA, 5 mM β-mercaptoethanol, 0.1 mg/mL BSA. When necessary, a light piperidine treatment was performed by adding 10% piperidine for 15 min at 37°C. Reaction products were analyzed by electrophoresis on denaturing 20% polyacrylamide gels (20:1, 7 M urea, 0.5x TBE), and visualized with a Storm 840 by PhosphorImager (Molecular Dynamics Inc.).

Electrophoretic Mobility Shift Assay

A 5'-^{32}P-end-labeled 42-mer double-stranded oligonucleotide was used as a probe for EMSA. Assays were performed as described previously [139]. In brief, approximately 0.1 ng of the labeled probe (corresponding to 1.5 x 10^4 cpm) was incubated with 15 ng of wild-type and mutant Apn1 proteins in buffer B [10 mM Hepes-NaOH (pH 7.9), 20 mM KCl, 10% glycerol, 0.1 mM EDTA, 0.5 mM DTT, 1 mM PMSF] for 20 min at room temperature. The formation of protein-DNA complexes was resolved by electrophoresis in a 140 cm x 175 cm x 0.75 cm, 6% native polyacrylamide gel (19:1 acrylamide:bisacrylamide ratio) in high-ionic strength Tris-glycine buffer [50 mM Tris-HCl (pH 8.8), 380 mM glycine, 2 mM EDTA] at 100 V for 4 h at 4°C, dried, and revealed by autoradiography [146]. The sequences of the two different probes, 42-mer U•G and 42-mer C•G double-stranded oligonucleotides, were 5'-GCTGCATGCCTGCAGGTCGA**U**TCTAGAGGATCCC-GGGTACCT-3' and the complementary strand 3'-CGACGTACGGACGTCCAGC-T**G**AGATCTCCTAGGGCCCATGGA-5' and 5'-GGTCTAAACGTTTATGCCTTT-GCTCTGGACCATACAATTATC-3' and the complementary strand 3'-CCAGATTTGCAAATACGGAAACGAGACCTGGTATGTTAATAG-5', respectively.

RESULTS

The construct GFP-APN1 expresses a functionally active fusion protein

The full length *APN1* gene was inserted in frame into the pYES-GFP vector to produce the plasmid pGFP-APN1, which expresses the Gfp-Apn1 fusion protein under the galactose inducible *GAL1* promoter (see below and Materials and Methods) [82]. To examine if the plasmid expressed a functionally active Gfp-Apn1 fusion protein, we tested for drug complementation in strain YW781 (*apn1Δapn2Δ*) [85]. This strain lacks both Apn1 and Apn2, and therefore is hypersensitive to various DNA-damaging agents, including MMS and H_2O_2, which that produce AP sites and strand breaks with blocked 3'-termini, respectively [85,89]. Introduction of pGFP-APN1 into strain YW781 conferred full parental resistance to MMS (Figure 2-1, lane 6) and H_2O_2 (data not shown), under noninducing conditions, as determined by gradient plate assays. In this assay, the drug-sensitive strains grow only a short distance into the gradient, whereas the resistant strains grow along the entire length of the gradient [138]. As expected, the pYES-GFP vector provided no drug resistance to strain YW781 (Figure 2-1, lane 5). The data suggest that plasmid pGFP-APN1 produces a biologically active fusion protein in yeast cells. It is noteworthy that the *GAL1* promoter is leaky and produces enough Gfp-Apn1 to restore drug resistance to strain YW781. Overproduction of Gfp-Apn1 by galactose induction conferred no additional drug resistance to strain YW781 (data not shown). Similar findings were previously observed in yeast with untagged Apn1 [40,81].

The Gfp-Apn1(E158G) and Gfp-Apn1(D192G) mutant plasmids confer no drug resistance to the AP endonuclease-deficient strain YW781

We determined if glycine substitution of amino acid residues E158 and D192 interferes with the biological function of Apn1. The two substitutions, E158G and D192G, were created by altering the DNA sequence in plasmid pGFP-APN1 by site-directed mutagenesis to produce the plasmids pGFP-APN1(E158G) and pGFP-APN1(D192G), respectively. Introduction of either mutant plasmid into strain

Figure 2-1. Drug resistance determination in *S. cerevisiae* strains YW465 (parent) and YW781 (*apn1Δapn2Δ*) harboring plasmids carrying either the native or mutant alleles of the *APN1* gene fused to GFP.

The results were obtained from gradient plate assays where the bottom layer contained 0.015 mmol of methyl methane sulfonate (MMS). Growth along the gradient is considered to be 100%. The picture was taken after incubation for 1 day at 30°C.

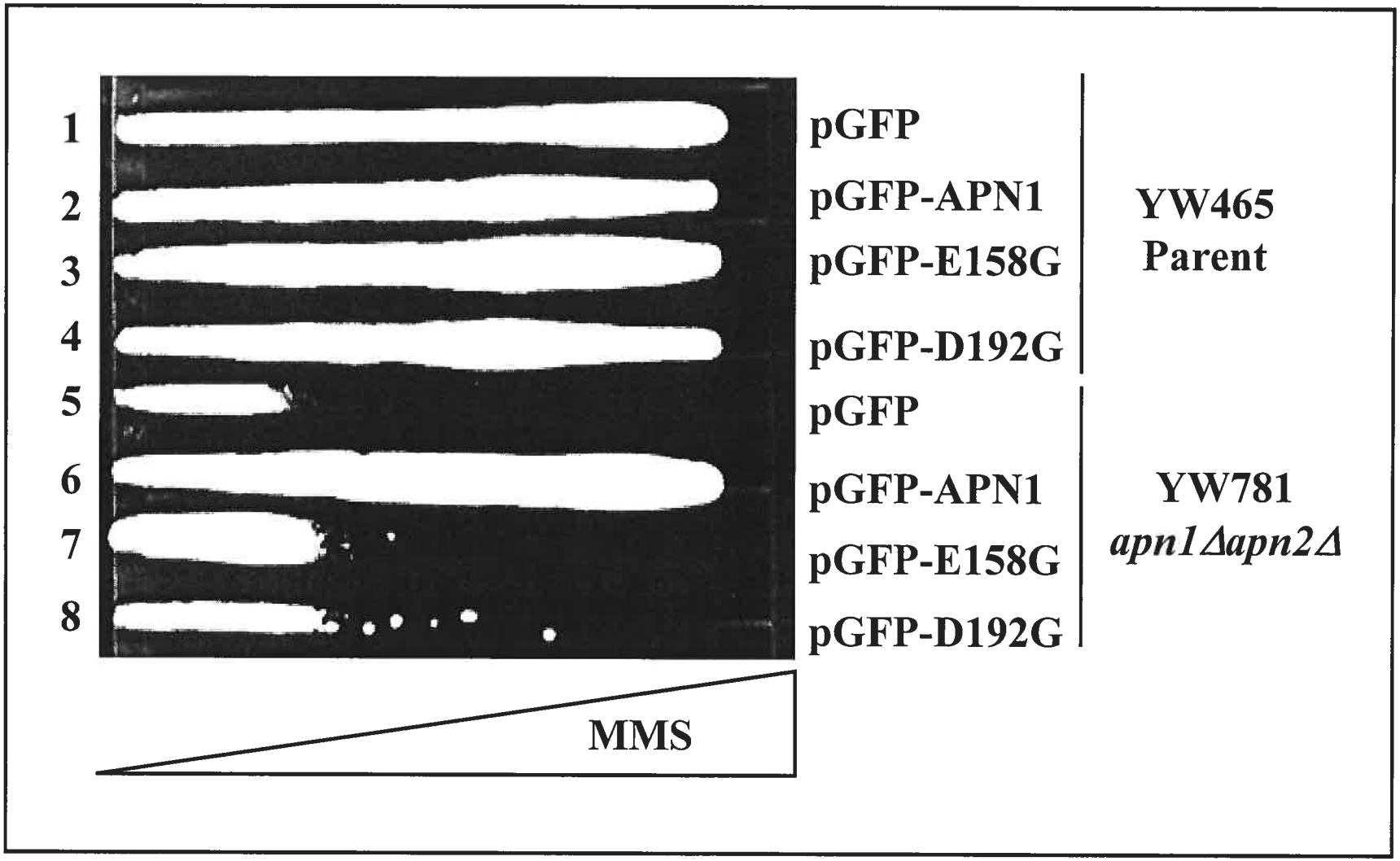

FIGURE 2-1. Jilani *et al.*, 2003

YW781 failed to confer resistance to MMS or H_2O_2, as compared to the pGFP-APN1 plasmid (Figure 2-1, lanes 7 and 8 vs lane 6, and data not shown). Similar results were obtained if the drug gradient plate assays were done under conditions of galactose induction (data not shown). The data suggest that the plasmids pGFP-APN1(E158G) and pGFP-APN1(D192G) are likely expressing inactive mutant proteins.

The Apn1 mutant plasmids express normal levels of the mutant proteins and are localized to the nucleus

To exclude the possibility that lack of complementation by these mutant plasmids might merely reflect a reduction in the level of protein expression, we examined levels of native and mutant proteins in total cell extracts (Figure 2-2). Extracts derived from either the parent, or strain YW781 harboring the plasmid pGFP-APN1, expressed the expected 66 kDa full-length fusion protein following galactose induction (0.5% for 4 h) (Figure 2-2, lanes 1 and 6, respectively). In the absence of galactose induction, the Gfp-Apn1 fusion protein could not be detected with anti-Gfp antibodies (lanes 4 and 5), although under these conditions enough Gfp-Apn1 is expressed to fully restore drug resistance to strain YW781 (Figure 2-1). Total extracts prepared from either the parent or strain YW781 harboring either of the two mutant plasmids also exhibited normal expression levels of the 66 kDa fusion protein (Figure 2-2, lanes 2, 3, 7, and 8, respectively). There was no significant degradation of either mutant fusion protein, suggesting that these do not exhibit any major structural deformation to trigger proteolysis, and thus are as stable as the native fusion protein. Another possibility that could explain the inability of the Apn1 mutants to complement the drug hypersensitive phenotypes of strain YW781 might involve prevention of protein translocation into the nucleus. We therefore examined the cellular location of the native and the mutant proteins by fluorescent microscopy (see Materials and Methods). The native Gfp-Apn1 and the Apn1 mutants were mainly localized to the nucleus in both strains following induction with

Figure 2-2. Comparison of the expression levels of native Apn1 and its mutant forms fused to Gfp.

Total protein extracts were derived from the indicated plasmid-bearing yeast strains YW465 and YW781 following induction for 4 h with (+, lanes 1-3 and 6-8) or without (-, lanes 4 and 5) 0.5 % galactose. Each lane contains 100 μg of total extract, and the Western blot was probed with a monoclonal anti-Gfp antibody. The arrow indicates the position of the native and mutant forms of Gfp-Apn1 (66 kDa). Molecular mass standards are shown at the left.

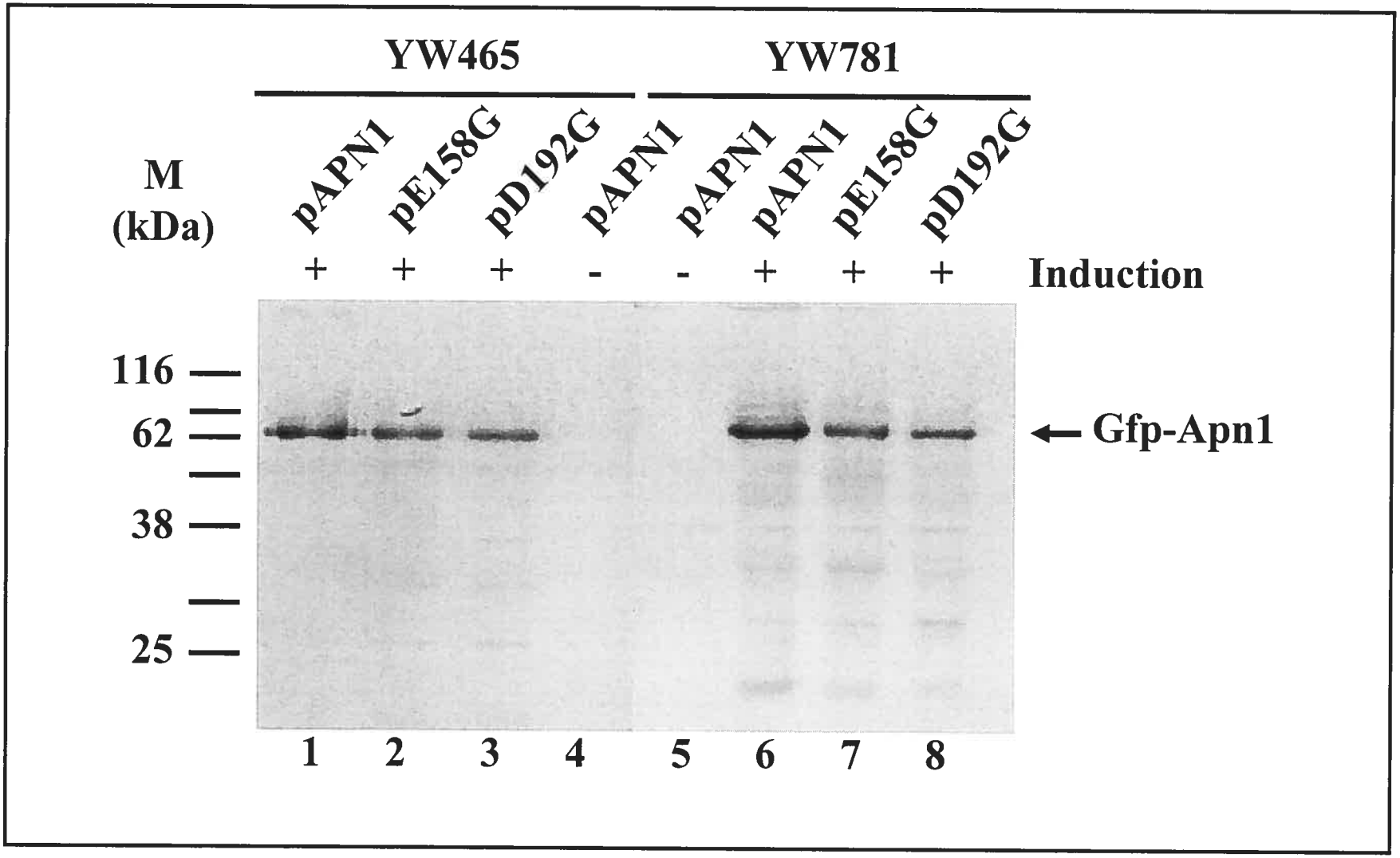

FIGURE 2-2. Jilani *et al.*, 2003

galactose (Figure 2-3). We conclude that the two plasmids pGFP-APN1(E158G) and pGFP-APN1(D192G) are indeed expressing the mutant protein, and that the mutant proteins do not harbor a defect in entering the nucleus, supporting the notion that these mutant proteins lack the ability to repair damaged DNA.

Expression and complementation analyses of Gst-Apn1 and the Gst-Apn1 mutant forms in the DNA repair deficient E. coli strain BW528

To determine if the Apn1(E158G) and Apn1(D192G) mutants have a defect in repairing damaged DNA, we designed an *E. coli* expression system to facilitate the purification of these proteins. The genes encoding the native *APN1* and the two mutant alleles, *APN1(E158G)* and *APN1(D192G)* were inserted in frame with the glutathione-*S*-transferase gene *Gst* in the vector pGEX-4T-1 to create a set of three plasmids [pGST-APN1, pGST-APN1(E158G), and pGST-APN1(D192G)], which were designed to produce Gst-Apn1, Gst-Apn1(E158G), and Gst-Apn1(D192G) fusion proteins, respectively, under the control of the IPTG-inducible *lac* promoter. The plasmids were introduced into the *E. coli* strain BW528, which in a manner analogous to that of its yeast counterpart strain YW781 is deficient in AP endonuclease activity, *i.e.,* is lacking both endonuclease IV and exonuclease III genes. This *E. coli* strain is also hypersensitive to various DNA-damaging agents because of an inability to repair damaged chromosomal DNA [136]. Total extracts derived from the exponentially growing *E. coli* strain BW528 carrying either plasmid pGST-APN1, pGST-APN1(E158G), or pGST-APN1(D192G), and induced by IPTG, expressed the expected 66 kDa fusion protein as observed by Coomassie staining (Figure 2-4A). The expression levels were similar for all three proteins and no major degradation was observed (Figure 2-4A).

We previously showed that expression of Apn1 complemented the drug hypersensitivities of strain BW528 [136]. We therefore tested if the fusion form of Apn1, Gst-Apn1, was also capable of complementing the drug hypersensitivites of strain BW528 [136]. Introduction of the plasmid pGST-APN1

Figure 2-3. Nuclear localization of Gfp-Apn1 and its mutant forms. Fluorescent analysis were performed with strains YW465 (parent) and YW781 (*apn1Δapn2Δ*) (YW778) bearing either the pGFP-APN1, or pGFP-APN1(E158G), or pGFP-APN1(D192G) plasmid. Cells were grown in selective medium with 2% raffinose and induced with 0.5% galactose for 4 h before being photographed at a magnification of 100 times with a Cool Snap camera attached to the Leitz immunofluorescent microscope.

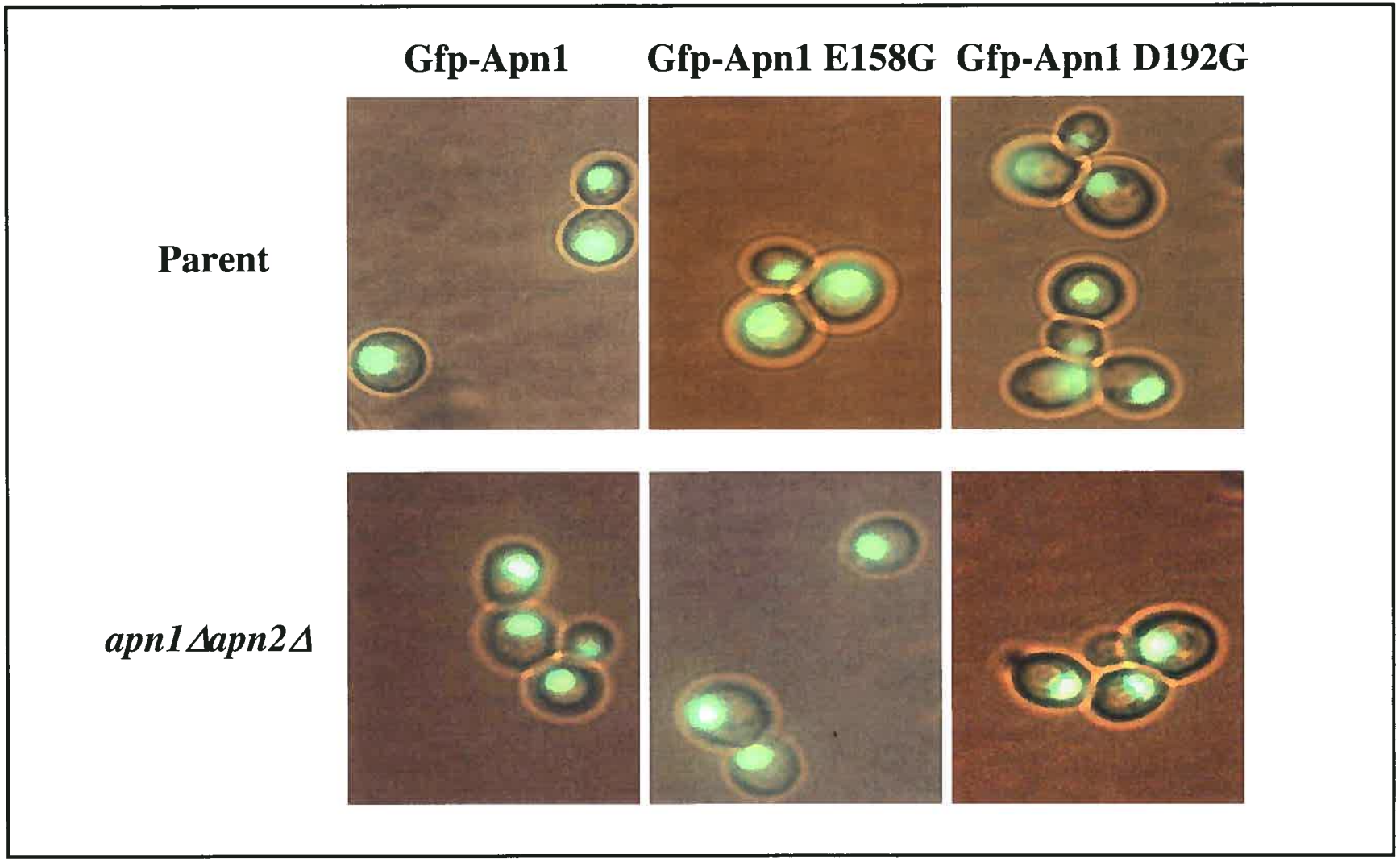

FIGURE 2-3. Jilani *et al.*, 2003

Figure 2-4. Expression and purification of native and mutant forms, E158G and D192G, of Apn1 using *E. coli*.

(A) Coomassie blue-stained SDS-PAGE gel of total extracts derived from strain BW528, and carrying either the pGST vector or the pGST-APN1 plasmid or the mutant forms: lane 1, molecular mass standards; and lanes 2-5, pGST, pGST-APN1(pAPN1), pGST-APN1(pE158G), and pGST-APN1(pD192G), respectively. Each lane (lanes 2-5) contained 60 μg of total protein extract. The plus and minus signs indicate whether the lane did or did not experience 1 mM IPTG induction. (B) Glutathione-*S*-transferase affinity column purification of Gst-Apn1 and its mutant forms. Total extracts derived from strain BW528 carrying either the pGST, pGST-APN1(pAPN1), pGST-APN1(E158G), or pGST-APN1(D192G) plasmid were purified on a Gst affinity column and analyzed on an SDS-PAGE gel stained with Coomassie blue. Each lane (lanes 2-5) contained 200 ng of the affinity-purified proteins. (C) Gst affinity-purified Apn1 and the variants were subjected to ion-exchange chromatography on monoS and analyzed on Coomassie-stained gel. Each lane (lanes 1-3) contained 200 ng of purified protein. For each panel, the arrow indicates the position of native and mutant forms of the fusion protein, Gst-Apn1.

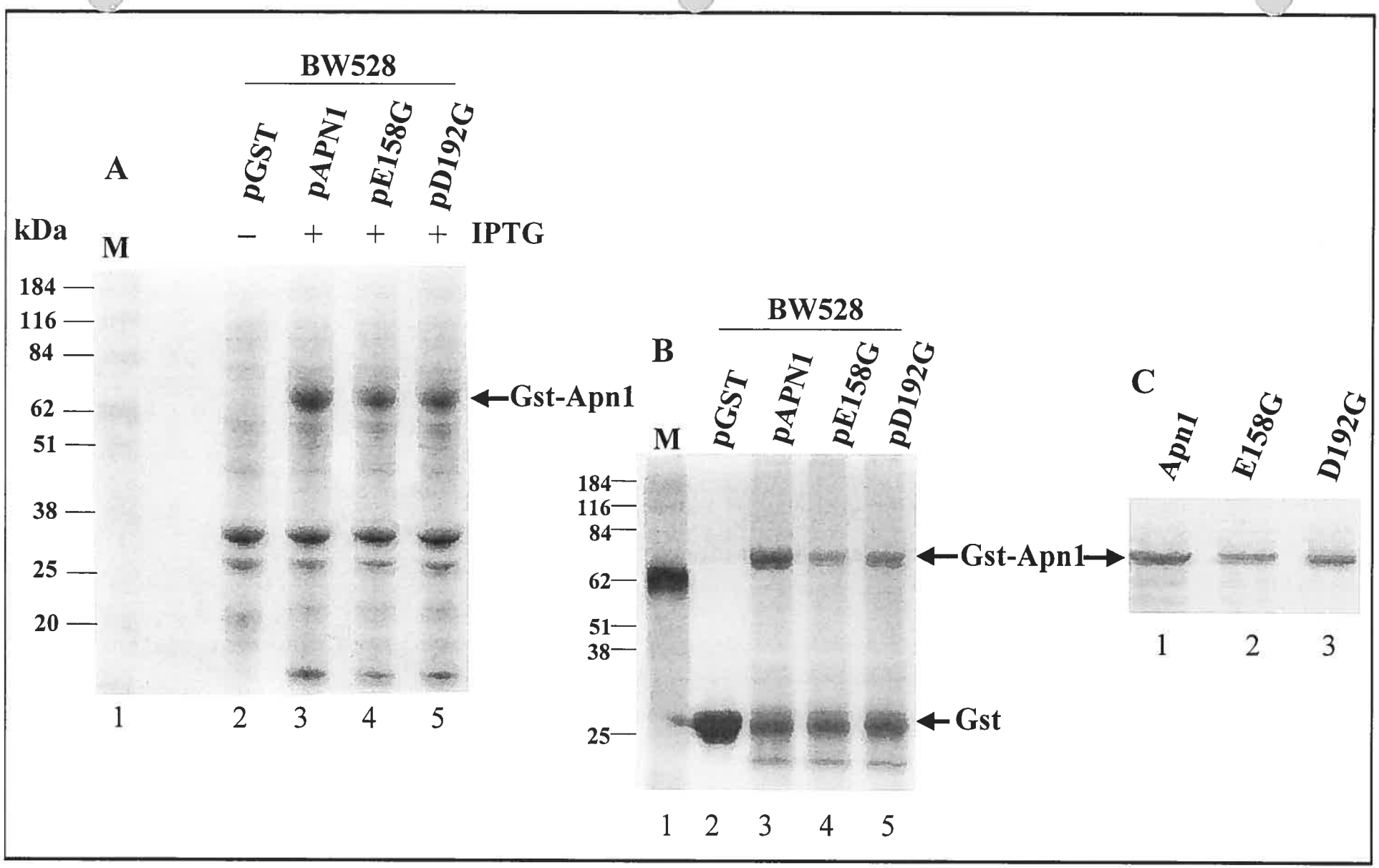

FIGURE 2-4. Jilani *et al.*, 2003

into strain BW528, but not the empty pGST vector (pGEX-4T-1), restored parental resistance to both MMS and H_2O_2 (Figure 2-5A,B, lane 3 vs lane 5), suggesting that the Gst-Apn1 fusion protein is functionally active in bacteria, as is the Gfp-Apn1 fusion protein in yeast. It should be noted that the *lac* promoter appears to be leaky since the drug complementation assay was performed in the absence of IPTG (Figure 2-5). However, in the presence of IPTG, Gst-Apn1 conferred no additional drug resistance to strain BW528 (data not shown). This is not surprising, as we have documented similar findings with the overexpression of Apn1 in strain BW528 [136]. Introduction of the mutant plasmids, either pGST-APN1(E158G) or pGST-APN1(D192G), into BW528 conferred no resistance to MMS or H_2O_2 (Figure 2-5A and B, lanes 1 and 2), clearly indicating that the mutant proteins expressed by these plasmids are unable to act on the damaged DNA.

Apn1 mutants lack DNA repair activities

We next examined the ability of the purified Gst-Apn1 and the mutant forms to process DNA lesions *in vitro*. Briefly, the Gst fusion proteins were affinity-purified on a glutathione column followed by ion-exchange chromatography on monoS (panels B and C of Figure 2-4, respectively). This second purification step was necessary to remove trace contamination of AP lyase activity, which bound to the Gst affinity column independent of Apn1. The purified Gst fusion proteins were assessed for all three enzymatic activities, i.e., AP endonuclease, 3'-diesterase, and the activity that incises oxidized base lesions. To monitor AP endonuclease activity, we used a labeled 42-mer double stranded oligonucleotide bearing a single AP site at position 21. Cleavage of the AP site substrate by AP endonucleases produces a labeled 20-mer product which can be readily detected on 10% polyacrylamide gels [147]. As shown in Figure 2-6A, the native Gst-Apn1, as well as purified endo IV, actively cleaved the substrate to produce the 20-mer product (lanes 1, 2, and 7). Interestingly, following the formation of the 20-mer product, purified Gst-Apn1 was able to remove additional nucleotides in a 3' to 5'-direction to create a smaller product (lane 1 or 2), but not the mutants even at higher protein concentration (>50 ng, data not shown).

Figure 2-5. Drug complementation analysis of strain BW528 carrying plasmids expressing the native and mutant forms of Apn1 fused to Gst. AB1157(endoIV$^+$exoIII$^+$) is the parent of BW528(endoIV$^-$exoIII$^-$). The complementation assays were performed on drug gradient plates with the bacterial strains bearing plasmids with the indicated Gst-APN1 fusion genes. The bottom layer of the gradient plate contained either 0.025 mmol of MMS (A) or 1.17 mM of H_2O_2 (B). Growth along the gradient is considered to be 100%. Pictures were taken after incubation for 24 h at 37°C.

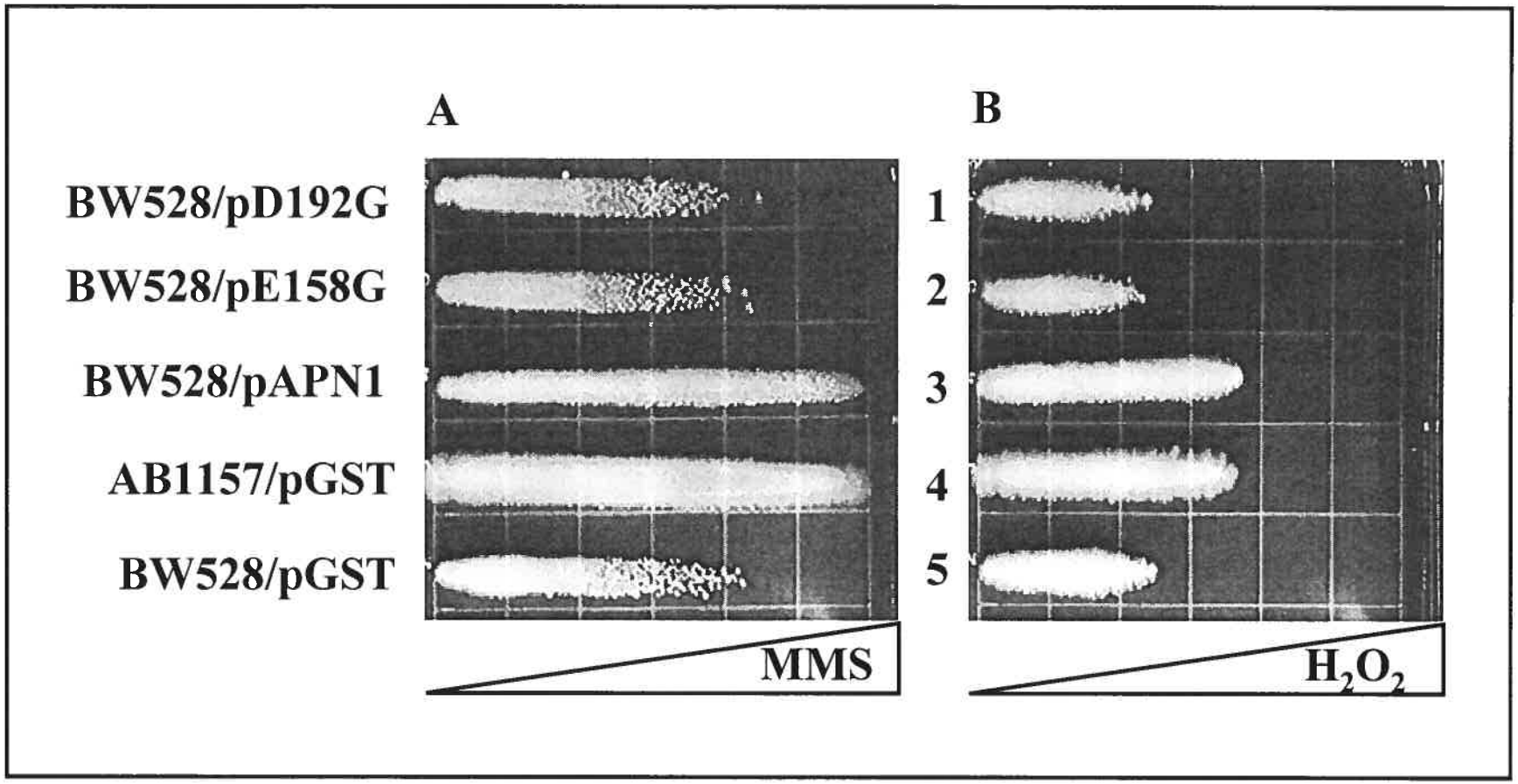

FIGURE 2-5. Jilani *et al.*, 2003

Figure 2-6. Comparison of the DNA repair activities of Apn1 and the mutant forms, E158G and D192G.

(A) Analysis of the AP endonuclease activity. The 5'-^{32}P-labeled 42-mer double-stranded oligonucleotide U•G substrate (40 nM) containing a single AP site at position 21 was treated with uracil DNA glycosylase to create an AP site, and then the AP endonuclease assay was carried out in a reaction volume of 10 μL at 37°C for 20 min with the following concentration of purified proteins: lanes 1 and 2, 3 and 6 ng of Gst-Apn1, respectively; lanes 3 and 4, 10 and 20 ng of Gst-Apn1(E158G), respectively; and lanes 5 and 6, 10 and 20 ng of Gst-Apn1(D192G), respectively. Purified endo IV (9 ng) was used as a positive control. Formation of the 20-mer AP endonuclease incision product was monitored by autoradiography following resolution on a 10% polyacrylamide (19:1 acrylamide:bisacrylamide ratio)-7 M urea sequencing gel. Arrows indicate positions of the 42-mer substrate and the 20-mer product. (B) Analysis of the 3'-diesterase activity. The labeled 42-mer double-stranded oligonucleotide AP site substrate was pretreated with excess purified endonuclease III to create the 20-mer product bearing the 3'-α, β-unsaturated aldehyde. Processing of this blocked end with 3'-diesterase activity creates a faster migrating 3'-hydroxyl group. The 3'-diesterase activity was performed in a reaction volume of 10 μL reaction at 37°C for 20 min with the same protein concentrations given for panel A. Purified endo IV (4 ng) was used as a control to cleave the AP site substrate and to reveal the position of the 3'-hydroxyl group. Arrows on the right indicate positions of the 3'-α, β-unsaturated aldehyde and 3'-hydroxyl group. (C) Analysis of the incision activity on substrates containing oxidized bases. The 5'-^{32}P-labeled duplex oligonucleotide substrates containing dHU/G (20 nM, lanes 1-5), dHT/A (20 mM, lanes 6-10), or THF/G (10 nM, lanes 11-15) were incubated with Apn1 (lanes 2, 7, and 12), Gst-Apn1 (lanes 3, 8, and 13), E158G (lanes 4, 9, and 14), and D192G (lanes 5, 10, and 15) under the same reaction conditions given for panel A. Control lanes 1 and 6 contained substrates that were treated with light piperidine. Arrows indicate the positions of the 30-mer substrates and the 10-mer product. The data is representative of two independent analyses.

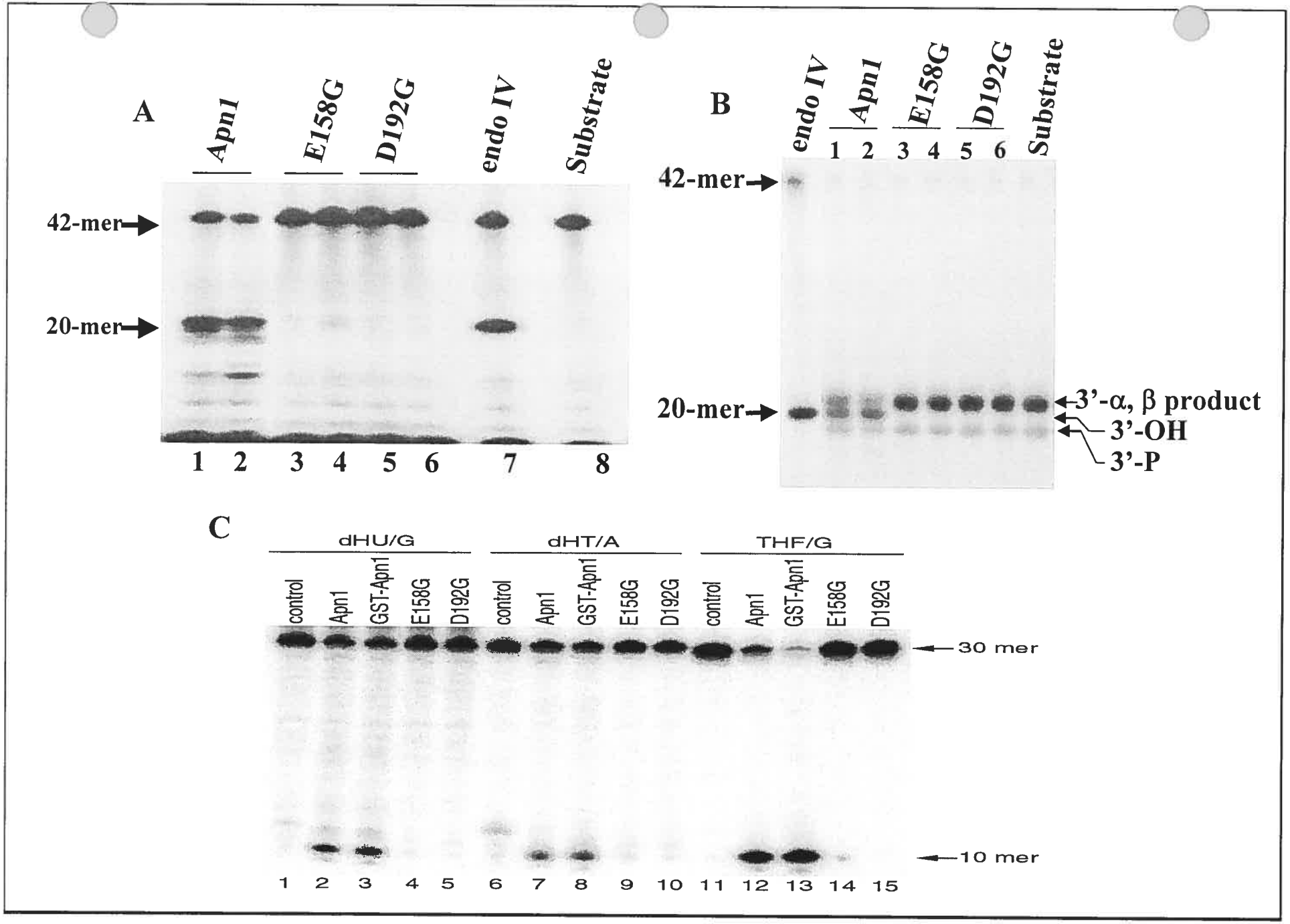

FIGURE 2-6. Jilani *et al.*, 2006

We further note that the 3'- to 5'-exonuclease activity is unlikely to be the result of a bacterial contaminant that is copurified with Gst-Apn1, as this activity was not detected with the mutant when incubated with the endo IV pre-incised AP site (data not shown). These data suggest that Apn1 may possess a 3'- to 5'-exonuclease activity (see the Discussion).

Analysis of the Gst-Apn1(E158G) mutant revealed that it was highly inefficient at cleaving the AP site substrate (Figure 2-6A, lane 4 vs lane 2). In separate experiments, we estimated that the Gst-Apn1(E158G) mutant exhibited a nearly 150-fold reduction in AP endonuclease activity, compared to that of the native Gst-Apn1 (data not shown). In contrast, the Gst-Apn1(D192G) mutant exhibited no detectable cleavage activity even at protein concentrations in excess of 200-fold (Figure 2-6A, lane 6 vs lane 2, and data not shown). These findings clearly indicate that the glycine amino acid substitution at either position 158 or 192 dramatically reduces or completely abolishes the AP endonuclease activity of Apn1, respectively, such that the resulting mutant proteins cannot repair MMS-induced AP sites in the DNA repair deficient strains.

We next monitored the 3'-diesterase activity of these proteins by following the removal of a 3'-blocking DNA lesion, 3'-α,β-unsaturated aldehyde. To create this lesion, the 42-mer oligonucleotide substrate containing the AP site was pretreated with the AP lyase endonuclease III, which cleaves the AP site by a β-elimination reaction 3' to the AP site, to generate the 20-mer product containing, at the 3'-end, *trans*-4-hydroxy-2-pentenal-5-phosphate (3'-α,β-unsaturated aldehyde) (Figure 2-6B). This endonuclease III preparation is contaminated with Fpg, an enzyme that can cleave AP sites to generate a 3'–phosphate (Figure 2-6B). Thus, the *trans*-4-hydroxy-2-pentenal-5-phosphate (3'-α,β unsaturated aldehyde) product also contained a minor amount of 3'–phosphate (Figure 2-6B). Both the 3'-α,β unsaturated aldehyde and the 3'–phosphate can be removed by a 3'-diesterase activity to create the intermediate migrating 20-mer containing a 3'-hydroxyl group (Figure 2-6B). As shown in Figure 2-6B, the native Gst-Apn1 actively processed the 3'-α,β-unsaturated aldehyde and the 3'–phosphate to generate the 20-mer product bearing the 3'-hydroxyl group, which migrated to the same position as the product produced by direct AP endonuclease

action, such as endonuclease IV on the 42-mer AP site substrate. In contrast, neither of the Gst-Apn1 mutants was capable of removing the 3'-blocking groups (Figure 2-6B, lane 3 or 4, and lane 5 or 6). Thus, substitution of the amino acid residues E158 and D192 of Apn1 with glycine abolishes the 3'-diesterase activity of this enzyme.

In addition to AP endonuclease and 3'-diesterase activities, Apn1 also possesses the ability to incise DNA at the site of oxidatively damaged bases, e.g., 5,6-dihydropyrimidines, that are the major products generated by γ-irradiation under anoxic conditions [84]. We therefore determined if this novel enzymatic activity of Apn1 was also altered by glycine substitutions at either E158 or D192. We used two independent substrates bearing either dihydrouracil paired with G (dHU/G) or dihydrothymidine paired with A (dHT/A). A third substrate bearing a modified AP site tetrahydrofuran (THF/G) was used as a control for AP endonuclease activity. Cleavage of these substrates can be monitored by the appearance of a 10-mer product on 20% denaturing polyacrylamide gels. Figure 2-6C revealed that the Gst-Apn1 mutants were unable to cleave the 5'-^{32}P-labeled dHU/G (lanes 4 and 5), dHT/A (lanes 9 and 10), and TFH/G substrates (lanes 14 and 15). In control experiments, cleavage of the DNA substrates with the purified Gst-Apn1 was as proficient as the untagged native Apn1 (Figure 2-6C lane 3 vs lane 2, lane 8 vs lane 7, and lane 13 vs lane 12). It is noteworthy that the 5,6-dihydropyrimidines, having lost their aromatic structure, are more susceptible to base loss. As shown in Figure 2-6C when the dHU/G- and dHT/A-containing oligonucleotides in the absence of enzyme are treated with piperidine, they are only minimally incised (<3%), suggesting that the AP site yield is negligible. Similar results were obtained when using 3'-[^{32}P]-dCMP labeled dHU/G, dHT/A, and TFH/G substrates (data not shown). On the basis of the findings described above, we conclude that glycine substitution at either E158 or D192 of Apn1 produces variant proteins with severe defects in their ability to process DNA lesions.

Gst-Apn1 mutants bind to double stranded oligonucleotide

We next examined if the DNA repair defects of the Apn1 mutants could be a consequence of an inability to bind DNA. We thus monitored the binding of the

purified proteins to two different double-stranded 42-mer oligonucleotides using an electrophoretic mobility shift assay (EMSA). One of the 42-mer double-stranded oligonucleotides contained a natural DNA sequence, and the other carried a central U•G mispair. Like the native Gst-Apn1, the two mutants retained the ability to bind the natural 42-mer oligonucleotide (Figure 2-7A, lanes 2 and 3 vs lane 1), as well as the 42-mer oligonucleotide carrying the U•G mispair (Figure 2-7A, lanes 7 and 8 vs lane 6). In addition, binding of the native Gst-Apn1 and the two mutants to the labeled 42-mer oligonucleotide was dependent on protein concentration (Figure 2-7B). Moreover, no difference in elution profile was observed between the native Gst-Apn1 and the mutants upon chromatography on double-stranded DNA agarose column (data not shown). These data suggest that neither of the two single-amino acid changes alters the ability of the protein to bind DNA. It is noteworthy that under identical conditions of the assay, when the native Gst-Apn1 bound to the U•G mispair 42-mer DNA, but not the native 42-mer DNA, it consistently showed a slower migration complex (Figure 2-7, lane 6 vs lane 1). However, this slower migration pattern was not observed with either of the two mutants (Figure 2-7, lanes 7 and 8). This phenomenon could be related to the mechanism by which members of the Endo IV family are proposed to recognize and bend the DNA at the site of the lesion (see the Discussion).

Figure 2-7. Mobility-shift analysis of a natural and a mismatch-containing 42-mer-labelled double stranded oligonucleotide by purified Gst-Apn1, Gst-Apn1(E158G), Gst-Apn1(D192G), and Gst.

(A) Binding of a fixed amount of purified proteins to the 42-mer labeled oligonucleotides. The purified proteins (5 ng) were incubated with 0.1 ng of 5'-^{32}P-labeled 42-mer double-stranded oligonucleotide (1.5 x 10^4 cpm), either the normal (C•G, lanes 1-4) or the mismatched (U•G, lanes 5-8), in 10 μL buffer B for 20 min at room temperature (see Materials and Methods). The protein-DNA complexes were resolved on a 6% native polyacrylamide (19:1 acrylamide:bisacrylamide ratio) gel by electrophoresis in a high-ionic strength Tris-glycine buffer, and the protein-DNA complexes were revealed by autoradiography. (B) Binding of increasing amounts of purified proteins to the 42-mer labeled (U•G) oligonucleotide: lane 1, free probe, and no protein; lanes 2-4, 10, 20, and 40 ng of purified Gst, respectively; lanes 5-7, 10, 20, and 40 ng of purified Gst-Apn1, respectively; lanes 8-10, 10, 20, and 30 ng of purified Gst-Apn1(E158G), respectively; and lanes 11-13, 5, 10, and 40 ng of purified Gst-Apn1(D192G), respectively.

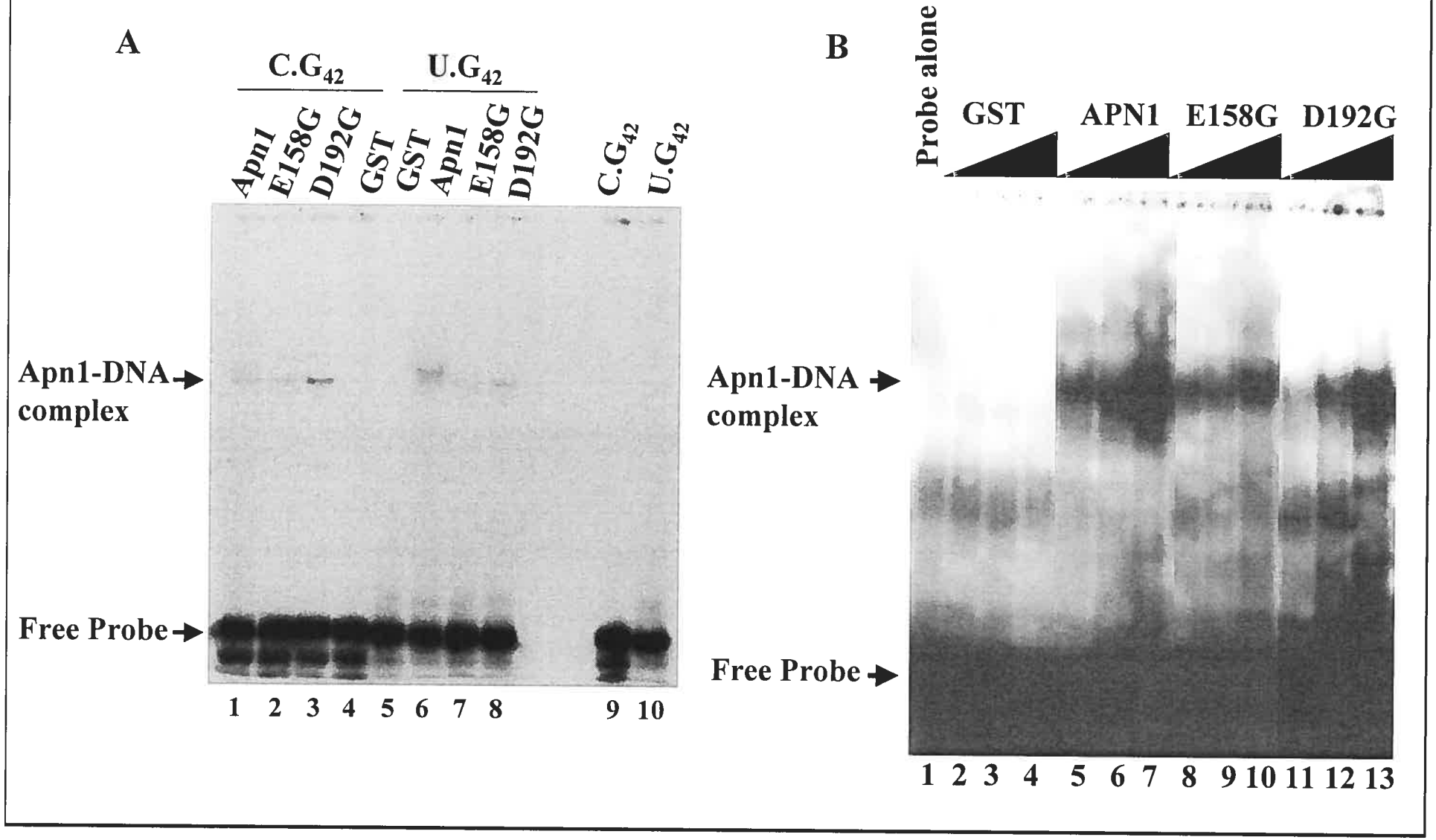

FIGURE 2-7. Jilani *et al.*, 2003

DISCUSSION

In this study, we created two variants of the DNA repair enzyme Apn1 from the yeast *S. cerevisiae* by replacing either the glutamate or aspartate amino acid residue at positions 158 and 192, respectively, with glycine. We show that the resulting mutants E158G and D192G have no apparent defects in protein stability or in the ability to enter the nucleus or to interact with DNA. However, these variant proteins were unable to restore resistance to MMS and H_2O_2 to a DNA repair deficient yeast strain, strongly suggesting that E158 or D192 is required for Apn1 to repair damaged DNA *in vivo*. In strong support of this, the purified mutant proteins were found to be either severely or completely deficient in Apn1-associated DNA repair activities including AP endonuclease and 3'-diesterase, as well as the incision of oxidized bases [78,84,136]. The fact that a single-amino acid change sharply diminishes all the DNA processing activities of Apn1 strongly suggests that the different enzymatic activities of this protein are governed by the same active site. It is therefore possible that the amino acid residues E158 and D192 play crucial role(s) in the enzyme catalytic center. In addition, it would appear that the function of D192 is more critical than that of E158, as the D192G substitution showed no residual enzymatic activities as compared to E158G which showed ~150-fold reduction.

Recently, the high-resolution atomic structure of *E. coli* endo IV was determined when the enzyme is bound to a 15-mer duplex DNA containing a synthetic AP site [67]. The crystal structure provided clear insight into the enzyme catalytic mechanism and revealed that endo IV consists of eight parallel β-strands each surrounded by peripheral α-helices in forming an $\alpha_8\beta_8$ TIM barrel fold, which is suitably arranged to bind DNA [67]. At AP sites, the enzyme acts by compressing and bending the DNA ~90^o such that it causes the orphan nucleotide and the AP site to flip out of the duplex [67]. The AP site is then sequestered within an enzyme active site pocket, where the 5'-phosphate bond is cleaved by a trinuclear zinc cluster that renders the phosphorus atom susceptible to a nucleophilic attack [67]. The endo IV enzyme pocket has the ability to discriminate between undamaged and damaged nucleotides [67]. The undamaged nucleotides exist in a β-configuration and are sterically excluded from the enzyme active site pocket [67]. However, damaged

nucleotides with an α-configuration, such as dihydropyrimidines, 5-hydroxypyrimidines, and formamidopyrimidines can be accommodated by the enzyme active site pocket, providing a reasonable explanation why members of the endo IV family can directly incise DNA containing oxidatively damaged bases [84,148]. In addition, the endo IV enzyme pocket is structured to accommodate strand breaks terminated with 3'-blocking groups such as 3'-phosphate and α, β-unsaturated aldehyde [67]. Thus, the structural and functional conservation that exist between endo IV and Apn1 strongly suggest that Apn1 is likely to use a similar enzyme active site pocket to process DNA lesions. However, this might not be the case, as our structure-function analyses revealed some key differences between endo IV and Apn1. Previously, we have established that a mutant form of endo IV, E145G, was unable to bind to DNA [139]. Consistent with our findings, the high-resolution structure of endo IV revealed that E145 indeed lies within one of the five DNA recognition loops, which the enzyme uses to make contact with double-stranded DNA [67]. Surprisingly, a glycine substitution of the identical amino acid residue E158 in Apn1 did not prevent this mutant from binding to double-stranded DNA, suggesting that E158 may play a single role perhaps making contact only with the metal ions required for catalysis, while the endo IV E145 residue plays a dual role in DNA binding and coordinating the trinuclear Zn cluster [67,139].

Another key difference between Apn1 and endo IV lies within one of the most conserved stretch of amino acid residues (^{175}GVCI**D**TCH^{182}) shared by the Endo IV family. In this region, replacement of the aspartate with glycine (D179G) reduces endo IV enzymatic activities by nearly 40-fold [139]. According to the endo IV crystal structure, Asp179 residue plays a role by stabilizing the positions of two of the three Zn (Zn2 and Zn3) atoms within the trinuclear Zn cluster required for the enzyme catalytic reaction [67]. In the case of Apn1, we found that the corresponding Asp192 residue showed no residual enzymatic activities. It is unlikely that differences in the Zn atom content can account for the disparity in the enzyme level of the endo IV and Apn1 mutants, as atomic absorption spectrometry revealed that Apn1 also contains at least three Zn atoms [149]. A reasonable explanation would be provided if one of the Zn atoms of Apn1 is only weakly held in the active site pocket by Asp192,

as compared to endo IV where the Zn atoms are held in place by the side chains of multiple amino acid residues. In fact, Apn1 treated with the metal chelator, 1,10-phenanthroline can be reactivated by addition of $ZnCl_2$, but not endo IV treated in a similar manner [149]. If indeed Asp192 forms a metal ligand, it is likely that the D192G mutant could have a lower Zn content, although addition of $ZnCl_2$ did not reactivate either the E158G or the D192G Apn1 mutant (data not shown). We anticipate that crystallographic studies of this D192G mutant of Apn1 in the presence of duplex DNA bearing an AP site should clearly define the role of this important amino acid residue.

We believe that the native Gst-Apn1 purified from *E. coli* may possess an intrinsic 3'- to 5'-exonuclease activity, which removes additional nucleotides following cleavage of the AP site. In fact, a recent study also documented that Gst-Apn1 purified from yeast can remove additional nucleotide(s) in the 3'- to 5' direction at a nick in double-stranded DNA to create a gap, although removal of the first nucleotide appears to be more rapid [85]. If indeed the 3'- to 5'-exonuclease activity is an inherent property of Apn1, as recently demonstrated for endo IV [150], then this activity could be regulated perhaps through protein-protein interaction as observed for Apn2 [93], and play an important function in maintaining the fidelity of DNA polymerase by removing incorrectly incorporated bases.

ACKNOWLEDGMENT

We are indebted to Dr. Elliot Drobetsky, Dr. Thomas Wilson, and Andrea Shatilla for critically reading the manuscript.

CHAPTER 3

Saccharomyces cerevisiae Ogg1 prevents poly(GT) tract instability in the mitochondrial genome

Published in *DNA Repair* **2006**, Vol. 5, No. 2, pp. 235-242.

Saccharomyces cerevisiae Ogg1 prevents poly(GT) tract instability in the mitochondrial genome

RATSAVARINH VONGSAMPHANH[1], J. RICHARD WAGNER[2], AND DINDIAL RAMOTAR[1ψ]

Running title: Ogg1 in the maintenance of poly(GT) tract stability

[ψ]Corresponding author:

[1]University of Montreal, Maisonneuve-Rosemont Hospital, Guy-Bernier Research Centre, 5415 de l'Assomption, Montreal, Quebec, Canada H1T 2M4. Telephone: (514) 252-3400 ext 4684. Fax: (514) 252-3430.

E-mail: [redacted]

[2]Département de Médecine Nucléaire et Radiobiologie, Faculté de Médecine, Université de Sherbrooke, Sherbrooke, Québec, Canada J1H 5N4.

ABSTRACT

Reactive oxygen species can attack the mitochondrial genome to produce a vast array of oxidative DNA lesions including 8-oxo-7,8-dihydro-2'-deoxyguanosine (8-oxo-dGuo). We assess the role of the *Saccharomyces cerevisiae* 8-oxo-dGuo DNA glycosylase, Ogg1, in the maintenance of a poly(GT) tract reporter system present in the mitochondrial genome. Deletion in the poly(GT) tract causes the reporter system to produce arginine-independent (Arg^+) colonies. We show that the mitochondrial form of Ogg1 is functionally active at processing 8-oxo-dGuo lesions and that Ogg1-deficient cells exhibit nearly 5-fold elevated rate of Arg^+ mutants under normal growth condition, as compared to the parent. Overexpression of Ogg1 completely suppressed the high rate of Arg^+ mutations to levels lower than the parental, suggesting that Ogg1 function could be limited in the mitochondria. Further analysis revealed that the Arg^+ mutations can be prevented if the cells are grown under anaerobic conditions. These findings provide *in vivo* evidence that oxidative stress induces the formation of lesions, most likely 8-oxo-dGuo, which must be repaired by Ogg1, otherwise the lesions can trigger poly(GT) tract instability in the mitochondrial genome. We also demonstrate that overproduction of the major apurinic/apyrimidinic (AP) endonuclease Apn1, a nuclear and mitochondrial enzyme with multiple DNA repair activities, substantially elevated the rate of Arg^+ mutants, but which was counteracted by Ogg1 overexpression. We suggest that Ogg1 might bind to AP sites and protect this lesion from the spurious action of Apn1 overproduction. Thus, cleavage of AP site located within or in the vicinity of the poly(GT) tract could destabilize this repeat.

Keywords: DNA repair enzymes, repeat sequences, yeast, mitochondria, genetic instability

INTRODUCTION

Haploid cells of the budding yeast *Saccharomyces cerevisiae* consist of nearly 50 copies of the mitochondrial genome (mtDNA), which is ~75-85 kb in size and 82% rich in AT sequences, and mainly encodes subunits of the electron transport system, as well as RNAs for assembling the mitochondrial translational machinery [151,152]. The mtDNA is constantly exposed to endogenous reactive oxygen species (ROS) produced, for example, during the four-electron reduction of oxygen to water in the oxidative phosphorylation process. It is estimated that each mitochondrion produce 10 x 10^6 ROS molecules per cell per day [153,154]. These ROS can damage the mtDNA to generate a repertoire of 70 known modifications, including isomers, of which 8-oxo-dGuo is a major lesion that can lead to G to T transversion mutations [155]. In fact, the mtDNA accumulate mutations one order of magnitude greater than that of the nuclear DNA, consistent with the vulnerability of the mitochondria to ROS-induced DNA damage [156,157]. In mammalian cells, the mtDNA is continuously replicated even in terminally differentiated cells such as nerve cells [158]. Thus, somatic mtDNA mutations are likely to cause severe effects on cellular function, as well as being involved in the pathogenesis of a variety of diseases including cancer and degenerative diseases such as Parkinson's, Alzheimer's, and Huntington's [159-162].

To date, several DNA repair enzymes have been found in the mitochondria that contribute to the maintenance of mtDNA integrity [82,163-165]. For example, inactivation of *S. cerevisiae* Ogg1, an enzyme that repairs 8-oxo-dGuo, leads to increased frequency of mitochondrial petite mutants due to deletions in the mtDNA [166]. However, these Ogg1-deficient cells do not appear to exhibit elevated point mutations in the large ribosomal RNA gene (21S rRNA) that give rise to erythromycin resistant colonies [166,167]. Thus, it would appear that unrepaired 8-oxo-dGuo lesions might cause deletions rather than base substitutions in the mitochondrial genome. In this study, we set out to investigate if Ogg1-deficiency would interfere with the stability of poly(GT) tracts installed within the mitochondrial genome. Essentially, the poly(GT) tract serves as a sensitive reporter system consisting of a derivative *ARG8m* that functions as a mitochondrial gene, instead of a

nuclear gene, and encoding an enzyme (acetylornithine aminotransferase) of the arginine biosynthetic pathway [168-170]. The derivative *ARG8m* gene contains either poly(GT) or poly(AT) tracts creating +1 or +2 frameshifts causing the cells to become phenotypically Arg^- [170]. Alterations in the poly(GT) or poly(AT) tracts restore the reading frame of the *arg8m* alleles to give rise to Arg^+ colonies [170]. For this study, we exploited only the poly(GT) tract with +2 frameshift as it is 25-fold more unstable in the mtDNA, undergoing a rate of ~40 $x10^{-7}$ changes in the tract per cell division when compared to the poly(AT) tracts, which changes at a rate of ~1.6 $x10^{-7}$ per cell division [170]. Using this system, we show that Ogg1-deficient cells exhibit nearly six-fold elevated rate of Arg^+ mutants, as compared to the parent. These Arg^+ mutants were completely suppressed by overexpression of the Ogg1 enzyme, suggesting that unrepaired 8-oxo-dGuo lesions can trigger instability of GT tract repeats in the mitochondrial genome. Interestingly, overproduction of the major apurinic/apyrimidinic (AP) endonuclease Apn1, a nuclear and mitochondrial enzyme with multiple DNA repair activities including the ability to incise AP sites, did not prevent the poly(GT) tract instability of the Ogg1-deficent cells, and instead potentiated the destabilization resulting in higher levels of Arg^+ mutants. However, the Apn1-induced GT tract instability was counteracted by the simultaneous overexpression of Ogg1. Because Ogg1 can bind to AP sites with high affinity, we suggest that it might serve to protect this lesion from the spurious action of Apn1 overproduction. Thus, cleavage of AP site within the poly(GT) tract could destabilize the repeat.

MATERIALS AND METHODS

Yeast strains

The *S. cerevisiae* strains used in this study were CAB193 (isogenic to DFS188; Mat α, *ura3-52 leu2-3, 112, lys2 his3 arg::hisG*; except carrying poly(GT) repeat in +2 reading frame) and CAB152 (also isogenic to DFS188, except carrying poly(AT) repeat in +2 reading frame) (kindly provided by Dr. E. Sia, University of Rochester, New York, USA). The following isogenic strains were derived from CAB193 and constructed using the one-step gene targeting approach [171]. RVY6 (*ogg1Δ::HIS3*), RVY7 (*apn1Δ::LEU2*), RVY8 (*ntg1Δ::LEU2*), RVY9 (*ogg1Δ::HIS3 ntg1Δ::LEU2*), and RVY10 (*ogg1Δ::HIS3 apn1Δ::LEU2*). Yeast cells were grown in either complete yeast peptone dextrose (YPD) or minimal synthetic (SD) medium, to which nutritional supplement were added at 20 μg/mL [172,173]. Standard genetic analysis and transformation were carried out as described previously [172,173]. The *Escherichia coli* DH5α strain was used for plasmid maintenance.

Construction of the plasmid pOGG1-GFP

The plasmid pOGG1 (kindly provided by Dr. S. Boiteux, CNRS-CEA, Fontenay aux Roses, France), which contains the entire *S. cerevisiae OGG1* gene, was used as the template to amplify by polymerase chain reaction (PCR) the entire coding region of the *OGG1* gene using the primers OGG1-F1 (5'-AAAGTTATTAG ACCTGAATTCACGACTACTCATAGAAAACG-3') and OGG1-F2 (5'-CTATGACTTTTTAGGGGTACCTATTTTTGCTTCTTTGATG-3') bearing the restriction sites (underlined) for *Eco*RI and *Kpn*I, respectively. This procedure yielded a 1.6 kb fragment which was digested with *Eco*RI and *Kpn*I and subcloned into the Yeplac195 yeast expression vector containing the *GFP* gene downstream of the cloning site. Thus, the *OGG1* gene was fused to the N-terminal of GFP in order to create the plasmid pOGG1-GFP.

To obtain a higher expression level of the Ogg1-Gfp fusion protein, the fragment containing the *OGG1* gene attached to the N-terminal of *GFP* was amplify by PCR using the primers OGG1-F2 (5'-CCGATTTTATTTATCAAGCTTA-

TGTCTTATAAATTCGGC-3') and GFP-SalI (5'-AGAACTAGTCGACCCTTATT-TGTATAG-3') bearing the restriction sites (underlined) for *Hind*III and *Sal*I, respectively. The 1.9 kb fragment was subcloned into the multicopy vector pYES2.0, bearing the galactose-inducible promoter *GAL1*, to produce the plasmid pYES-OGG1-GFP.

Preparation of mitochondrial fractions from yeast

Mitochondrial extracts were prepared from the purified organelle as previously described [82]. The cell pellets were weighed, washed with H_2O, resuspended (0.3 g/mL) in 100 mM Tris-SO_4 (pH 9.3) buffer containing 10 mM dithiothereitol, incubated with gentle shaking at 30°C for 10 min, and centrifuged 3,000 × *g* for 5 min at room temperature. Following centrifugation, the pellets were washed once with buffer B (1.2 M D-sorbitol, 20 mM KPB [pH 7.4]), and zymolyase at 2.5 mg/g of cell pellet in 0.1 g of cell pellet/mL of buffer B was added. The pellets were incubated for 60 min at 30°C with gentle shaking until the cell wall was completely digested. The spheroplasts were collected at 3,000 × *g* for 5 min at room temperature and washed three times (1 g/10 mL of buffer B). From this point, all manipulations were performed at 4°C. The spheroplasts were suspended at 1 g/2 mL of MIB (0.6 M D-mannitol, 20 mM HEPES-KOH [pH 7.4], 0.5 mM phenylmethylsulfonyl fluoride) and broken in a Dounce homogenizer with 15 strokes using the pestle (glass and Teflon). The homogenate was then diluted 2-fold in MIB and centrifuged at 3,000 × *g* for 5 min. The pellet contained crude nuclei, and the supernatant represents the crude cytoplasm and mitochondria. The supernatant was spun at 12,000 × *g*; the resulting pellet contained the crude mitochondria.

To obtain purified mitochondria, the crude mitochondria were diluted in 200 µL of MIB and layered on a two-step Nycodenz (Sigma) gradient made in a 14- by 89-mm Ultra-Clear centrifuge tube. The bottom layer of the gradient contained 5 mL of 18% and the top layer contained 5 mL of 14% Nycodenz in MIB. The tubes were spun at 40,000 × *g* in an SW41 rotor for 30 min, and the purified mitochondria were recovered between the two layers as a light brown band. The purified

mitochondria were diluted fivefold in MIB and centrifuged at 12,000 × *g* for 10 min. The resulting mitochondrial pellet was lysed by addition of 200 µL of yeast extraction buffer to produce the mitochondrial fraction.

Western blot

The proteins were separated on 12.5% SDS-PAGE gel, transferred onto a nitrocellulose membrane (8 cm x 10 cm) (Amersham Life Science) which was then blocked with buffer TSEM [10 mM Tris-HCl (pH 7.45), 150 mM NaCl, 0.1% Tween, 1 mM EDTA, 5% powdered milk] for 1 h. After the blocking, the membrane was probed with 10 mL of buffer TSEM containing monoclonal Gfp antibodies at a dilution of 1:5000 for 16 h at 4°C. Following the probing, the membrane was washed three times for 15 min with TSEM before adding 10 mL of the anti-mouse IgG conjugated to horseradish peroxidase at a dilution of 1:2500 (BIO/CAN Scientific Inc., Ont., Canada) for 1 h at room temperature. Finally, the membrane was washed again three times for 15 min with TSEM and immunoreactive polypeptides were detected by chemiluminescence (Dupont-NEN).

Preparation of DNA substrate and assay for Ogg1 activity

A 30 base synthetic oligonucleotide containing a unique 8-oxo-dGuo residue at position 11 (5'-TGACTGCATA$^{8\text{-oxo-dGuo}}$CATGTAGACGATGTGCAT-3') was 5'-^{32}P-end-labeled (provided by Dr. Murat Saparbaev, France). The specific activity of the labeled oligonucleotide was determined by running an aliquot on a 10% polyacrylamide gel and quantitating the amount of incorporated radioactivity. The oligonucleotide was ethanol precipitated, resuspended in TE [10 mM Tris-HCl (pH 7.5) and 1 mM EDTA], and annealed with an equimolar amount of the complementary oligonucleotide (5'-ATGCACATCGTCTACATGCCTATGCAG-TCA-3') by heating at 83°C and slow-cooling to room temperature. The 8-oxo-dGuo cleavage reactions were carried out in buffer containing 25mM Tris-HCl (pH 7.4), 50mM KCl, 2mM EDTA, 1 pmol oligonucleotide substrate, and the indicated concentration of mitochondrial extracts or purified bacteria fpg protein in a final

volume of 12.5 µL. Incubation were carried out at 37°C for 30 min and stopped by the addition of 5 µL formamide loading buffer. Samples were prepared for gel electrophoresis by heating at 65°C for 5 min. Reaction products were analysed on 10% denaturing polyacrylamide gels.

Measurement of mutations rates of mitochondrial DNA

The rate of mutation to Arg^+ was performed as previously described [170]. Briefly, 10 to 15 independent colonies of the indicated strains were grown in 1 mL of SD medium supplemented with 20 µg/mL of the appropriate auxotrophic requirements and grown at 30°C overnight in an orbital incubator shaker set at 250 rpm. The following day, the cells were centrifuged, washed twice with sterilized distilled water, resuspended in 1.5 mL of YPD, and incubated at 30°C with shaking for 4 h until OD_{600} reach ~0.8 to 1.0. After centrifugation, cells were again washed twice with sterile water, and resuspended in 1 mL of sterile water. Serially diluted cells (typically 100 µL of the 10^{-4} and 10^{-1} dilutions) were plated on SD solid medium plates containing arginine (for total colony count) and without arginine (for scoring the Arg^+ revertants), respectively. Total colonies were counted after 2 days, while the Arg^+ revertants colonies were counted after 2, 5, 10, and 15 days following incubation at 30°C. The rate of Arg^+ revertants, which possess alterations in the repeat tracts that restore the reporter gene reading frame, was calculated by method of the median [174]. For the measurement of Arg^+ revertants under anaerobic conditions, the BBL GasPak Pouch system was used. Cells were grown, plated as above, and incubated in the GasPak system for 5, 10, and 15 days at 30°C.

Analysis of the length of mitochondrial microsatellites

The types of alterations present in the repeat tracts were determined by PCR analysis of the *ARG8*^{m} as previously described [170]. The length of the poly(GT) tract without deletion is 88 nucleotides [170].

Analysis of 8-oxo-dGuo in mtDNA by HPLC

Mitochondrial DNA (mtDNA) was separated according to the protocol in "basic methods of yeast genetics" [175]. Briefly, cells were suspended in 0.9 M sorbitol and 0.1 EDTA (pH 7.5), treated with 7.5 mg/mL of Zymolyase 20 000 and incubated at 37°C for 70 min. The cells were lysed in 50 mM Tris-HCl (pH 7.4), 20 mM EDTA with 10% SDS. The nuclear and mitochondrial fractions were then separated by two cycles of differential centrifugation (2000 x g for nuclei followed by 10,000 x g for mitochondria). mtDNA was purified by the mtDNA Extractor CT kit (291-55301) according to the recommended protocol (Wako Chemicals USA, Inc., Richmond, VA). The yield of purified mtDNA varied from 2 to 5 μg for samples containing 50 μg of crude mtDNA (4-10%). Purified mtDNA (40-50 μg) was dissolved in 50 μL of freshly drawn nanopure water (Millipore, Bedford, MA). The sample was incubated for 20 min at 40°C with nuclease P1 [5 μL; 1 unit/μL in acetate buffer 50 mM (pH 4.8)], and then for another 40 min at 40°C with alkaline phosphatase [5 μL of alkaline phosphatase; 1 unit/μL in 50 mM Tris-HCl buffer (pH 7.4) plus 7 μL of 1.2 M ammonium acetate (pH 7.0)]. The mixture of nucleosides was acidified (pH 4) by addition of 5 μL of 0.22 M phosphoric acid, and then extracted with 50 μL of chloroform by brief vortexing and centrifugation at 13 200 x g for 5 min to eliminate excess proteins. The aqueous phase was recovered and transferred to 150 μL plastic vials for HPLC analysis. Analysis of 8-oxo-7,8-dihydro-2'-deoxyguanosine (8-oxo-dGuo) by HPLC was carried out using a Model 2690 Alliance system (Waters, Milford, MA) connected to a Model 2487 UV detector (Waters) and a Coulochem II electrochemical detector (ESA Associates, Chelmsford, MA) equipped with a Model 5011 analytical cell (ESA Associates). Nucleosides were separated on a ODS-A, 250 mm x 6 mm, 5 μm particle size analytical octadecylsilyl column (YMC, Kyoto, Japan) connected to a Model CH-30 Eppendorf column heater set at 30°C (Hamburg, Germany) with 8% methanol in 50 mM phosphate buffer at pH 5.0 as the mobile phase at a flow rate of 1 mL/min. For optimal detection of 8-oxo-dGuo, the first and second electrodes of the electrochemical cell were set at 250 and 450 mV, respectively (voltage versus Pd reference electrode). The amount of

damage (8-oxo-dGuo/ 10^6 dGuo) was estimated from the ratio of peak areas for 8-oxo-dGuo, obtained by electrochemical detection, and non-modified 2'-deoxyguanosine (dGuo), obtained by UV detection, during the same chromatographic run.

RESULTS

The mitochondrial form of Ogg1 is active at processing 8-oxo-dGuo lesions

Previously, it was shown that a GFP tagged form of Ogg1 can be distributed to the mitochondria of yeast cells, although this report did not monitor for the enzyme activity in this organelle [166]. To examine if Ogg1 is enzymatically active in the mitochondria, we deleted the *OGG1* gene in the parent strain CAB193 to produce the *ogg1Δ* mutant strain RVY6 and examined the purified mitochondria derived from these strains for Ogg1 activity. To monitor the activity of Ogg1, we used a 30-mer double-stranded oligonucleotide bearing a single 8-oxo-dGuo lesion at position 11 in the upper strand [82,176]. As shown in Figure 3-1, extract derived from the purified mitochondria obtained from the parent strain cleaved the 30-mer substrate to produce the expected 10-mer product (lanes 5 and 6), similar to the product generated by purified fpg protein (lane 2), the bacterial counterpart of the yeast Ogg1 [176]. In contrast, extracts derived from purified mitochondria obtained from the *ogg1Δ* null mutant showed no detectable cleavage of the substrate even at the highest concentration of mitochondrial extract used in the assay (Figure 3-1, lane 10). On the basis of our findings, we conclude that Ogg1 is indeed present in the mitochondria, as previously reported [166], and in an enzymatically active form. In control experiment, mitochondrial extracts derived from either the parent or the *ogg1Δ* mutant equally cleaved an abasic site substrate [82] (data not shown), suggesting that the absence of Ogg1 is unlikely to cause alteration in the levels of other base excision repair enzymes.

*ogg1*Δ mutants exhibit elevated poly(GT) tract instability

We next tested if Ogg1 is required for maintenance of poly(GT) or poly(AT) tract stability. To do this, we exploited the parent and *ogg1Δ* null strains carrying the derivative $arg8^{m}$ alleles with +2 frameshift mutations created by the insertion of either a poly(GT) or a poly(AT) tract [170]. These strains are unable to grow on medium lacking arginine, unless a 2-bp deletion occurs in the GT or AT tract to

Figure 3-1. Mitochondrial Ogg1 is functionally active.

Ogg1 assay was carried out with the following concentrations of the purified mitochondrial extracts prepared either from the parent strain CAB193 (lanes 3-6) or the *ogg1Δ* mutant (lanes 7-10); 0 (lanes 3 and 7), 20 (lanes 5 and 9), and 60 μg (lanes 6 and 10). Purified fpg 100 ng (lane 2) was used as a positive control. Arrows indicate position of the 30-mer substrate and the 11-mer product. The data is representative of two independent experiments.

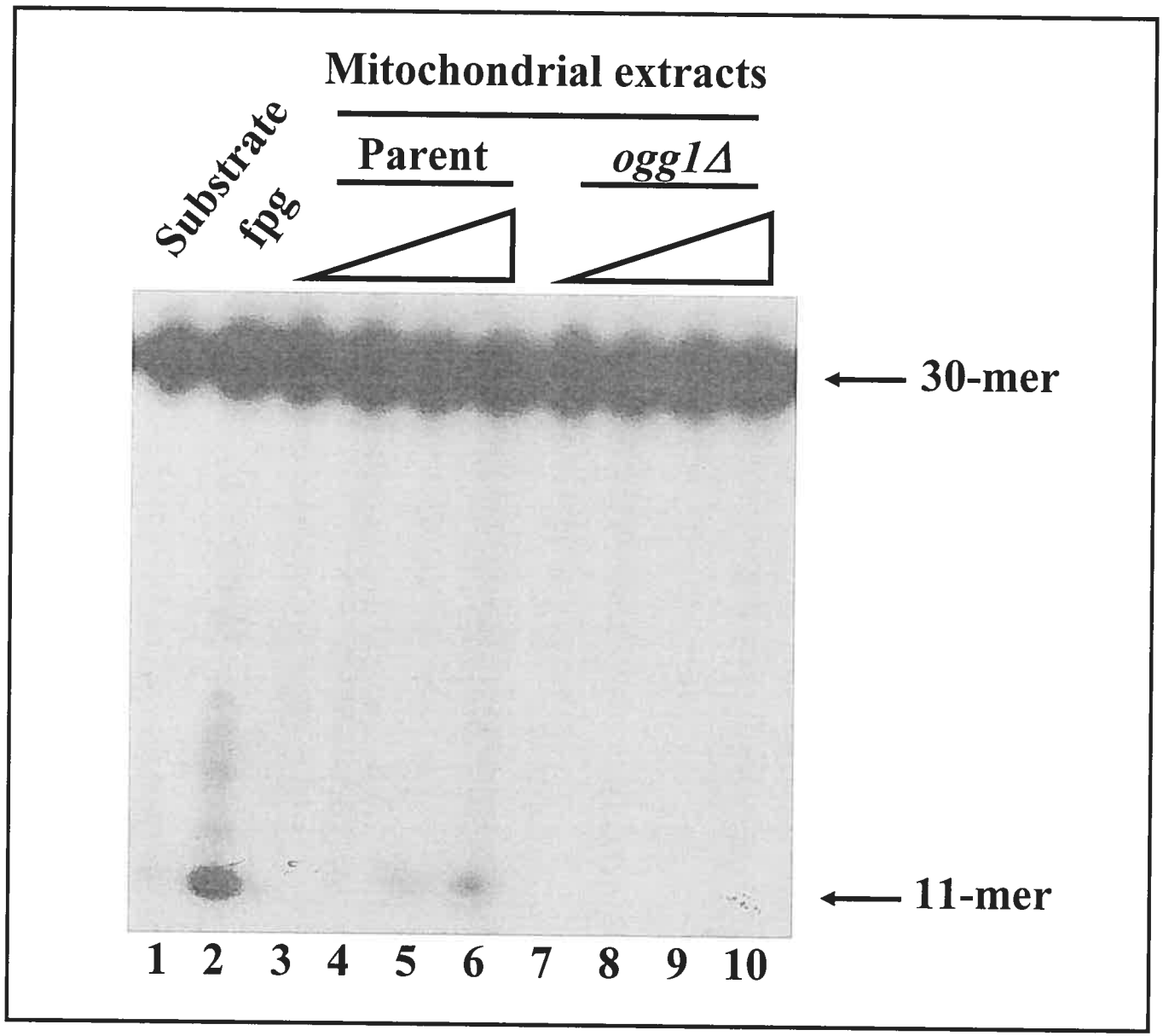

FIGURE 3-1. Vongsamphanh *et al.*, 2006

restore the *ARG8*^{m} reading frame thereby reverting the cells to the Arg^{+} phenotype [170]. As shown in Figure 3-2, following 2-5 days of selection of multiple independent cultures on minimal medium plate lacking arginine, both the parent and the *ogg1Δ* mutant carrying the poly(GT) tract generated Arg^{+} revertants at the same rate. However, after 10 days of selection the rate of Arg^{+} mutations increased very modestly (and no significant increased by 15 days) for the parent, while that of the *ogg1Δ* null mutant increased nearly 3-fold by 10 days and a further 3.5-fold by 15 days (Figure 3-2). No significant increase in Arg^{+} mutations was observed after 20 days of selection at which point the experiment was terminated (Figure 3-2). In the case of the parent and the *ogg1Δ* mutant carrying the poly(AT) tract, there was no significant differences in the rate of Arg^{+} revertants, even after 15 days of selection (data not shown). On the basis of these finding, it would appear that Ogg1 is required to suppress the poly(GT), but not the poly(AT), tract instability.

To confirm that the poly(GT) tract instability is a result of Ogg1 deficiency, we examined the rate of Arg^{+} revertants produced by the *ogg1Δ* mutant carrying a multicopy plasmid pOGG1 overexpressing the Ogg1 protein [176]. As shown in Figure 3-2, plasmid pOGG1 completely abolished the high levels of Arg^{+} revertants in the *ogg1Δ* mutant. Moreover, Ogg1 overexpression further reduced the level of Arg^{+} revertants (nearly 1.5-fold lower), as compared to the level observed in the parent strain carrying only the empty vector (Figure 3-2). Introduction of pOGG1 in the parent also reduced the basal level of Arg^{+} revertants, suggesting that Ogg1 function might be limiting in the mitochondria. Consistent with our findings, Singh *et al.* [166] showed that overexpression of either yeast Ogg1 or human Ogg1 in a parent yeast strain or the isogenic *ogg1Δ* mutant further decreased the formation of petite colonies to levels lower than that observed in the parent strain carrying only a vector. It is noteworthy that plasmid pOGG1 did not completely eliminate all the Arg^{+} revertants in either the parent or *ogg1Δ* mutant, suggesting that other factors might be limiting which could contribute to the poly(GT) tract stability.

Figure 3-2. Ogg1 is required to maintain poly(GT) tract stability.

The rate of mutation to Arg^+ was performed as previously described (see the Materials and Methods). Briefly, 10-15 independent colonies of the parent strain CAB193 (open circles), the *ogg1Δ* null mutant (filled circles), the parent with the plasmid pOGG1 (open squares), and the *ogg1Δ* null mutant with pOGG1 (filled squares) were analyzed for Arg^+ revertants. These colonies were scored after 2, 5, 10, 15, and 20 days on solid medium plates without arginine. Day 2 represents the spontaneous Arg^+ mutants arising from the overnight culture (see Table III-I). The data is the average of three independent experiments.

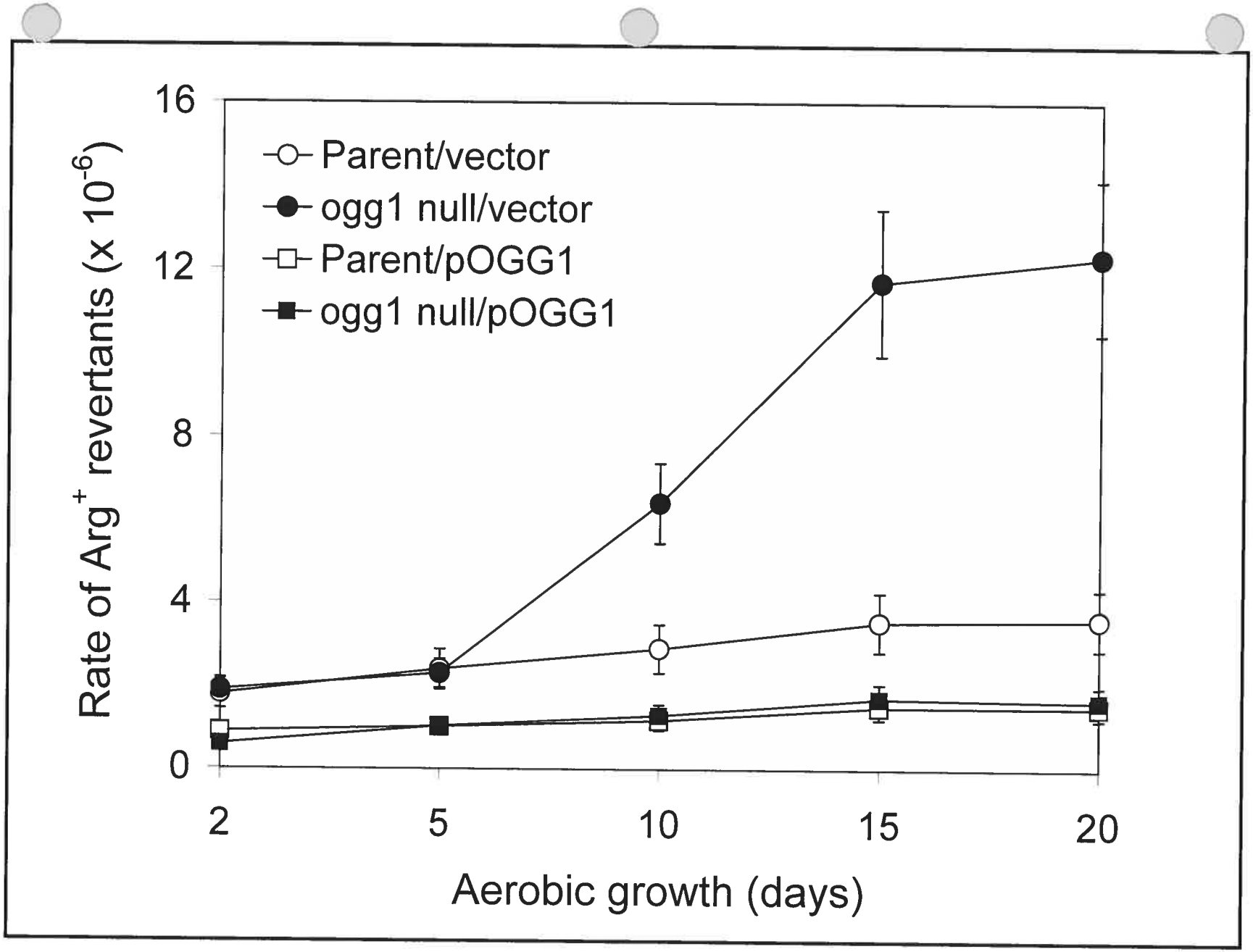

FIGURE 3-2. Vongsamphanh *et al.*, 2006

Since Ogg1 is known to repair the mutagenic 8-oxo-dGuo lesion, it is likely that accumulation of this lesion in the poly(GT) tract may cause the instability. As such, we isolated the mtDNA from purified mitochondria and quantitatively measured the level of 8-oxo-dGuo base using HPLC (see the Materials and Methods). However, in three independent determinations, this approach failed to reveal any significant difference in the levels of 8-oxo-dGuo between the mtDNA obtained from the *ogg1Δ* mutant (198 $\pm$ 12 lesions/ 10^6 G), as compared to the parent (184 $\pm$ 10 lesions/10^6 G) (see the Discussion).

PCR analysis of GT tract instability in the parent and the *ogg1Δ* mutant

We next examined the types of alterations that occurred in the poly(GT) tract by PCR analysis of 15 independent Arg^+ colonies derived from both the parent and the *ogg1Δ* mutant. All (15/15) of the independent Arg^+ colonies derived from the parent contained 2-bp deletion, indicating that the poly(GT) tract give rise primarily to deletions (Figure 3-3 showing PCR analysis of two representative Arg^+ colonies). Similarly, all (15/15) of the independent Arg^+ colonies derived from the *ogg1Δ* mutant contained deletions, but of these 7 showed 2-bp deletions and 8 contained 14-bp deletions or larger (Figure 3-3). This data suggests that in the absence of Ogg1, unrepaired 8-oxo-dGuo lesions might be the cause of the larger deletions in the poly(GT) tract. Consistent with this notion, it has been documented that inactivation of Ogg1 causes deletion, but not complete loss of the mtDNA [166].

Anaerobic condition eliminates the elevated mutations in the *ogg1Δ* null

If indeed the increased rate of Arg^+ revertants is due to oxidative DNA damage caused by the production of ROS during aerobic metabolism, then we anticipate that cells grown under anaerobic conditions should decrease the level of Arg^+ revertants. To perform this experiment, the cells were grown under normal growth conditions in liquid medium, plated onto solid medium lacking arginine, followed by incubation in

Figure 3-3. PCR analysis for poly(GT) tract instability.

Mitochondrial DNA was extracted as described in the Materials and Methods from the parent strain CAB193 (lane 1), the *ogg1Δ* mutant (lane 2), two Arg^+ derivatives of the parent (lanes 3 and 4), and two Arg^+ revertants of the *ogg1Δ* mutant (lanes 5 and 6) strains. Following PCR amplification in the presence of labeled dATP, the products were ran on 6% polyacrylamide gel and analyzed by autoradiography. The left arrow indicates a 86 nt marker and the right arrows show the poly(GT) tract without deletion (88 nt), and in frame deletions of -2, -5, and -20 corresponding to 86, 83, and 68 nt, respectively. The data are representative of two independent experiments.

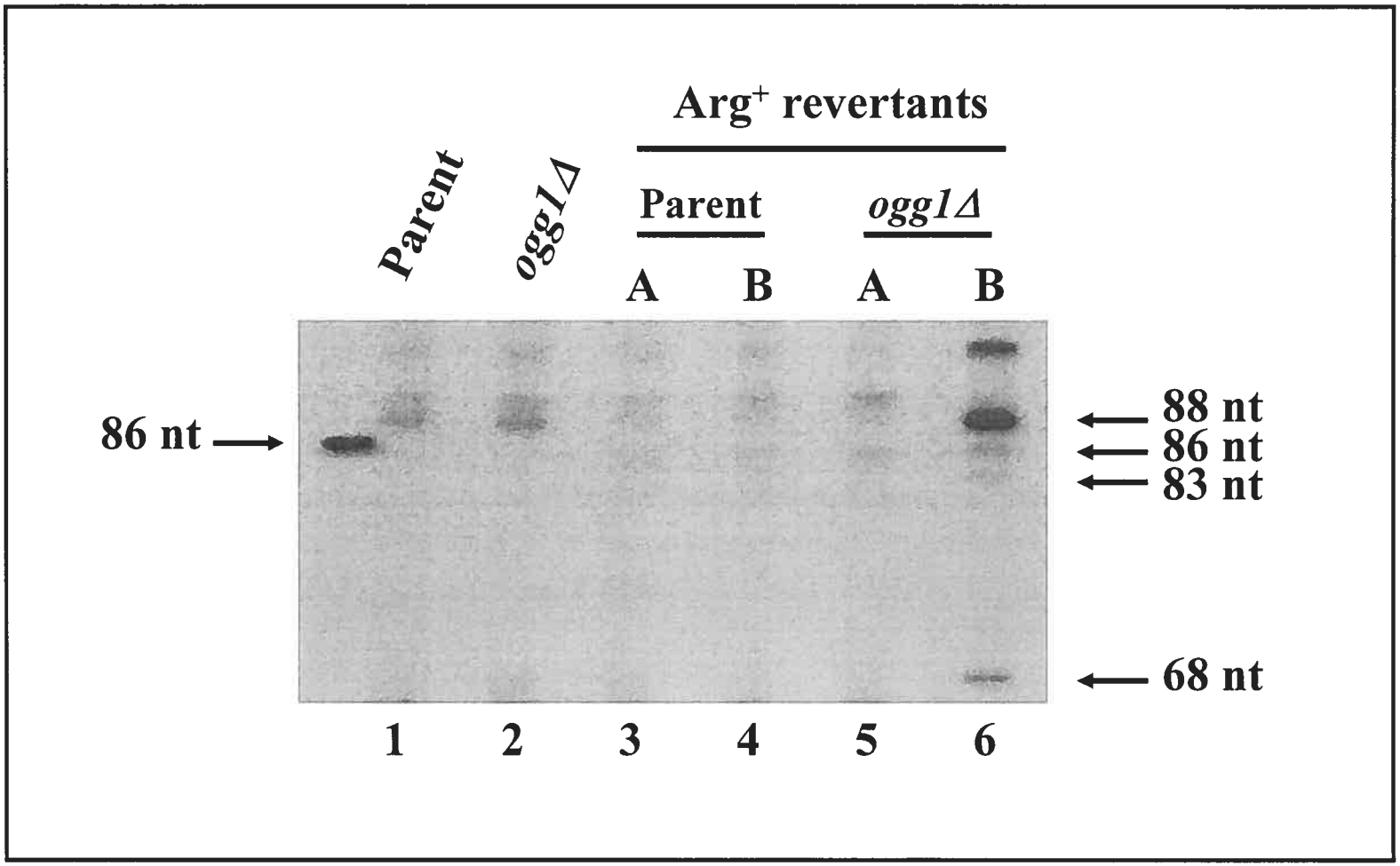

FIGURE 3-3. Vongsamphanh *et al.*, 2006

anaerobic bags (see the Materials and Methods). Following 5, 10, and 15 days of incubation under this condition, the parent strain showed a slightly reduced level of Arg^+ revertants (Figure 3-4), as compared to growth under the aerobic condition (Figure 3-2). Interestingly, the *ogg1Δ* mutant behaved like the parent strain under the anaerobic condition and displayed nearly the same level of Arg^+ revertants (Figure 3-4). Since the *ogg1Δ* mutant showed a substantial increase in Arg^+ revertants during aerobic growth, but not under the anaerobic condition, it suggests that the poly(GT) tract instability is due to ROS-induced DNA lesions which must be processed by Ogg1.

Apn1 overexpression in the *ogg1Δ* mutant stimulates poly(GT) tract instability

We recently demonstrated that the major AP endonuclease Apn1 in *S. cerevisiae* possesses a strong 3'→5'-exonuclease activity, which is capable of removing 8-oxo-dGuo that is derived from the oxidized dNTP pool and misincorporated into DNA during replication [86]. As such, we tested if overexpression of Apn1 might play a role in reducing poly(GT) tract instability in the *ogg1Δ* mutant, by preventing 8-oxo-dGuo misincorporation into the mtDNA. Unexpectedly, introduction of a plasmid pAPN1, which overproduces Apn1 [81], in the *ogg1Δ* mutant stimulated the rate of Arg^+ revertants by an additional two-fold after 10 days of selection, when compared to the mutant carrying only the empty vector (Table III-I). This effect was not specific for the *ogg1Δ* mutant, as introduction of pAPN1 into the parent strain also stimulated the appearance of Arg^+ revertants by three- to four-fold (Table III-I). Since Apn1 has multiple enzymatic functions including AP endonuclease, nucleotide incision, as well as 3'-5'-exonuclease activities [86,177], it is possible that the uncontrolled action of this enzyme could lead to increase nicking of the mitochondrial genome causing instability of the poly(GT) tract (see the Discussion). We, therefore, tested if overexpression of Ogg1 could counteract the poly(GT) tract destabilization triggered by Apn1 overexpression. As shown in Table 3-1, introduction of plasmid pOGG1 into either the parent or *ogg1Δ*

Figure 3-4. Anaerobic conditions reduce the poly(GT) tract instability.

The same experimental procedure as in the aerobic conditions was used to measure Arg^+ revertants under anaerobic growth, for the exception that BBL GasPaK Pouch system was used to create the anaerobic conditions. Open circles represent the parent strains and the filled circles represent the *ogg1Δ* mutant strain, respectively. The data are the average of three independent experiments.

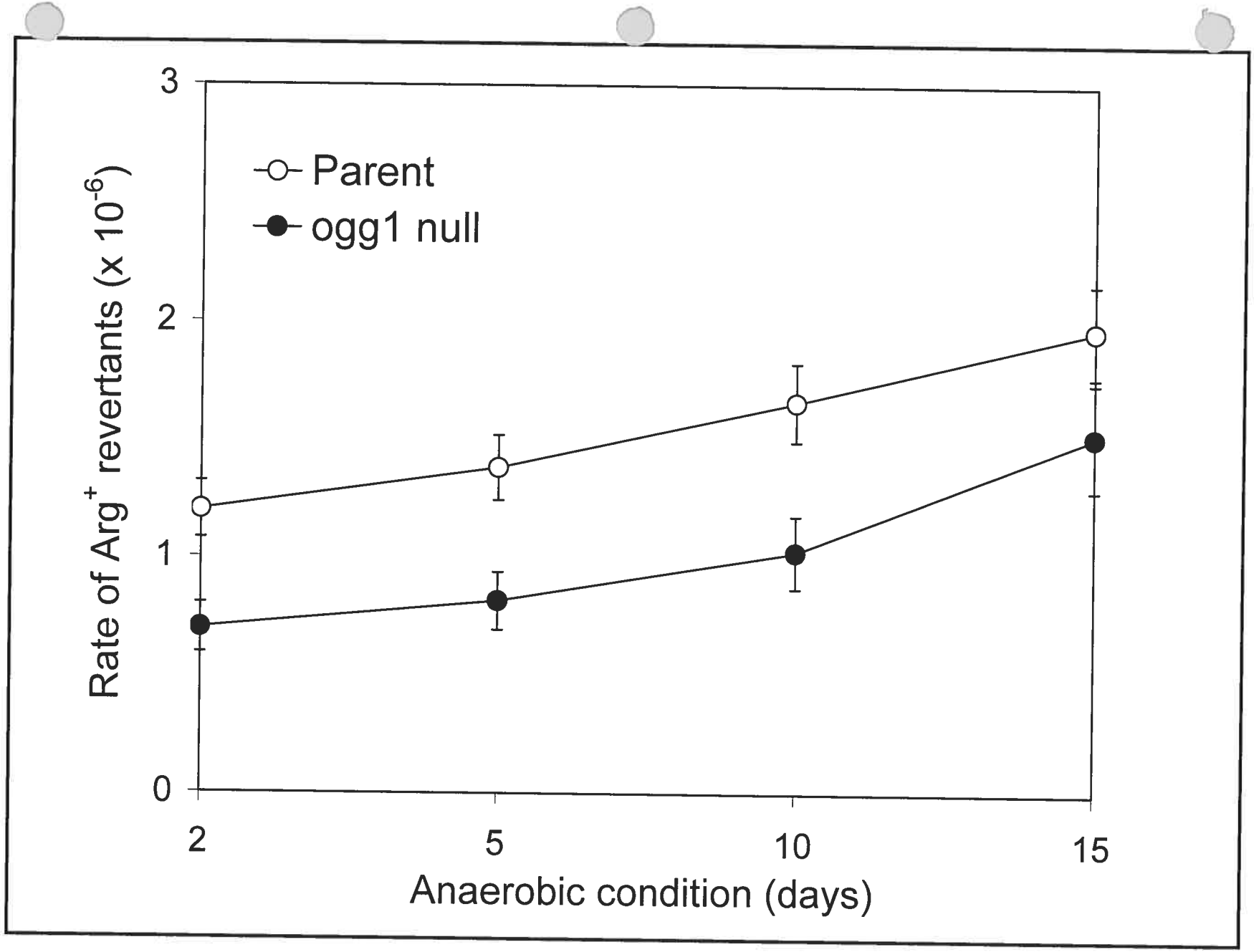

FIGURE 3-4. Vongsamphanh *et al.*, 2006

mutant overexpressing Apn1 decreased by four- to six- fold, respectively, the elevated rate of Arg^+ revertants that was observed when the strains were only overexpressing Apn1. From these data, we reasoned that Ogg1 might protect a distinct lesion, e.g. AP site, within the vicinity of the poly(GT) tract from the mutagenic action of Apn1 overproduction.

Poly(GT) tract instability is not affected by *NTG1* deletion

Previous studies showed that the *NTG1* gene encodes a mitochondrial DNA repair enzyme, which functions in the base excision repair pathway to process oxidized pyrimidines and purines, e.g., 2, 6-diamino-4-hydroxy 5N-methylformamido pyrimidines, as well as abasic sites and 8-oxo-dGuo mispaired with adenine [178,179]. Mutants devoid of Ntg1 display an elevated level of oxidative damage to the mtDNA and exhibit a nearly two-fold increased in mtDNA point mutations, but do not show the mitochondrial respiration-deficient (petite) phenotype [165]. Because of the broad substrate specificity of Ntg1, we tested if deletion of the *NTG1* gene in the parent strain would affect the poly(GT) tract instability. As shown in Table III-I, the resulting *ntg1Δ* mutant showed no increase in the rate of Arg^+ revertants, as compared to the parent strain. Moreover, *ogg1Δ* mutant deleted for the *NTG1* gene also showed no further increase in Arg^+ revertants, when compared to the *ogg1Δ* single mutant (Table III-I). These genetic data strongly indicate that DNA lesions that are primarily repaired by the Ntg1 enzyme might not be produced within the poly(GT) tract.

Table III-I. Effect of DNA repair proteins on the rate of poly(GT) tract instability in the mitochondrial genome.

Strains/vector or plasmid	Rate of mutation to Arg^+(10^{-6} per cell division)				Fold-induction
	Day 2	Day 5	Day 10	Day 15	
CAB193 (Parent)/vector	1.8 (1.4-2.2)	2.4 (2.3-2.5)	2.9 (2.8-3.1)	3.6 (3.4-3.8)	2
RVY6 (*ogg1Δ*)/ vector	2.1 (1.9-2.3)	2.3 (2.1-2.4)	7.4 (5.9-8.4)	11.7 (11.3-12.5)	6.5
RVY7 (*apn1Δ*)/ vector	0.9 (0.7-1.1)	1.3 (0.9-1.5)	2.4 (2.1-2.6)	3.1 (2.7-3.3)	1.7
CAB193/pOGG1	1.2 (1.0-1.5)	1.6 (1.1-1.8)	1.9 (1.7-2.1)	2.3 (2.1-2.4)	1.3
RVY6 (*ogg1Δ*)/ pOGG1	0.6 (0.6-0.7)	1.2 (1.1-1.3)	1.4 (1.2-1.7)	1.7 (1.5-1.9)	0.9
RVY6 (*ogg1Δ*)/ pOGG1-GFP	1.3 (1.1-1.7)	2.1 (1.9-2.3)	2.4 (2.0-2.7)	2.6 (2.2-2.8)	1.4
RVY8 (*ntg1Δ*)/ vector	1.2 (1.0-1.4)	1.6 (1.1-2.2)	3.5 (3.2-3.7)	3.3 (3.1-3.5)	1.8
RVY9 (*ogg1Δ ntg1Δ*)/ vector	2.2 (2.0-2.4)	2.5 (2.4-2.6)	6.3 (5.9-6.7)	11.6 (11.4-11.8)	6.4
RVY10 (*ogg1Δ apn1Δ*)/ vector	1.1 (0.8-1.4)	1.9 (1.7-2.0)	4.0 (3.5-4.1)	5.3 (4.5-6.1)	2.9
CAB193/pAPN1	2.4 (2.1-2.7)	2.8 (2.7-2.9)	8.4 (7.2-9.6)	12.4 (11.5-13.4)	6.9
CAB193/pAPN1 + pOGG1	0.9 (0.7-1.2)	1.5 (1.2-1.7)	3.1 (2.6-3.6)	3.4 (3.2-3.6)	1.9
RVY6 (*ogg1Δ*)/ pAPN1	2.7 (2.5-3.1)	3.0 (2.8-3.2)	16.7 (15.8-17.6)	18.9 (18.1-19.8)	10.5
RVY6 (*ogg1Δ*)/ pAPN1 + pOGG1	0.7 (0.7-0.8)	1.2 (1.0-1.4)	2.9 (2.5-3.4)	3.1 (2.7-3.5)	1.7

The mutation rate was determined by using 10-15 individual colonies, and repeated three times for each strain. The values in the brackets show the range of the mutation rate. Fold-induction was determined by dividing the values obtained for day 15 by that of day 5 for the parent carrying only the vector. Day 2 represents the spontaneous Arg^+ colonies arising during the overnight culture in liquid SD medium.

DISCUSSION

In this study, we investigate the role of Ogg1 in maintaining the stability of a poly(GT) tract installed within the *ARG8*^{m} reporter gene, that is embedded in the mitochondrial genome [170]. We demonstrate that Ogg1-deficient mutants exhibit an elevated rate of poly(GT) tract instability in a time-dependent manner, increasing to nearly six-fold following incubation of the cells at standard growth conditions for 15 days. Several findings indicate that the poly(GT) tract destabilization is likely due to the accumulation of unrepaired oxidized DNA base lesions, particularly 8-oxo-dGuo. Firstly, overexpression of Ogg1, which is known to repair 8-oxo-dGuo lesions, completely abolished the elevated rate of mutations in the poly(GT) tract (Table III-I) [180]. Secondly, anaerobic growth conditions, which greatly reduces the production of reactive oxygen species and consequently oxidative DNA lesions, e.g., 8-oxo-dGuo, prevented the destabilization of the poly(GT) tract. Thirdly, the deficiency of Ntg1, an enzyme which repairs primarily oxidized pyrimidines base lesions, did not affect the poly(GT) tract stability [178,179]. Finally, Ogg1-deficiency had no detectable effect on the stability of the poly(AT) tract.

Although the above observations present a convincing argument that the oxidized DNA lesions are most likely to cause the poly(GT) tract instability is 8-oxo-dGuo, we were unable to demonstrate that this lesion accumulated in the mtDNA derived from the *ogg1Δ* mutant, as compared to the parent. The levels we determined by HPLC were almost indistinguishable being 198 $\pm$ 12 and 184 $\pm$ 10 lesions /10^6 G for the *ogg1Δ* mutant and the parent, respectively. These levels are much higher than levels recently reported for 8-oxo-dGuo in mtDNA from normal rodent tissue (~1-14 lesions /10^6 G), although the level appears to increase in OGG1-defective animals (about 125 lesions /10^6 G) [181,182]. In contrast, there is very little data available on the levels of 8-oxo-dGuo lesions present in the mitochondrial genome of yeast. Using a similar method of analysis, one study reported levels greater than 500 8-oxo-dGuo lesions /10^6 G in the mitochondrial genome of *S. cerevisiae* [183]. The similarity of DNA damage for *ogg1Δ* mutant and parent suggests that total DNA damage is a poor indicator of mutagenesis in small localized poly(GT) targets. Alternatively, the assay

for DNA damage may artificially induce damage that is above the level of damage associated with mutagenesis.

The observation that overproduction of the AP endonuclease, Apn1, triggers destabilization of the poly(GT) tract, but which was obliterated by the simultaneous overexpression of Ogg1, suggests that (i) it is crucial to maintain the correct balance of Apn1 within the mitochondria [82] and (ii) both Apn1 and Ogg1 are likely competing to recognize a lesion that has the propensity to trigger genome instability. We speculate that the common lesion might be spontaneous AP sites arising within or in the vicinity of the poly(GT) tract. This is supported by the observation that human OGG1 can also bind very tightly to AP sites and only released from the lesions following the recruitment of the human AP endonuclease, APE1 [119,184]. As such, yeast Ogg1 could possibly compete for binding to AP sites and protect a fraction of the lesions from spurious cleavage by the uncontrolled action of the overproduced Apn1, which could create excessive nicked DNA and consequently single stranded gaps by the action of its 3'-5'-exonuclease activity [86]. Thus, the observation that deletion of the *APN1* gene in the *ogg1Δ* mutant reduces the high rate of poly(GT) tract instability (Table III-I) is consistent with a model whereby Apn1 activity levels must be tightly regulated in order to preserve the mtDNA integrity. Whether Apn1-induced DNA nicks and or single stranded DNA gaps within a repeated DNA sequence in the mitochondrial genome can interfere with the fidelity of DNA polymerase γ such that it undergoes slippage remains to be determined.

While it has been demonstrated that deletion of the *NTG1* gene reduces the frequency of petite mutants in the *ogg1Δ* mutant [166], this gene deletion does not appear to rescue or potentiate the poly(GT) tract instability in the *ogg1Δ* mutant. The mechanism by which Ntg1-deficiency prevents petite mutations in the *ogg1Δ* mutant is not known, although *ntg1Δ* single mutants do not exhibit the petite phenotype [166]. However, the Ntg1 enzyme can act on a variety of DNA lesions including dihyrouracil, dihyrothymidine, 5-hydroxyuracil, Fapy G, and abasic site [185], and it is, therefore, possible that minimizing incision of the spontaneously damaged sites in the mtDNA could prevent deletion in the genome that causes the petite phenotypes [166]. This phenomenon has been previously documented for the *mag1Δapn1Δ*

double mutant, whereby deletion of the *MAG1* gene, encoding 3-methyadenine-DNA-glycosylase, reduces the load of the mutagenic AP sites in the *apn1Δ* mutant [186,187]. Since in our experiments Ntg1 deficiency did not prevent the poly(GT) tract instability in the *ogg1Δ* mutant, it may suggest that Ntg1-repairable lesions are not likely present in this repeated sequence possibility due to the small target size.

So far, the only other gene known to play an important role in the maintenance of the poly(GT) tract stability is *MSH1*, which encodes the yeast homolog Msh1 of the bacterial MutS protein [170]. Msh1 is also important to maintain the overall integrity of the mtDNA, as *msh1Δ* mutants loss mtDNA within 20 generations [188]. The precise mechanism by which Msh1 prevents genome instability is not known, although it is believed to serve a function to recognize DNA mismatches [170]. Studies performed in yeast indicated that the Msh1 homologs, Msh2 and Msh6, are required to remove adenine mispaired with 8-oxo-dGuo in order to prevent the incidence of 8-oxo-dGuo induced G to T transversion mutations [189]. Moreover, Msh2 acts in a synergistic manner with Ogg1 to avoid G to T mutations [190]. It is noteworthy that these Msh1 homologs exist as complexes (Msh2-Msh3 and Msh2-Msh6) to repair DNA mismatches and loop structures [191]. However, no partner has emerged yet for Msh1 and raises the question as to how this protein might prevent poly(GT) tract instability. Whether Msh1 serves to recognize a multitude of DNA distortions in the mtDNA including DNA mismatches, loop structures, as well as 8-oxo-dGuo lesions, and recruit the corresponding DNA repair proteins remains a challenging task to be investigated.

In short, we found that the poly(GT) tract reporter system can be a useful assay to study the contribution of DNA repair enzymes in the repair of oxidative DNA damage. This system might be amenable to examine the role of these DNA repair proteins on other types of repeat, such as the triple (CAG) repeat involved in Huntington's disease [192].

ACKNOWLEDGEMENTS

We thank Drs. E.A. Sia for the yeast strains and S. Boiteux for the pOGG1 overproducing plasmid. This study was supported by a grant to D.R. from the Canadian Institutes of Health Research. R.V. is awarded a student fellowship from the National Cancer Institute of Canada, and D.R. is supported by a senior fellowship from the Fonds de la Recherche en Sante du Quebec.

CHAPTER 4

Human GAPDH functions as a redox factor to reactivate the oxidized form of the DNA repair enzyme APE1

In preparation

Human GAPDH functions as a redox factor to reactivate the oxidized form of the DNA repair enzyme APE1

ARSHAD JILANI[1Ψ], RATSAVARINH VONGSAMPHANH[1Ψ], SONISH AZAM[1], and DINDIAL RAMOTAR[1‡]

Running title: GAPDH reactivates oxidized APE1

[‡]Corresponding author:
[1]University of Montreal
Maisonneuve-Rosemont Hospital
Guy-Bernier Research Centre
5415 de l'Assomption
Montreal, Quebec, Canada H1T 2M4
Telephone: (514) 252-3400 ext 4684. Fax: (514) 252-3430
E-mail: [redacted]

[Ψ] authors with equal contributions

ABSTRACT

The glycolytic enzyme glyceraldehyde-3-phosphate dehydrogenase (GAPDH) has been implicated in many biological processes including its role as a cellular sensor of oxidative stress. We show that GAPDH physically associates with APE1, an enzyme involved in DNA repair, as well as redox regulation of several transcriptional factors. This interaction allows GAPDH to convert the oxidized forms of APE1 to the reduced form, resulting in reactivation of AP endonuclease activity. While three GAPDH variants, C152G, C156G, and C247G, retain the ability to interact with APE1, only C247G could reactivate the oxidized APE1 suggesting that Cys152 and Cys156 of GAPDH are indispensable for APE1 reactivation. Interestingly, overproduction of GAPDH confers upon DLD-1 cells additional resistance specifically to DNA damaging agents, which generate lesions that are repaired by APE1. In contrast, GAPDH-siRNA knockdown sensitized the cells to these agents. Our data provide compelling evidence that the nuclear translocation of GAPDH during oxidative stress constitutes a protective mechanism involving the activation of APE1.

INTRODUCTION

The evolutionary conserved enzyme glyceraldehyde-3-phosphate dehydrogenase (GAPDH) catalyzes a critical reaction in the second stage of the glycolytic pathway [193]. It uses the oxidized form of nicotinamide adenine dinucleotide (NAD+) and converts glyceraldehyde-3-phosphate to 1,3-bisphosphoglycerate, which eventually generates lactate and the production of an ATP molecule. Recent studies have documented that GAPDH is also involved in several other biological processes that include cellular response to DNA damage (DNA repair and replication) [194,195], tRNA export [196,197], apoptosis [198], as well as histone H2B gene expression [199].

The implication of GAPDH in DNA damage response may be predicted based on several compelling evidences. First, GAPDH translocates from the cytoplasm to the nucleus upon induction of oxidative stress by H_2O_2 [200]. Second, exposure to H_2O_2 reduces significantly GAPDH glycolytic (or dehydrogenase) activity thus endowing GAPDH with the ability to interact with some proteins [201]. Finally, GAPDH was found associated with a novel protein complex distinct from mistmatch repair protein complexes, following its nuclear translocation upon treatment with mercaptopurine, an agent used for treating acute lymphoblastic leukemia. This protein complex containing GAPDH binds directly to thioguanylated DNA [202]. Together, these data strongly indicate that GAPDH acts as an intracellular sensor of DNA damage.

Therefore, GAPDH is no more just a historical glycolytic enzyme but has become a multifunctional protein of great importance. In this paper we report another important function of GAPDH. We have found that GAPDH interacts and reduces APE1, a known DNA repair enzyme, which plays a crucial role, for example, in processing spontaneous and drug-induced apurinic/apyrimidinic (AP) sites [103]. APE1 has conserved cysteines and has been reported to reduce p53 [203], and many transcriptional factors such as AP-1 (c-Fos and c-Jun), NF-κB, Myb, and HIF-1α [109,204,205]. APE1 is thus a dual function enzyme which can regulate the redox state of a number of proteins and also function as a DNA repair (AP) endonuclease. We further show that overexpression of GAPDH conferred additional resistance to

agents, for example, MMS and H_2O_2 that create lesions, which require processing by APE1. Consistent with this finding, siRNA knockdown of GAPDH sensitizes cells to MMS and H_2O_2 exposure, but not to 254 nm UV light (UVC). We propose that GAPDH might play a key role in promoting the DNA repair functions of APE1 during oxidative stress.

MATERIALS AND METHODS

Bacteria strains

The *E. coli* strains used in this work were BW528 [Δ(*xth-pnc*), *nfo1*::*kan*] (kindly provided by B. Weiss, Emory University, Atlanta, GA) and BL21(DE3)pLysS [*dcm ompT hsdS* (r_B-m_B-) *galλ*(DE3) (pLysS Cam^r)] (Stratagene). Strains were transformed with the indicated vector or plasmids (see below) by the $CaCl_2$ method [136].

Cell culture

Human lung fibroblast (LF1) and colon carcinoma cell lines (HCT116) were kindly provided by Dr. Elliot Drobetsky (University of Montreal, Montreal, QC), and DLD-1 (human colon cancer cells) stably transfected with either pGFP or pGFP-GAPDH plasmid were generously provided by Dr. W.E. Evans (University of Tennessee, Memphis, TN). The cells were maintained in Ham's F10 nutrient medium (Sigma-Aldrich, St-Louis, MO), McCoy5A cell medium (Invitrogen, Carlsbak, CA), or RPMI-1640 medium (BioWhittaker Inc., Walkersville, MD); supplemented with 5% calf serum or 10% fetal bovine serum; 0.1 mg/mL penicillin; and 0.1 mg/mL streptomycin.

AP endonuclease assay

This assay was performed using a 5'-end labeled 42-mer U21•G oligonucleotide substrate as previously described [143].

Purification of a protein with associated AP endonuclease activity

All the purification steps were done at 4°C and an AP endonuclease assay [143] was performed after each step of purification. Approximately 5 x 10^6 human lung fibroblast cells were broken in a Dounce homogenizer with 10 strokes using the

pestle (glass and Teflon) in 1 mL of buffer A which consisted of 50 mM Tris-HCl (pH 7.0), 20 mM NaCl, 10% glycerol, and protease inhibitor cocktail (Complete Mini, EDTA-free, Roche Diagnostics GmbH). Cell extracts were centrifuged at 14 000 rpm at 4°C for 10 min and the supernatants were incubated with pre-equilibrated 1.6 mL DEAE-Sepharose resin (Amersham Pharmacia Biotech) in buffer A by rotating at 4°C for 15 min. The supernatants were then loaded onto a 500 uL ssDNA agarose column (Amersham Pharmacia Biotech) in buffer A. The proteins were eluted by step gradient using 100 mM (250 uL), 200 mM (250 uL), 300 mM (250 uL), and 500 mM (360 uL) NaCl in buffer A. The AP endonuclease activity of the eluted fractions was assayed and based on the activity as revealed by autoradiography, fractions from 200, 300, and 500 mM NaCl elutions were pooled (pool volume = 860 uL) and were dialysed in an Amicon Ultra Centricon (Millipore Corp.) with buffer B [50 mM Tris-HCl (pH 7.5), 20 mM NaCl, 0.5 mM DTT, and 0.5 mM EDTA] by repeated concentration and 10-fold dilution with buffer B four times. The last concentration step was diluted 10-fold in buffer B and loaded onto a 200 uL MonoQ column (Bio-Rad) pre-equilibrated in buffer B. The flow-through fraction was dialyzed by repeated concentration and 10-fold dilution with buffer C [50 mM Tris-HCl (pH 8.0), 20 mM NaCl, 0.5 mM DTT, and 0.5 mM EDTA). The last concentration step was diluted 10-fold with buffer C and loaded onto a 200 uL MonoQ column (Bio-Rad) pre-equilibrated in buffer C. The flow-through fraction was then loaded onto a 200 uL CMSepharose column (Amersham Pharmacia Biotech) pre-equilibrated in buffer C The column was washed three times with buffer C and eluted with 100, 200, 400, and 600 mM NaCl. The eluated proteins from 200, 400 and 600 mM NaCl elution showed AP endonuclease activity and were pooled and concentrated to 25 uL and desalted by centrifugation using an Amicon Ultra Centricon (Millipore Corp.) in buffer C. The concentrated proteins were then loaded onto a 150 uL MonoS column (Bio-Rad) pre-equilibrated with buffer C. The column was washed three times with 300 uL buffer C and eluted with 100, 200, 400, and 600 mM NaCl in buffer C. The AP endonuclease assay on these eluted fractions revealed an activity in the 200 and 400 mM elution and the activity correlated with a 37 kDa band on a SDS-PAGE gel.

Protein sequencing

An analysis on 12% SDS-PAGE was performed on a preparative scale and the 37 kDa band was cut, washed with 50% acetonitrile in water and sequenced by LC-MS (Harvard Microchemistry).

Plasmids

PCR was used to amplify the entire GAPDH cDNA from the plasmid template (ATCC #817954R), digested with *Bam*H1 and *Eco*R1, and cloned into the *E. coli* expression vector pGEX-4T-1 (Amersham Biosciences) to produce the plasmid pGST-GAPDH. The pGST-GAPDH plasmid was used as the template to generate the pGST-GAPDH C152G, pGST-GAPDH C156G, and pGST-GAPDH C247G mutant plasmids with the QuickChange Site-Directed Mutagenesis kit (Stratagene, La Jolla, CA).

Proteins

GST-GAPDH fusion proteins were overexpressed in *E. coli* BW528 strain and purified by glutathione-Sepharose 4B mini columns (Amersham Biosciences). Briefly, the protein extracts were loaded onto the GST affinity column pre-equilibrated with buffer A which consisted of 50 mM Tris-HCl (pH 7.5), 100 mM NaCl, 0.5 mM EDTA, 0.5 mM DTT, and the protease inhibitor cocktail tablets (Complete Mini, EDTA-free, Roche Diagnostics GmbH). The column was then washed three times with buffer A and eluted with 250 μL of 50 mM Tris-HCl (pH 8.0) containing 10 mM reduced glutathione. The purified fusion protein GST-GAPDH was analyzed on an SDS-PAGE gel stained with Coomassie blue and then was assayed for AP endonuclease activity. In the case of His6-APE1, it was overexpressed in *E. coli* BL21(DE3) pLysS strain and purified by TALON Metal Affinity column (BD Biosciences) according to the instructions of the manufacturer with slight modifications. Briefly, the protein extracts (15 mg) were loaded onto the affinity column (0.3 mL) pre-equilibrated with binding buffer which consisted of 20

mM Tris (pH 8.0), 500 mM NaCL, 10% glycerol, 0.01% NP-40, and the protease inhibitor cocktail (Complete Mini, EDTA-free, Roche Diagnostics GmbH). The binding reaction was carried out at room temperature for 20 min. Then, the column was washed three times with 50 mM sodium phosphate, 300 mM NaCL and eluted with 300 μL of elution buffer consisting of 50 mM sodium phosphate, 300 mM NaCL, and 150 mM imidazole. Human, rabbit, chicken, porcine, and yeast GAPDH were purchase from Sigma-Aldrich.

GAPDH assay

GAPDH glycolytic activity of purified GST-GAPDH or commercial preparations of GAPDH from human, rabbit, chicken, porcine, and yeast was measured by spectrophotometric assay at 340 nm. Briefly, the assay was carried out in 0.015 M sodium pyrophosphate, 0.03 M sodium arsenate (pH 8.5) (Sigma), in the presence of 3.5 mM DTT, 0.26 mM NAD^+, and 0.51 mM glyceraldehyde 3-phosphate (Sigma). The reactions were performed for 10 min at 25°C.

Binding of GST-GAPDH to HIS-APE1 column

To analyze the GAPDH/APE1 interaction using the Talon metal affinity resin (Clonetech), 400 μL of matrix slurry was placed in a plastic disposable 10 mL gravity-flow column (Bio-Rad). The resin was equilibrated with 10 mL of buffer B [50 mM sodium phosphate (pH 7.0) and 300 mM NaCl]. At least 10 μg of purified HIS-APE1 protein was then incubated with the resin for 30 min at room temperature with gentle shaking. The column was washed with 30 mL of buffer B, followed by the addition of either 1 μg of purified GST-PNKP, GST-GAPDH, GST-GAPDH C152G, GST-GAPDH C156G, or GST-GAPDH C247G, and incubation for 1 h at room temperature. The column was washed with 30 mL of binding buffer (see above). Bound material was eluted with buffer B containing 150 mM imidazole and the eluted fraction was analyzed by Western Blot.

GST pull down assays

Glutathione-Sepharose 4B beads (100 μL) alone or bound to 10 μg GST-tagged protein allowed to mixed with purified N-terminal 6His-tagged APE1 (1 μg) in 0.5 mL in buffer A and incubated for 30 min at room temperature with gentle rotation. The beads were washed three times buffer A and an aliquot was analyzed for bound proteins by SDS-PAGE followed by Western blots probed with either anti-HIS or anti-GST monoclonal antibody.

Immunoprecipitation

IP was performed on whole-cell lysates prepared in lysis buffer [62.5 mM Tris-HCl (pH 6.8), 10% glycerol, 2% SDS, and the protease inhibitor cocktail (Complete Mini, EDTA-free, Roche Diagnostics GmbH)], and then diluted 10-fold with RIPA buffer [50 mM Tris-HCl (pH 7.4), 1% NP-40, 0.25% sodium deoxycholate, 1 mM EDTA, and 150 mM NaCl]. Following preclearing with 30 μL of Protein G plus/A agarose beads (Santa Cruz Biotechnology, Santa Cruz, CA), 1.5 mg of total protein was incubated with anti-APE1 antibodies overnight at 4°C, and then incubated with 50 μL of Protein G plus/A agarose beads for another 1 h at 4°C. The beads were washed four times with RIPA buffer, and then boiled in 2X SDS sample buffer. The immunoprecipitates were then subjected to SDS-PAGE and the specific proteins were detected by immunoblotting with monoclonal anti-GAPDH antibody (Chemicon).

Immunodetection

The antibodies used in this study were monoclonal anti-HIS (Santa Cruz) and anti-GAPDH (Chemicon), and polyclonal anti-GST (Sigma). For Western analysis, the antibodies were used at a dilution of 1:5000, 1:2000 and 1:5000, respectively, in 10 mM Tris-HCl (pH 7.5), 150 mM NaCl, and 5% powdered milk [206]. Ten milliliters of this mixture were used to probe nitrocellulose blots (8 cm x 10 cm) overnight at 4°C. The secondary antibodies were anti-mouse for the HIS and GAPDH

monoclonal antibodies and anti-rabbit for the GST antibodies. Anti-mouse and anti-rabbit were used at a dilution of 1:2500 and 1:5000, respectively, and detected by the enhanced chemiluminescence system (Dupont, NEN).

Oxidation of His-APE1 protein with H_2O_2

The His6-APE1 proteins bound to the TALON metal affinity column (BD Biosciences) were treated with 15 mM H_2O_2 (Sigma), washed 3 times with buffer B [50 mM sodium phosphate (pH 7.0) and 300 mM NaCl], and then eluted using buffer B containing 150 mM imidazole. The eluted proteins were dialyzed in a Spectra/Por 1 dialysis tube (MWCO 6K-8K, Spectrum) by repeated concentration and dilution with 18 mM Tris-HCl (pH 7.5), 48 mM NaCl for five times. The concentrations of the proteins were estimated on a Coomassie blue-stained 12% SDS-PAGE gel.

Site-directed mutagenesis

The QuickChange Site-Directed Mutagenesis kit (Stratagene) was used to change the cysteine residues to glycine using the pGST-GAPDH plasmid as the template. Oligonucleotides GAPDH C152G-F1 (5'-CATCAGCAATGCCTCCGG-CACCACCAACTGCTTAGC-3'), GAPDH C156G-F2 (5'-GCCTCCTGCACCA-CCAACGGCTTAGCACCCCTGGC-3'), and GAPDH C247G-F3 (5'-GTGGTGGACCTGACCGGCCGTCTAGAAAAACCTGCC-3') were used to generate the pGST-GAPDH C152G, pGST-GAPDH C156G, and pGST-GAPDH C247G mutant plasmids, respectively. The mutations were verified by DNA sequence analysis. All the above oligonucleotide primers were synthesized by Invitrogen, Life Technologies, USA.

Chemical oxidation of GST-GAPDH

The GST-GAPDH proteins bound to the glutathione-Sepharose 4B resin (Amersham Pharmacia Biotech) were treated with 15 mM H_2O_2 at 37°C for 10 min. The column was then washed three times with buffer A which consisted of 50 mM

Tris-HCl (pH 7.5), 100 mM NaCl, 0.5 mM EDTA, 0.5 mM DTT, and the protease inhibitor cocktail tablets (Complete Mini, EDTA-free, Roche Diagnostics GmbH) and eluted with 250 μL of 50 mM Tris-HCl (pH 8.0) containing 10 mM reduced glutathione. The eluted proteins were dialyzed in a Spectra/Por 1 dialysis tube (MWCO 6K-8K, Spectrum) by repeated concentration and dilution with 18 mM Tris-HCl (pH 7.5), 48 mM NaCl for five times.

siRNA-mediated GAPDH silencing

Small interfering RNA (siRNA) was used to knockdown the expression of GAPDH. HCT116 cells (100 000 cells/mL/well) were seeded in 6-well plates and transfected with 75 nM of GAPDH siRNA or the control siRNA (that has not significant homology to any known gene sequences from mouse or human) using lipofectamine (Invitrogen) in Opti-MEM (Invitrogen). The transfection was allowed to proceed at 37°C for 4 h after which the cells were incubated in 2 mL of McCoy5A media containing 10% FBS for 48 h. These transiently transfected HCT116 cells were subjected to different treatments as described below or harvested for Western blotting.

Drug exposure and clonogenic assay

The washed confluent cells were exposed to different drugs. H_2O_2 was diluted in the medium at a final concentration of 25 mM whereas MMS was prepared as 250 mM stock solution in distilled water. All of the drugs were dissolved in RPMI for DLD-1 cells whereas in McCoy5A for HCT116 cells prior to incubation. Drug incubation was conducted in the incomplete medium for 30 min at 37°C at a cell density of 2×10^6 cells/mL in 5 mL and 100 000 cell/mL in 2 mL. After the treatment the cells were rinsed with 1X PBS, trypsynized, counted and plated in duplicates for the colony forming unit assay (CFU). The cells were cultured for 14 days at 37°C with 5% CO_2 in humidified atmosphere. Colonies were counted after staining them with methylene blue [207].

UV irradiation

Cells were irradiated with monochromatic 254 nm UV light (UVC) and UVB at a dose rate ranging from 0-20 J/m^2 and 50-200 J/m^2, respectively, in 1X PBS. The cell cultures were irradiated with acute doses of either polychromatic UVB (290–320 nm) or monochromatic UVC at room temperature. The UVB source consisted of two fluorescent tubes (F15T8 UVB lamp; Ultraviolet Products) generating a dose rate of 4 J/m^2/s. The incident UVB was filtered by using a sheet of cellulose acetate (Kodacel TA-407 0.015 in; Eastman Kodak) to virtually eliminate contaminating wavelengths below 290 nm. In the case of UVC, cells were irradiated with a G25T8 germicidal lamp (Sankyo Denki) at a dose rate of 0.2 J/m^2/s. UVB and UVC fluences were measured with a Spectroline DRC 100× digital radiometer (Spectronics, Westbury, NY) equipped with DIX 300 and 254 sensors, respectively. It should be noted that the UVB lamp emitted some measurable incident energy within the UVA range (320–400 nm), which could not be eliminated. Although we cannot categorically rule out that this UVA component exerted some effect, the total UVA output under our exposure conditions, i.e., ≈50 J/m^2, was unlikely to elicit any significant biological response given that UVA is ≈50,000-fold less genotoxic than UVB on a per-joule basis [208].

Western blot

The transfected cells were harvested by trypsinization and subjected to protein extraction by cell lysis. The supernatant was collected and the protein was quantified by Bradford's dye binding method with bovine serum albumin (BSA) as a standard. Western blotting was performed to evaluate the expression of GAPDH in the transfected cells. 80 μg of the protein lysate was resolved on a 10% denaturing polyacrylamide gel (with 3% polyacrylamide stacking) and transferred electrophoretically to a nitrocellulose membrane (Amersham Biosciences). After blocking with 5% nonfat dry milk in TBS, the membrane was incubated with mouse anti-GAPDH (Chemicon) for overnight at 4°C. Immunoreactive proteins were localized with horseradish peroxidase–conjugated secondary antibodies membrane (Amersham Biosciences) for 1 h at room temperature. After washing with TBS, the

reactants were developed using the enhanced chemiluminescence kit (Amersham Biosciences).

RESULTS

Purification of a Mg^{2+}-independent AP endonuclease activity

We used total cell extracts derived from cultured LF1 human lung fibroblasts as a source to search for a Mg^{2+}-independent AP endonuclease(s) that could share similar enzymatic properties as those reported for members of the *E. coli* endonuclease (endo) IV family [60,133]. The total human cell extracts were subjected to six chromatographic columns and monitored for a Mg^{2+}-independent AP endonuclease activity by enzymatic assay after each step of purification (see the Materials and Methods). The final protein purification step was achieved by a NaCl discontinuous gradient on a MonoS column, which yielded a single polypeptide of approximately 37 kDa as visualized by Coomassie blue staining (Figure 4-1A). No additional polypeptide was detected in the MonoS purified fractions upon extensive staining with either Coomassie blue or silver stain (Figure 4-1A and data not shown). The intensity of the purified polypeptide corresponded with the level of AP endonuclease activity, that is, most of the activity was present in the 0.4 M NaCl fraction (Figures 4-1A, lane 4, and B). Increasing amount of the purified polypeptide present in the 0.4 M NaCl fraction resulted in an increase production of the 20-mer product, strongly suggesting that the purified protein contained AP endonuclease activity (Figure 4-1C). This purified protein also cleaved acid treated plasmid DNA containing a single AP site, indicating that the activity is not specifically acting on the 42-mer substrate (data not shown). The protein was unable to nick native single-stranded or double-stranded DNA, suggesting that it lacks endonuclease activity (data not shown). Moreover, the protein cannot cleave the 42-mer double-stranded oligonucleotide containing the U•G mismatch, unless the uracil is removed consistent with the notion that the purified protein fraction has associated AP endonuclease activity (data not shown). In additional control experiments, we assessed the purified protein fraction for the presence of enzymes that belong to the base excision DNA repair pathway including AP lyase, DNA polymerase, and DNA ligase. However, none of these enzymatic activities was displayed by the purified protein fraction, indicating that the AP endonuclease activity is not associated with other base excision repair proteins (data not shown).

Figure 4-1. Purification of a Mg^{2+}-independent AP endonuclease enzyme.

(A) The eluted fractions from the final step of purification on a Mono S column were analyzed by an SDS-PAGE gel stained with Coomassie blue. (B) The eluted fractions from A were assayed for AP endonuclease activity (see Materials and Methods). (C) An increasing amount the purified polypeptide was assayed for AP endonuclease activity (lanes 1 to 5, 1, 5, 10, 25, and 50 ng, respectively). Purified endo IV (lane 6; 100 ng) was used as a positive control. The AP endonuclease assay was monitored by autoradiography following resolution on a 10% polyacrylamide (19:1 acrylamide:bisacrylamide ratio)-7 M urea sequencing gel. Arrows indicate positions of the 42-mer substrate and the 20-mer product.

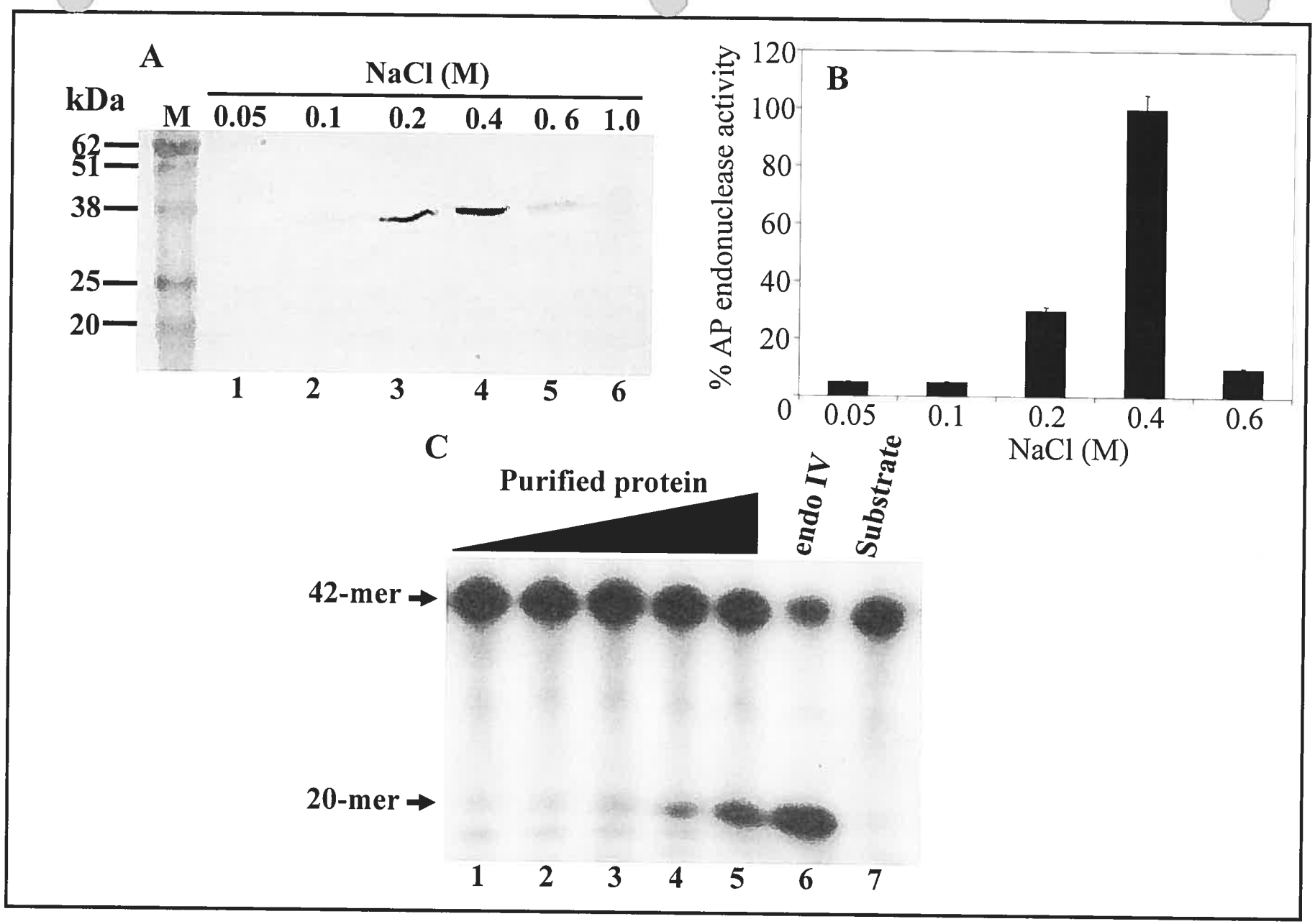

FIGURE 4-1. Jilani *et al.*, 2006

Identification of GAPDH in the purified protein fraction

To determine the identity of the 37 kDa purified protein, the polypeptide band was excised and analyzed by mass spectrometry [209]. Of 59 individual sequences (MS/MS spectra) analyzed, all showed 95 to 100% identity to the human GAPDH enzyme. GAPDH was originally discovered as a glycolytic enzyme, which uses the cofactor NAD+ to catalyze the conversion of glyceraldehyde-3-phosphate to 1,3-diphosphoglycerate with the concomitant release of NADH in an oxidation-reduction reaction [193]. To ascertain that our purified protein is indeed GAPDH, we tested for its enzymatic activity by monitoring NADH formation via absorption at 340 nm [160]. The purified protein displayed a comparable level of GAPDH activity when compared to a commercial preparation of human GAPDH (Figure 4-2A).

Purified GAPDH exhibits no AP endonuclease activity

GAPDH has been demonstrated to play a role in DNA repair, for example, binding to specific DNA lesions [210]. To directly test if that our purified GAPDH protein has either an intrinsic or a tightly associated protein with AP endonuclease activity, we inserted in-frame the cDNA encoding the entire human retina GAPDH next to the glutathione S-transferase (GST) gene in the pGEX-4T-1 bacterial expression vector to produce the plasmid pGST-GAPDH. The pGST-GAPDH plasmid was introduced into the *E. coli* strain BW528 (which lacks AP endonuclease activity, see below) and the protein extracts derived from transformed bacteria were passed onto a glutathione column to purify the GST-GAPDH fusion protein. The full length GST-GAPDH (63 kDa) appeared to be the major polypeptide, although some minor lower molecular weight species that could be degradation products were also detected by Coomassie blue staining (Figure 4-2B). Moreover, the GAPDH assay revealed that the purified GST-GAPDH fusion protein exhibits a significant level of activity as compared to the purified native untagged form of GAPDH (Figure 4-2A), thus suggesting GST-GAPDH is functionally active.

Figure 4-2. Purified polypeptide is the glycolytic enzyme GAPDH.

(A) Measurement of the GAPDH glycolytic activity from the commercial preparation of human GAPDH (opened circles), the purified polypeptide (filled circles), and the fusion proteins GST-GAPDH (filled squares), GST-GAPDH C152G (opened triangles), GST-GAPDH C156G (filled triangles), and GST-GAPDH C247G (opened squares) was done by spectrophotometric assay at 340 nm. (B) Expression and purification of GST-GAPDH using *E. coli*. Total extracts derived from BW528 strain carrying the pGST-GAPDH plasmid were purified on GST affinity columns and analyzed on a SDS-PAGE gel stained with Coomassie blue. Lane 3 contained 200 ng of the purified GST-GAPDH fusion protein. Molecular mass standards (kDa) are shown in lane 1.

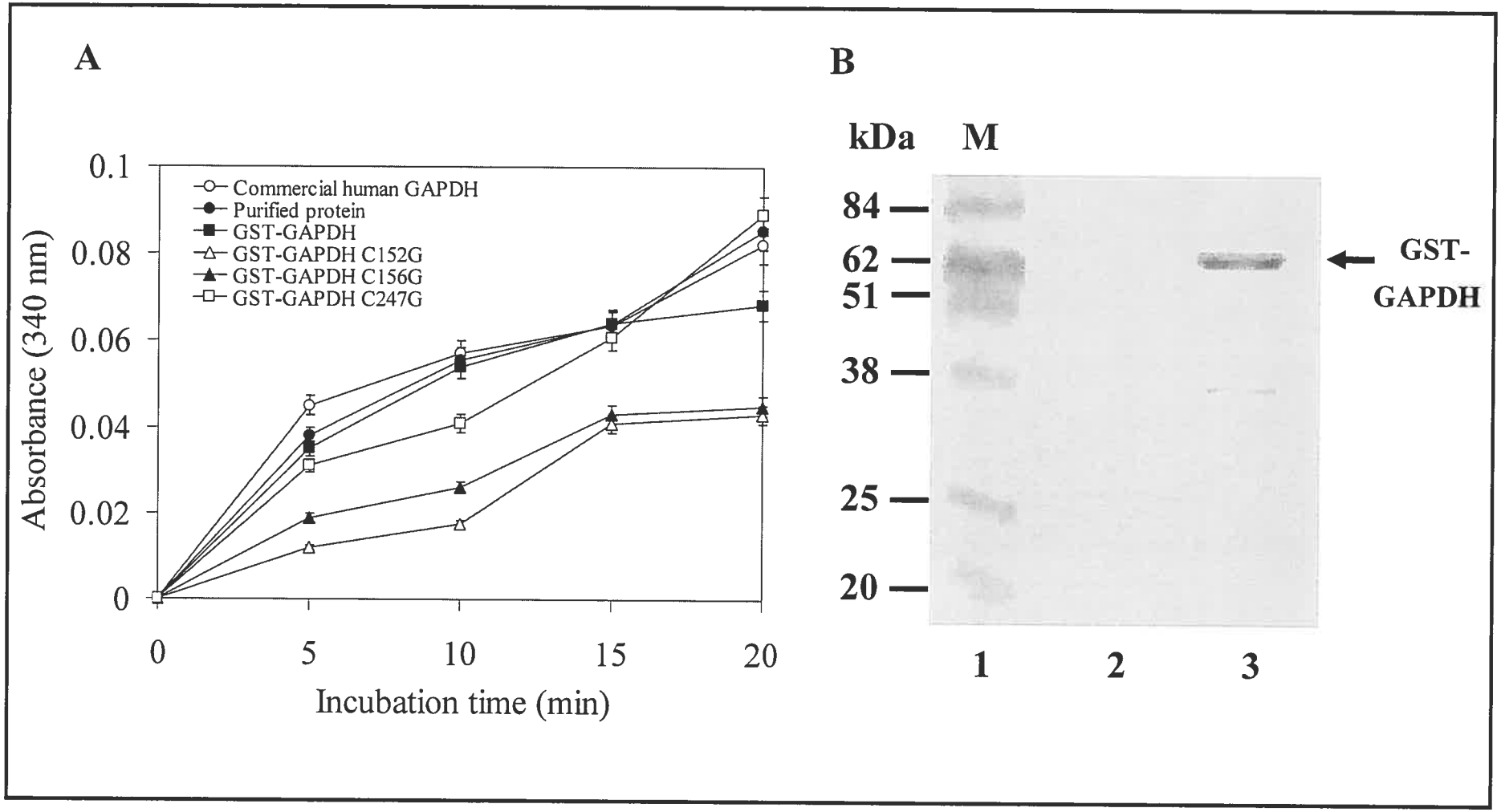

FIGURE 4-2. Jilani *et al.*, 2006

We next examined if the GST-GAPDH fusion protein possessed the ability to cleave the AP site substrate. No 20-mer products was observed with the GST-GAPDH fusion protein (see Figure 4-4 below), indicating that it lacks AP endonuclease activity and free of contamination by AP endonucleases. Furthermore, sequence comparison of GAPDH with the two known families of AP endonucleases, Endo IV and Exo III, yielded no significant similarity, thus excluding the possibility that GAPDH bears a nuclease motif (data not shown).

On the basis of these above findings, we strongly believe that GAPDH does not contain an intrinsic AP endonuclease activity, and may instead be tightly associated with such an activity.

Interaction of GAPDH with APE1

To examine whether GAPDH is associated with an AP endonuclease activity, we generated affinity chromatography columns of GST-GAPDH-Sepharose 4B or GST-Sepharose 4B as described under Materials and Methods. The columns were loaded with LF1 cell extracts, washed and directly tested for AP endonuclease activity. The GST-GAPDH column retained an AP endonuclease activity, whereas in contrast, no AP endonuclease activity was detected with the GST column (data not shown). Since the major AP endonuclease present in human lung fibroblasts is due to APE1, we strongly suggest that this protein is likely interacting with GAPDH resulting in the observed associated AP endonuclease activity.

To analyze if the interaction between GAPDH and APE1 is direct, we prepared a Talon affinity column consisting of functionally active N-terminal His-tagged APE1 and performed affinity chromatography assays (see Materials and Methods). Thus, purified GST-GAPDH was applied onto a HIS-APE1 column and the binding analyzed by Western blotting using anti-GST antibody. As shown by Figure 4-3A, GST-GAPDH did directly bind to the HIS-APE1 column, but not to the empty Talon column (lane 4 vs lane 3, lanes 5-10 are discussed below). In additional control experiments, the DNA repair protein PNKP (polynucleotide kinase 3'-phosphatase) fused to GST did not bind to the HIS-APE1 column, suggesting that

Figure 4-3. GAPDH interacts directly with APE1.

(A) Equal amounts (200 ng) of purified GST-PNKP (lanes 1 and 2), GST-GAPDH (lanes 3 and 4), GST-GAPDH C152G (lanes 5 and 6), GST-GAPDH C156G (lanes 7 and 8), and GST-GAPDH C147G (lane 9 and 10) fusion protein were loaded onto either empty TALON (lanes 1, 3, 5, 7, and 9) or HIS-APE1-conjugated TALON columns (lanes 2, 4, 6, 8, and 10), followed by extensive washing and direct analysis of the column matrix by Western blotting with an anti-GST antibody. Molecular weight standards (kDa) are shown on the left. (B) Purified HIS-APE1 fusion protein was loaded onto either GST-PNKP (lane1), GST (lane 2), or GST-GAPDH (lane 4) column and assayed for binding. Bound HIS-APE1 fusion proteins were eluted and analyzed by Western blotting with anti-HIS antibody (right panel). Inputs of HIS-APE1 (lane 3), GST (lane 5), and GST-GAPDH (lane 6) were also loaded. Molecular weight standards (kDa) are shown in the middle. (C) Immunoprecipitation experiment. Polyclonal anti-APE1 antibodies specifically precipitated GAPDH from HCT116 cell extracts (lane 4). GAPDH was not immunoprecipitated in a mock immunoprecipitation reaction (lane 3). 10% (150 μg) and 20% (300 μg) of the total input are shown in lanes 1 and 2, respectively. Molecular weight standards (kDa) are shown on the left. (D) AP endonuclease assay with commercial preparations of GAPDH from pig (lanes 3-5; 20, 40, and 60 ng, respectively) and yeast (lanes 6-8; 20, 40, and 60 ng, respectively). Purified endo IV (lane 2; 100 ng) was used as a positive control. Arrows indicate positions of the 42-mer substrate and the 20-mer product.

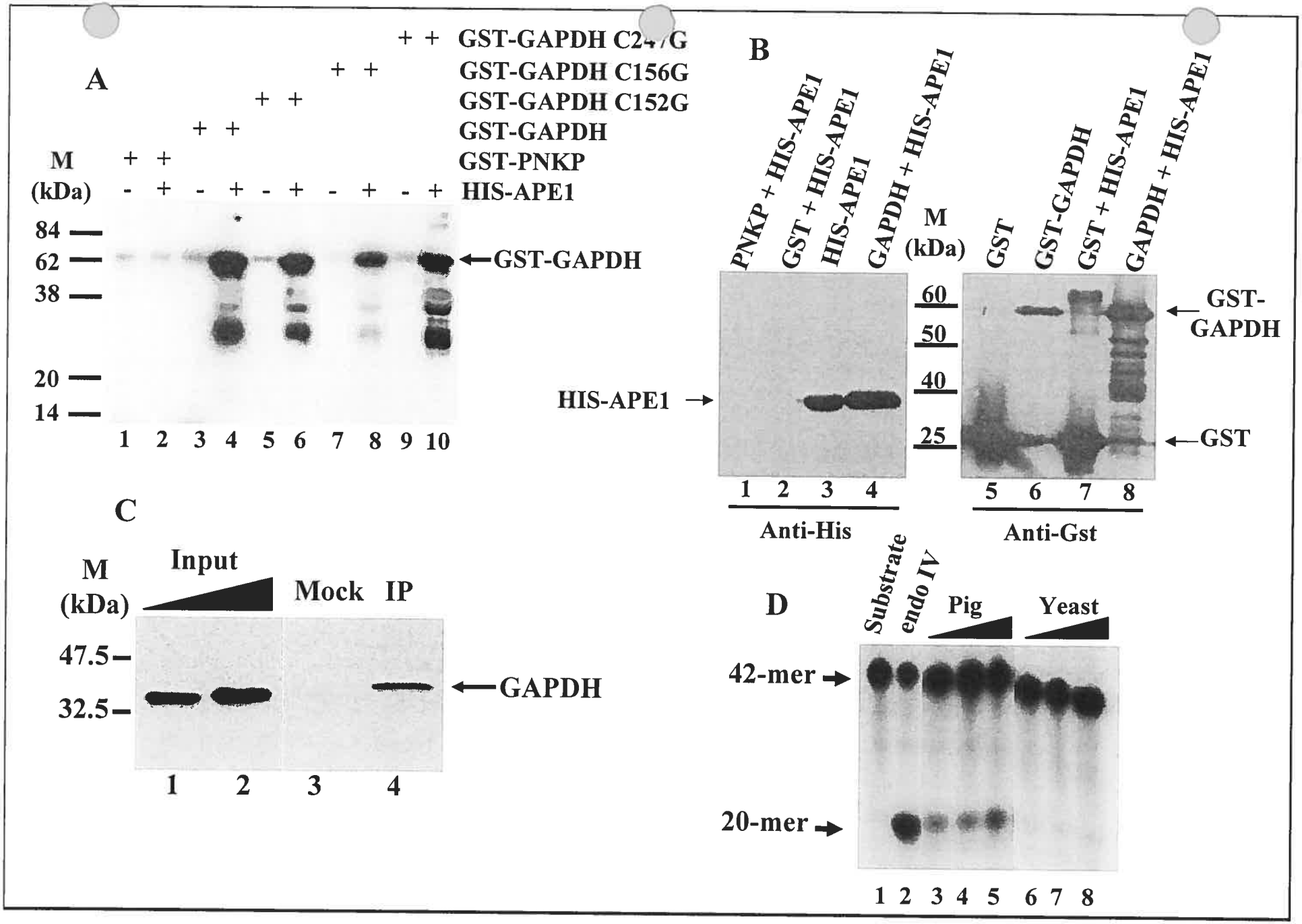

FIGURE 4-3. Jilani *et al.*, 2006

APE1 interacts specifically with GAPDH *in vitro* (Figure 4-3A, lane 2). To confirm that GAPDH directly binds to APE1, a reverse affinity chromatography was performed using purified HIS-APE1 and Sepharose 4B columns containing either GST-GAPDH, GST-PNKP, or GST alone. Purified HIS-APE1 was then loaded separately onto the three Sepharose 4B columns. Results revealed that HIS-APE1 associated with the GST-GAPDH column, but neither to the GST-PNKP nor the GST column, confirming that APE1 and GAPDH interact specifically *in vitro* (Figure 4-3B, lane 4 vs lanes 1-2).

To investigate whether GAPDH and APE1 may interact *in vivo*, immunoprecipitation experiments were carried out. HCT116 cell extracts were immunoprecipitated using an anti-APE1 antibody and the presence of GAPDH in the immunoprecipitates was analyzed by Western blotting, using anti-GAPDH antibodies. As shown in Figure 4-3C, endogenous APE1 and GAPDH coimmunoprecipitated, suggesting that both proteins might be associated in the cells.

Together these *in vitro* and *in vivo* results indicate that commercial preparations of GAPDH are also likely to be associated with APE1 AP endonuclease activity. To test this assumption, we performed AP endonuclease assays using commercial source of GAPDH derived from human, rabbit, chicken, pig, and yeast. GAPDH from a mammalian source such as pig nicked the AP site substrate, but not from yeast which does not possess APE1 protein (Figure 4-3D, lanes 3-5 vs lane 6-8). In control experiments, the glycolytic enzymes pyruvate dehydrogenase and 6-phosphofructokinase obtained from the same commercial source did not contain any detectable level of AP endonuclease activity (data not shown).

Activation of AP endonuclease activity of APE1 by GAPDH

It is well documented that APE1 exists in the oxidized and reduced forms [116] and that the reduced form is necessary to activate transcription factors including p53, NF-κB, and c-Jun and c-Fos, subunits of AP-1 [109,203,204]. Moreover, it has been shown that thioredoxin is required to activate APE1 in order to potentiate AP-1 transcriptional activity [116]. As such, we explored the possibility if GAPDH could

function to activate APE1 AP endonuclease activity. In this experiment, we first determined the minimal amount of purified HIS-APE1 that showed no detectable AP endonuclease activity. Purified HIS-APE1 in the range of 0.1 to 2 ng showed no measurable AP endonuclease activity (Figure 4-4, lane 3 showing 1 ng), while a significant level of activity was observed with 10 ng of the protein (Figure 4-4, lane 4). We next assessed if preincubating a fixed amount (1 ng) of HIS-APE1 with increasing amounts of GST-GAPDH would reveal any level of AP endonuclease activity. As shown in Figure 4-4, the HIS-APE1 AP endonuclease activity was indeed revealed by increasing amounts of GST-GAPDH (lanes 13 to 16). In control experiments, neither purified GST nor GST-PNKP activated the HIS-APE1 AP endonuclease activity (lanes 9 to 12, and data not shown). Since the purified GST-GAPDH from *E. coli* is free of contaminating AP endonuclease activity (Figure 4-4, lanes 7 and 8, and also above), we suggest that GAPDH may play a role to reactivate an inactive form of APE1.

GAPDH functions to reduce the oxidized form of APE1

Since APE1 exists in the oxidized and reduced forms, which correspond to its inactive and active state, respectively, we therefore assessed whether APE1 redox status is affected by GAPDH. Silver stain analysis under nonreducing conditions of purified HIS-APE1 revealed a set of heterogenous bands (Figure 4-5A, lane 1). When HIS-APE1 was incubated with an excess of purified GST-GAPDH, the heterogenous bands of APE1 migrate as a single band (or monomer) and became more intensely stained (Figure 4-5A, lane 4). This phenomenon was not observed when HIS-APE1 was incubated with either glutathione or purified GST (Figure 4-5A, lanes 2 and 3, respectively). When the same experiment was performed with a reducing buffer (Figure 4-5A, lanes 7-9), monomers of HIS-APE1 were intensely stained by silver nitrate independently of the presence of GST-GAPDH (Figure 4-5A, lane 9). Analysis of the purified protein under reducing conditions (Figure 4-5A, lane 6)

Figure 4-4. GAPDH stimulates APE1 AP endonuclease activity.

Increasing concentrations: 1, 10, 25, and 50 ng, of either purified GST (lanes 9 -12) or GST-GAPDH (lanes 13-16) were added to 1 ng of purified HIS-APE1 (lanes 9-16). Purified HIS-APE1 (1 and 10 ng, lanes 3 and 4, respectively), GST (1 and 50 ng, lanes 5 and 6, respectively), and GST-GAPDH (1 and 50 ng, lanes 7 and 8, respectively) were assayed alone in control experiments. Arrows indicate positions of the 42-mer substrate and the 20-mer product.

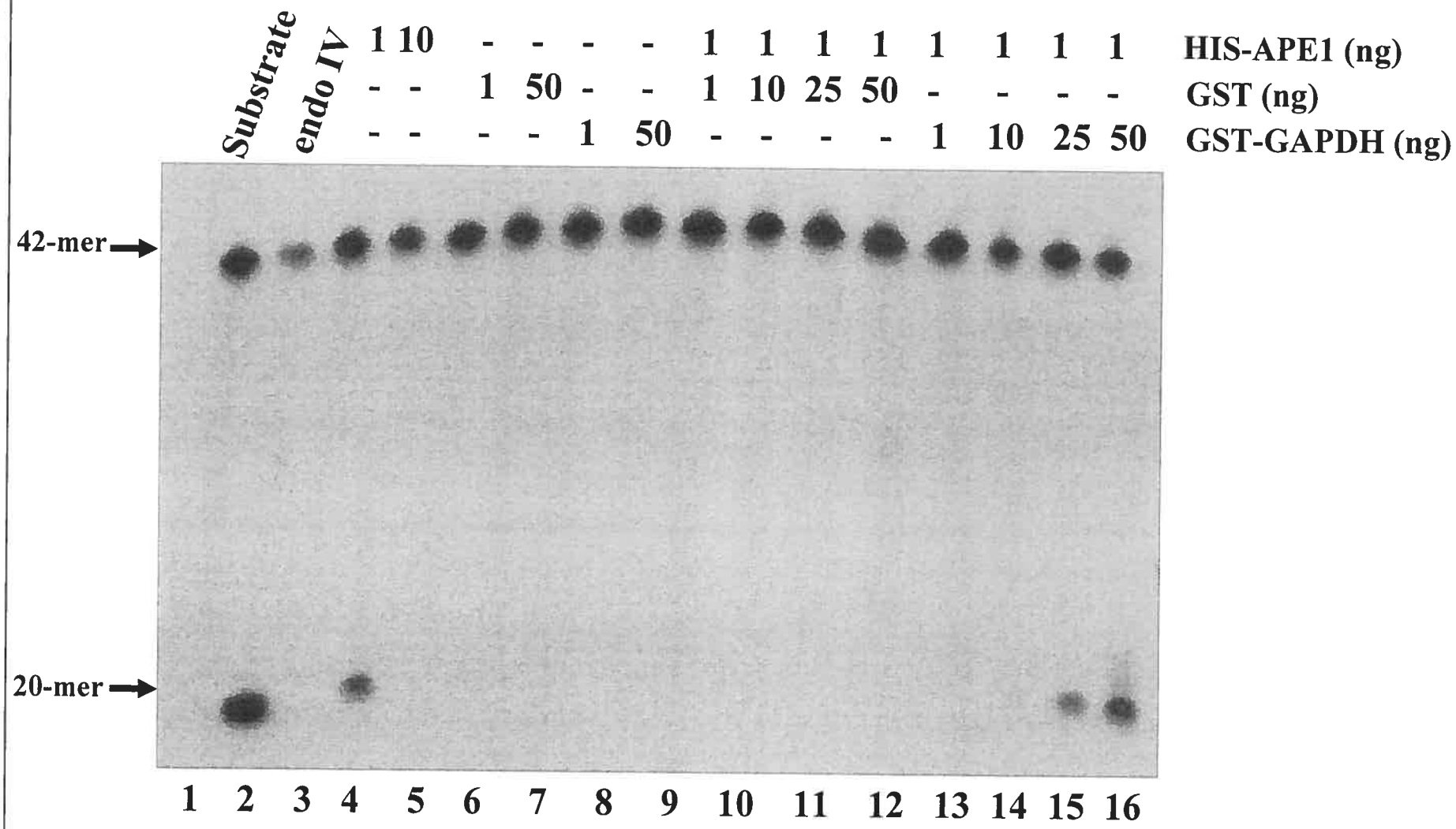

FIGURE 4-4. Jilani *et al.*, 2006

Figure 4-5. GAPDH stimulates APE1 AP endonuclease activity via a redox reaction.

(A) GAPDH affects the redox state of APE1. Either glutathione (lanes 2 and 7), GST (lanes 3 and 8), or GST-GAPDH (lanes 4 and 9) was incubated with HIS-APE1 (lanes 1-4 and 6-9) at 37°C for 30 min. Reactions were analyzed on SDS-PAGE gel under non-reducing (lanes 1-5) or reducing conditions (lanes 6-9) and stained with silver nitrate. The right arrows indicate the positions of the reduced and oxidized forms of HIS-APE1. The left arrows indicate the positions of the purified GST-GAPDH, HIS-APE1, and GST proteins. Molecular mass standards (kDa) are shown on the left. (B) GAPDH stimulates oxidized APE1 AP endonuclease activity in a dose-dependent manner. Chemically oxidized HIS-APE1 (20 ng) was added to either 5, 20 and 50 ng of purified GST (lanes 10-12, respectively) or 5, 20, 50, and 100 ng of purified GST-GAPDH (lanes 13-16, respectively); 1, 10, and 50 ng of purified HIS-APE1, lanes 3-5, respectively; 20 and 100 ng of oxidized HIS-APE1, lanes 6 and 7, respectively; 50 ng of purified GST, lane 8; and 50 ng of GST-GAPDH, lane 9. Purified endo IV (lane 2; 100 ng) was used as a positive control. Arrows indicate positions of the 42-mer substrate and the 20-mer product.

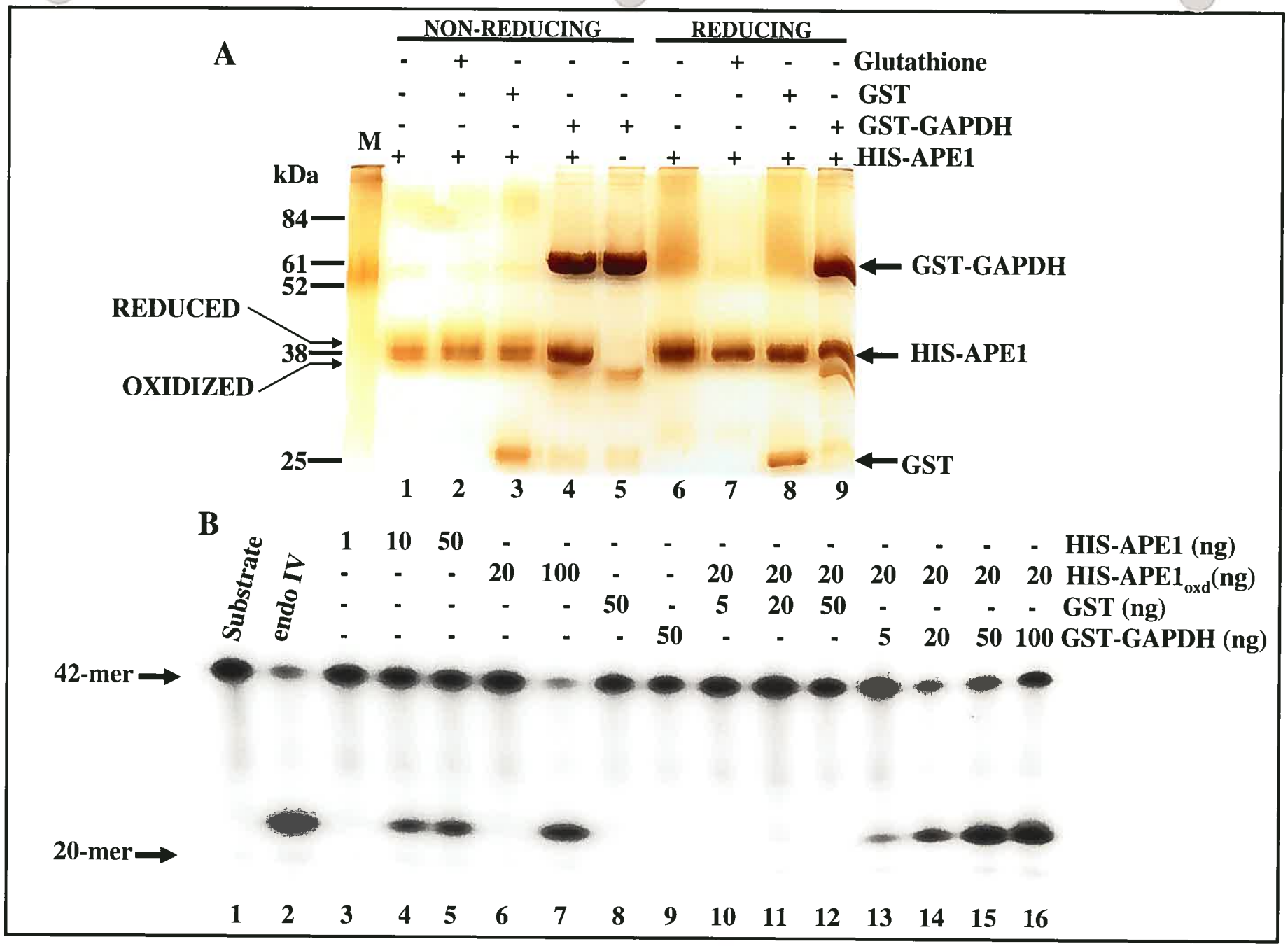

FIGURE 4-5. Jilani *et al.*, 2006

confirms previous data which showed that APE1 moves as a monomer under reducing conditions [116]. Taken together, these results suggest that stimulation of APE1 AP endonuclease activity results from a reduction reaction mediated by GAPDH.

To further test whether GAPDH can affect AP endonuclease activity of oxidized APE1, we performed an AP endonuclease assay with chemically oxidized purified HIS-APE1 (HIS-APE1$_{oxd}$) and different amounts of purified GST-GAPDH. As shown in Figure 4-5B, in the presence of 20 ng of HIS-APE1$_{oxd}$, which does not show any detectable AP endonuclease activity (lane 6), GAPDH stimulated AP endonuclease activity in a concentration-dependent fashion (lanes 13-16). Moreover, reducing agents such as NAC (N-acetylcysteine), glutathione, and DTT (dithiothrietiol), used at 1 and 5 mM concentrations, did not have a stimulatory effect on HIS-APE1$_{oxd}$ AP endonuclease activity (data not shown). These results indicate that GAPDH might perform a specific role regarding the reactivation of oxidized APE1 AP endonuclease activity via a redox reaction.

Mutation of cysteine 152 and 156 of GAPDH to glycine affects the reactivation the AP endonuclease activity

If indeed GAPDH serves as a redox factor for APE1, we expect that it should contain redox cysteines. Analysis of GAPDH amino acid sequence revealed that it possesses two cysteine amino acid residues at positions Cys152 (C152) and Cys156 (C156) (152CTTNC156) that showed similarities with the conserved redox center of thioredoxin (32CGPC35). As such, we investigated whether the cysteine residues C152 and C156 in GAPDH are important for the interaction and/or the reactivation of oxidized APE1, we substituted these residues with glycine by site-directed mutagenesis in the pGST-GAPDH plasmid. Another glycine substitution at cysteine 247 (C247) was done to serve as a control. The mutated and wild type plasmids were transformed in *E. coli* and the corresponding fusion proteins purified as described under Materials and Methods. The mutated proteins migrated on gels at the same position as wild type GST-GAPDH and were expressed with similar efficiency

(Figure 4-3A), suggesting that mutations did not induced major structural deformation to trigger proteolysis. The mutant fusion proteins were thus as stable as the wild type GST-GAPDH. However, conversion of C152 and C156 to glycine reduced GAPDH activity by approximately 33%, when compared to either the C247G or wild type protein (Figure 4-2A).

To test whether the cysteine to glycine substitution in GAPDH affects the interaction with APE1, we used the affinity chromatography approach to monitor for retention of GAPDH and its variants. As shown in Figure 4-3A, all GAPDH variants bind to HIS-APE1 columns (lanes 6, 8, and 10), suggesting that glycine substitution did not affect the ability of GAPDH to interact with APE1.

To address the contribution of C152 and C156 residues in the stimulation of oxidized APE1 AP endonuclease activity, we used the purified mutated proteins in *in vitro* AP endonuclease assays. The conversion of C152 and C156 to glycine abolished the stimulation of HIS-APE1$_{oxd}$ (Figure 4-6, lanes 6-9 and 10-13). In contrast, amino acid change at C247 did not affect the reactivation of HIS-APE1$_{oxd}$. Taken together, these data strongly suggest that GAPDH utilizes C152 and C156 in the redox reaction to reactivate HIS-APE1$_{oxd}$.

Overexpression of GAPDH enhances cellular resistance to MMS and H2O2, but not UVC

As our results indicate that GAPDH is able to modulate APE1 activity *in* vitro, we aimed to study whether overexpression of GAPDH affect cellular sensitivity to DNA damaging agents. Thus, we examined the response of DLD-1 cells that are stably transfected with an expression vector harboring GFP-GAPDH or GFP (that was used as a control) [211] to MMS, H_2O_2, and UVC. MMS and H_2O_2 are known to induce APE1-repairable DNA lesions, whereas UVC produces DNA damage that are repaired by the NER pathway. DLD-1 cells overexpressing GAPDH displayed 2- to 3-fold increase in protection against MMS and H_2O_2 (Figure 4-7A, left and right panel, respectively). In contrast, overexpression of GAPDH did not confer additional

Figure 4-6. Cysteine 152 and 156 residues of GAPDH are important to stimulate APE1 AP endonuclease activity.

The following amounts of either GST-GAPDH (lanes 2-5), GST-GAPDH C152G (lanes 6-9), GST-GAPDH C156G (lanes 10-13), or GST-GAPDH C247G (lanes 14-17) was incubated with 20 ng of purified HIS-APE1$_{oxd}$ (lanes 1-17): 1, 10, 25, and 50 ng. Endo IV (lane 19) was used as a positive control. Arrows indicate positions of the 42-mer substrate and the 20-mer product.

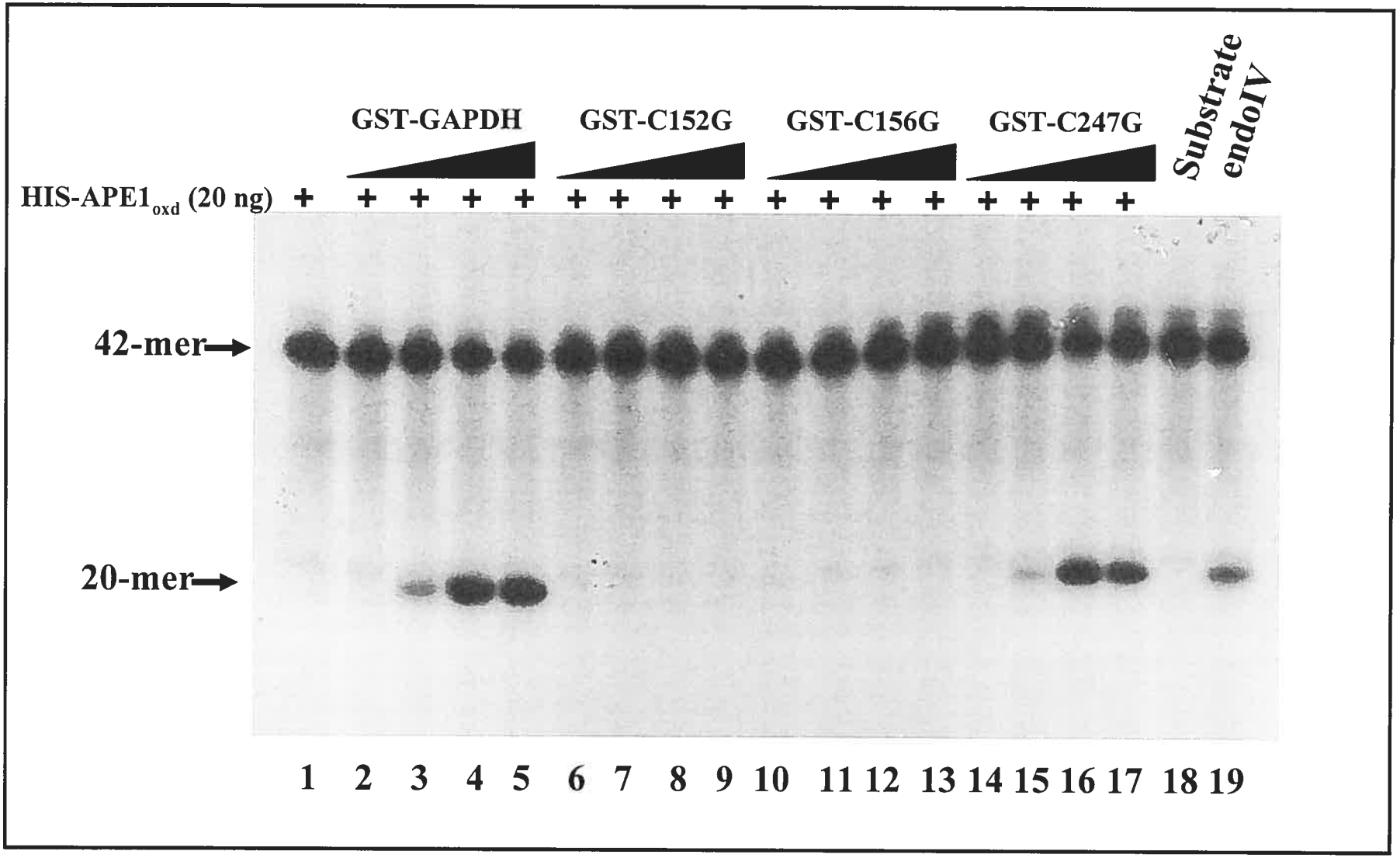

FIGURE 4-6. Jilani *et al.*, 2006

resistance to UVC in comparison to cells transfected with the GFP control vector (Figure 4-7A, center panel). Thus, the increase cellular resistance observed in DLD-1 cells overexpressing GAPDH to MMS and H_2O_2 appears to reflect the stimulation of APE AP endonuclease activity by GAPDH.

GAPDH function is necessary for protection against APE1-repairable DNA damage

To further address the role of GAPDH in response to DNA damage, we took advantage of siRNA technology to inhibit GAPDH function. HCT116 cells were transfected with either the control or GAPDH siRNAs. The transfected cells were then screened for suppression of GAPDH levels by Western blot analysis. As shown in Figure 4-7B, the three cell populations that were chosen exhibited >50% reduction in GAPDH protein levels (lanes 2-4). The GAPDH knockdowns showed no apparent differences in growth rate as compared with their counterparts that have normal levels of GAPDH (data not shown). Then, we exposed GAPDH knockdowns to various concentrations of MMS, H_2O_2, and to increasing doses of UVC, following which we performed cell viability assays. The results showed that suppression of GAPDH by siRNA markedly sensitized HCT116 cells to MMS and H_2O_2 (Figure 4-7C, left panel, and data not shown). However, GAPDH silencing did not produce sensitization to UVC, but interestingly provided partial resistance to UVC as compared to control siRNA (Figure 4-7C, right panel).

Figure 4-7. GAPDH plays an important role in protecting cells against MMS and H_2O_2, but not UVC.

(A) The percentage of DLD-1 viable cells overexpressing pGFP-GAPDH (filled circles) or control pGFP (open circles) (as shown in the inset) after treatment with varying concentrations of MMS (left panel) and H_2O_2 (right panel), and increasing doses of UVC (center panel). (B) Inhibition of GAPDH by siRNA. HCT116 cells were transfected by 75 nM of either siRNA against GAPDH (lanes 3 and 4) or control siRNA (lanes 1 and 2). Western blotting was done to confirm the knockdown using either anti-GAPDH (upper panel) or anti-APE1 (middle panel) antibody with 15 and 30 μg of cell extracts (lanes 1-3 and 2-4, respectively). Ponceau red staining is shown as a loading control (lower panel). (C) The percentage of survival of HCT116 cells transfected with GAPDH siRNA (open circles) or non-transfected (filled circles) after treatment with various concentrations of MMS (left panel) and with various doses of UVC (right panel).

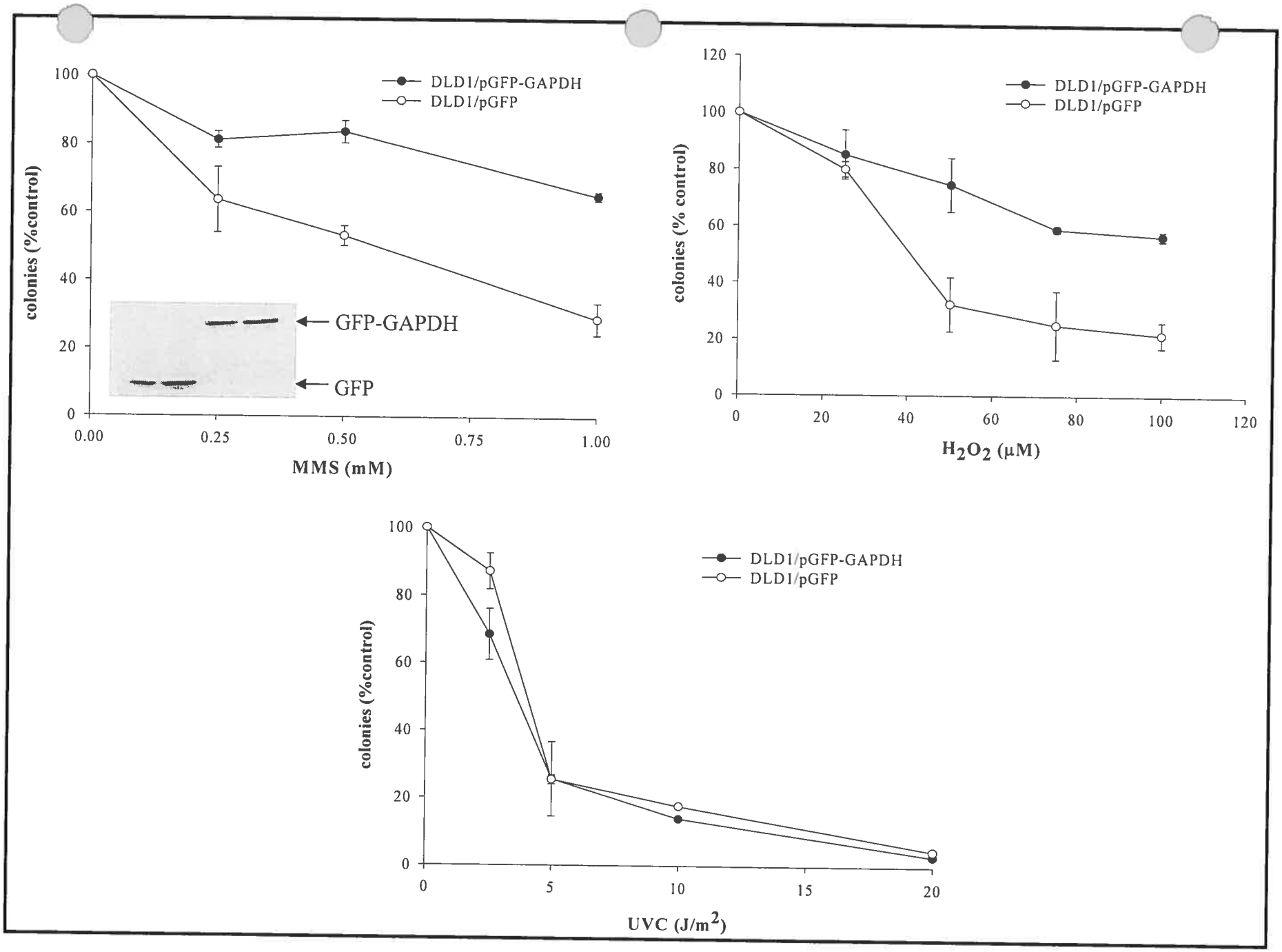

FIGURE 4-7A. Jilani *et al.*, 2006

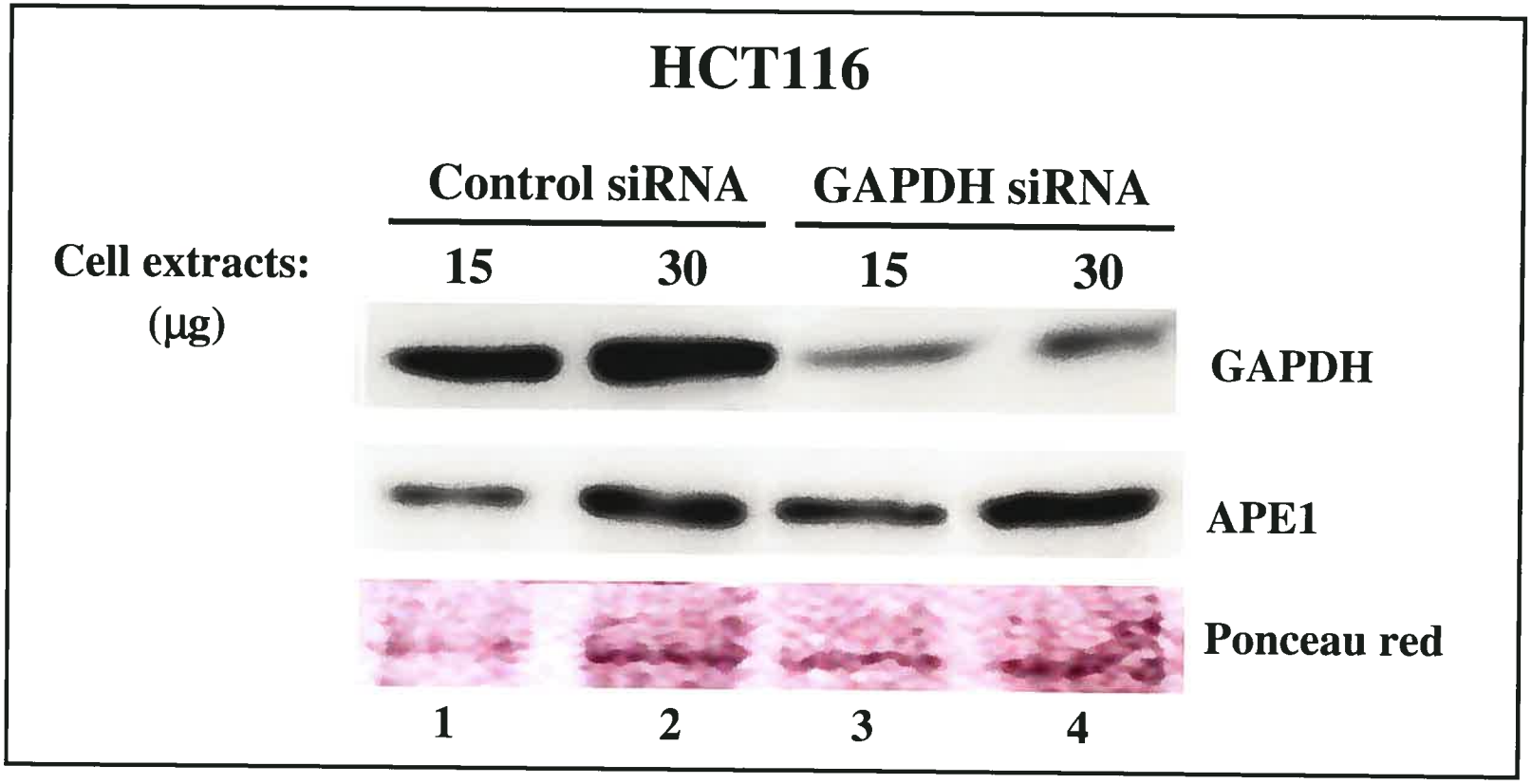

FIGURE 4-7B. Jilani *et al.*, 2006

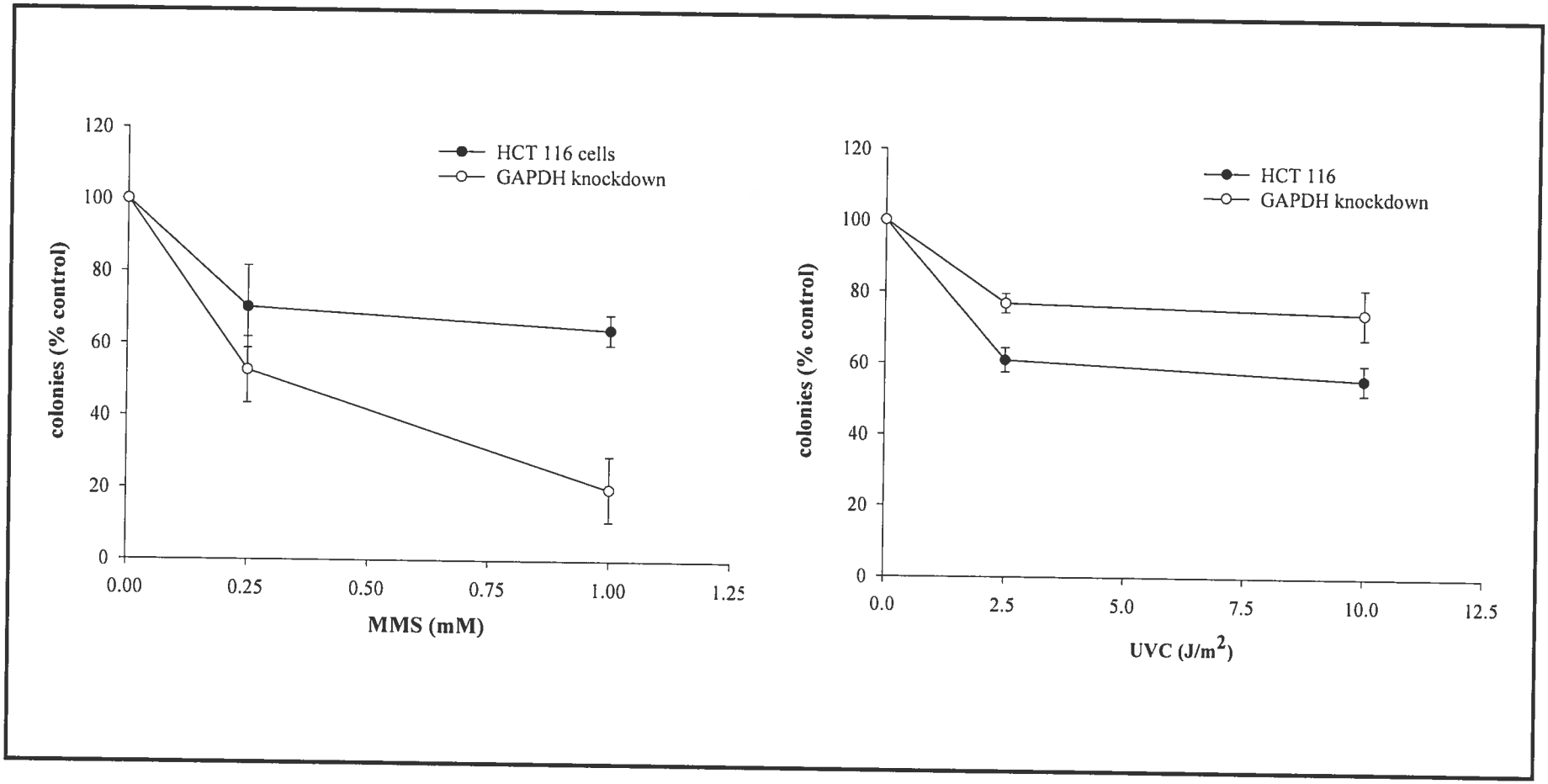

FIGURE 4-7C. Jilani *et al.*, 2006

DISCUSSION

The human AP endonuclease APE1 plays a central role in the BER pathway by performing various DNA repair functions, with the most important being its AP endonuclease activity. However, uncontrolled cleavage by APE1 could lead to increased genomic instability, similarly to our previous findings which showed that overexpression of yeast AP endonuclease Apn1 enhanced poly(GT) tract instability in the mitochondrial genome [212]. Thus, the DNA repair functions of APE1 must be regulated to prevent undesired DNA cleavage. Posttranslational modification by oxidation/reduction is emerging as a critical mechanism for the regulation of protein activities, in particular for modulating the BER enzymes. Previously, Kelley and Parson reported that the DNA repair function of APE1 was modulated by a change in the redox status of the protein [118]. Under oxidizing condition, APE1 protein is completely inhibited [118]. More recently, Bravard *et al.* demonstrated that the activity of human DNA glycosylase OGG1, which initiates the BER process, is also regulated in a redox-dependent manner [213]. They showed that an acute exposure to cadium, a ubiquitious environmental pollutant that is classified as a human carcinogen, caused nearly complete inactivation of OGG1 8-oxoG DNA glycosylase activity, but which was reversed after the removal of the heavy metal in human cells [213]. Here, we provide strong evidence that GAPDH might contribute a redox role to regulate the AP endonuclease activity of oxidized APE1.

GAPDH was identified by mass spectrometry analysis following our search for a protein exhibiting Mg^{2+}-independent AP endonuclease in human cells. Our *in vitro* enzymatic assays allowed us to clearly establish that GAPDH lacks intrinsic AP endonuclease activity, and thus it must be associated with the known AP endonuclease, APE1. Indeed, GAPDH interact with APE1 both *in vitro* and *in vivo* as demonstrated by affinity chromatography and immunoprecipitation experiments, respectively. We strongly believe that GAPDH binds to a minor form of APE1 with a different mobility pattern since we could not detect any polypeptide bands besides GAPDH by neither Coomassie blue nor silver staining as well as by mass spectrometry. In addition, the Mg^{2+}-free buffers used during our purification procedure can not sustained APE1 DNA repair activities as Mg^{2+} plays a major role

by promoting an activated (or open) DNA backbone conformation for DNA incision by APE1 [214]. However, APE1 was shown to possess some incision activity for ring-closed AP sites even in the presence of EDTA, a metal chelating agent [214]. It remains to be investigated whether GAPDH stimulates APE1 AP endonuclease activity towards *in vivo* AP site substrates that are susceptible to Mg^{2+}-independent cleavage.

GAPDH is now recognized as a multifunctional protein which displays a distinct membrane, cytosolic, and nuclear localization [215]. This latter cellular location of GAPDH has been questionable until recently, when reports showed that GAPDH possesses a CRM1-dependent nuclear export signal and that it is able to translocate to the nucleus by binding to the nuclear localization signal-containing protein, Siah1 [211,216]. These studies support the several new nuclear functions of GAPDH which have recently emerged. These includes the transcriptional regulation of H2B gene expression [199], the role of GAPDH in maintenance of telomere structure [217], in membrane cell fusion [218], in the recognition of drug-induced DNA lesions arising, e.g., from cancer chemotherapy [219], and in triggering apoptosis [216,220].

Here, we clearly demonstrated that GAPDH stimulates the AP endonuclease activity of oxidized APE1, as measured by an *in vitro* AP endonuclease assay. This stimulation of oxidized APE1 occurs perhaps through a redox reaction involving the Cys152 and Cys156 residues of GAPDH. However, neither cysteine residue has been shown to play a role in redox reaction, except for participating in the reduction of the glyceraldehyde-3-phosphate to produce 1,3-diphosphoglycerate in the glycolytic pathway [215]. The cysteines of GAPDH are separated by one additional amino acid residue (152CTTNC156), as compared to the redox active cysteines of thioredoxin (32CGPC35) [221]. Whether the cysteines of GAPDH are involved in a redox reaction or catalyzed protein disulphite isomerization of redox sensitive proteins awaits further analysis. It is noteworthy that APE1 protein possesses seven cysteine residues any number of which could be targets for regulation through redox modification. In fact, Cys310 of APE1 has been previously shown to be involved in the redox control of the enzyme repair functions [118].

The interaction of GAPDH with a key BER enzyme, APE1, is further supported by a report which demonstrated that GAPDH acts as a uracil DNA glycosylase which initiates the BER pathway by removing uracil bases generated by oxidative deamination of cytosine bases from the DNA [195]. Thus, GAPDH appears to play a dual role in the BER process. On the one hand, GAPDH removes the uracil to create an AP site and on the other, it stimulates APE1 AP endonuclease activity which will remove the AP sites. Since, OGG1 DNA glycosylase activity has been demonstrated to be regulated through redox reaction [213], it is tempting to speculate that GAPDH may serves a redox factor for several other BER proteins. GAPDH is one of the most abundant cellular proteins, thus mammalian cells may have found an efficient way to increase BER efficiency by utilizing an abundant protein to regenerate the activities of oxidatively damaged DNA repair proteins [222].

The biological importance of GAPDH in stimulating APE1 activity was suggested by cell survival assays performed following exposure to genotoxic agents. Our results clearly demonstrated that overexpression of GAPDH protects DLD-1 cells against MMS and H_2O_2, which are known to induce APE1-repairable DNA lesions, but not to UVC. Consistent with these results, siRNA knockdown of GAPDH sensitizes HCT116 cells to MMS, but not to UVC.

The overexpression of GAPDH in DLD-1 human colon carcinoma cell line did not result in apoptosis as observed by other groups. The role of GAPDH in apoptosis has been of great interest since this cellular process is believed to be the major mechanism underlying the pathophysiology of a variety of neurodegenerative diseases, including Huntington's [223], Alzheimer's [224], and Parkinson's [225]. GAPDH binds to some disease-related proteins such as huntingtin, β-amyloid precursor protein, atrophin, ataxin, and the andogren receptor [223,224,226]. The precise molecular mechanism by which GAPDH exerts its proapoptotic effects remains unknown, but it involves nuclear translocation of GAPDH [215]. Moreover, six isoforms of GAPDH has been reported in purified nuclei of cerebellar granule cells and whose level increases after cytosine arabinoside treatment which is known to induce apoptosis in neuronal cells [198]. Interestingly, only the more acidic

isoforms are rapidly translocated in the nucleus and could be the forms that regenerate oxidized proteins to the reduced forms.

In conclusion, the state of our knowledge with respect to the functional diversity of mammalian GAPDH and the underlying basic mechanisms which provide for its multidimensional nature is still growing. Several areas appear promising namely the protein interactions of GAPDH with disease proteins as well as BER enzymes. Of particular interest is to determine if there is a key cysteine amino acid residue that is regenerated from its oxidized to the reduced state by GAPDH.

CHAPTER 5

GENERAL DISCUSSION

DISCUSSION

Endogenous and exogenous reactive oxygen species (ROS) constantly cause damage to the cellular DNA. The consequence of oxidative DNA damage is generally undesirable, contributing to degenerative processes such as aging and cancer [1,2]. Oxidative DNA damage is an important source of apurinic/apyrimidinic (AP) sites and base damaged, such as 8-oxo-7,8-dihydroguanine (8-oxo-dGuo) and thymine glycol (Tg). AP sites can also result from spontaneous hydrolysis of the *N*-glycosylic bond and the removal of damaged bases by DNA glycosylases in the course of the base excision repair (BER) process [227]. It has been calculated that normal human liver cells present a steady-state level of about 50 000 AP sites per genome [228]. Thus, AP sites are considered to be one of the most frequent endogenous lesions in DNA [20]. In addition to being abundant, AP sites can induce mutations, which are mainly single base-pair substitutions, and cell death by blocking DNA replication and transcription [1]. To counteract the deleterious action of AP sites, organisms have evolved several DNA repair pathways, including BER which constitutes the chief defense mechanism against AP sites and the NER, a backup pathway [21].

AP endonucleases of the exo III (e.g. *E. coli* exo III and human APE1) and endo IV (*E. coli* endo IV and yeast Apn1) family are key enzymes in the BER pathway [60]. These enzymes recognize, and cleave the AP sites on the 5' side of the DNA phosphodiester backbone to create a free 3'-OH end for DNA polymerase synthesis. The pivotal crystallographic studies performed on representative members of the two AP endonuclease families (i.e. bacteria exo III and endo IV, and human APE1) have lead to a detailed comprehension of the relationship between the structure and function of AP endonucleases [60].

Our report on the first structure/function analysis of the eukaryotic counterpart of bacteria endo IV, yeast Apn1, has also provided insights into how AP sites are recognized and cleaved by AP endonucleases (Chapter 2) [177]. More importantly, our study revealed that although AP endonucleases are related, they still can use slightly different mechanisms to process damaged DNA [177]. Indeed, we observed that the Apn1 E158G and D192G mutants display different characteristics when

compared to the corresponding endo IV E145G and D179G mutants. The Apn1 E158G variant is able to bind DNA, but not endo IV E145G mutant. Moreover, the D192G variant of Apn1 completely lacks DNA repair activity, whereas the activity of endo IV D179G mutant is reduced 40-fold. To account for the disparity in the DNA binding capacity, we propose, based on the crystal structure of bacteria endo IV, that the Apn1 E158 residue serves solely in the binding of the Zn^{2+} ions required for catalysis, while the endo IV E145 residue is involved in both DNA binding and coordinating the trinuclear Zn cluster [177].

However, the difference in the enzymatic activity of the endo IV D179G and Apn1 D192G mutant can not be explained based on the endo IV crystal structure. The endo IV D179 and Apn1 D192 residues appear both to be involved in the stabilization of the catalytic Zn cluster. Still, glycine substitutions of these residues do not appear to affect the Zn content of both mutant enzymes [149]. Moreover, it is unlikely that the substrate specificity can account for the disparity in the enzyme activity of the endo IV and Apn1 variants, as kinetics studies demonstrated that both enzymes cleave various susbstrates, such as AP sites, THF, 5,6-dihydropyrimidines (DHU and DHT), and α-anomeric 2'-deoxynucleosides (αdN) with similar efficiencies [229,230]. On the other hand, the presence of an additional bipartite nuclear localization signal at the C-terminus of Apn1 may cause the protein to fold differently, which might result in a changed conformation of the active site pocket [81,231]. Likewise, it would be certainly very insightful to compare the crystal structures of the endo IV D179G and the apn1 D192G mutant proteins in order to determine whether any changes in active site structure occur as a result of these mutations and whether the NLS of Apn1 affects its protein conformation. In addition, these structural studies should allow for a comprehensible interpretation of the observed differences between the endo IV D179G and the Apn1 D192G mutant proteins in terms of catalytic efficiencies.

The importance of AP endonucleases has been established by the fact that AP endonuclease-deficiency leads to cellular hypersensitivity to certain genotoxic agents and to genomic instability and mutations [94]. Guillet and Boiteux demonstrated that the simultaneous inactivation of two AP endonucleases (Apn1 and Apn2) and of the

nuclease Rad1-Rad10 causes cell death in *Saccharomyces cerevisiae*, because of the inablity of the *apn1Δapn2Δrad1Δ* triple mutant to repair endogenous AP sites and related 3'-blocked single strand breaks [94]. In mammalian cells, knockout of the major AP endonuclease APE1 causes embryonic lethality, whereas APE1 knockdown induces inhibition of cell proliferation and activation of apoptosis which was correlated with accumulation of AP sites [102,103]. Together, these studies strongly suggest that the burden of AP sites is not compatible with life in absence of DNA repair.

AP endonucleases play a vital role by acting on AP sites that arise either spontaneously or from the removal of damaged bases by DNA glycosylases. AP endonuclease can also recognize modified bases independently of DNA glycosylases and incise the damaged DNA to generate a 3'-OH group and a 5'-phosphate [84]. Moreover, Simonelli *et al.* provided strong evidence that AP site-related lesions, such as 3'- or 5'-blocked single strand breaks [e.g. 3'-αβ-unsaturated aldehyde or 5'-deoxyribose-5-phosphate (5'-dRp), respectively], are mutagenic and possibly more toxic than AP sites themselves [232]. Thus, one can assume that eukaryotic cells require a control repair by AP endonucleases in order to prevent the accumulation of mutagenic intermediates.

Our recent study (Chapter 3) supports the existing evidence that AP endonucleases are responsible for generating mutagenic intermediates [212]. In fact, we demonstrated that overexpression of Apn1 in an *ogg1Δ* strain increased mitochondrial poly(GT) tract instability in yeast cells, which was however counteracted by Ogg1 DNA glycosylase overexpression. Consistent with our observation, Padnis *et al.* showed that Ntg1 DNA glycosylase-deficient yeast cells overexpressing Apn1 exhibited an increased frequency of mitochondrial mutations, which could be suppressed by deletion of Apn1 [233]. Likewise, Doudican *et al.* demonstrated that oxidative DNA damage causes mtDNA instability in *Saccharomyces cerevisiae* and that the mitochondrial helicase, Pif1, and Ntg1 cooperate to preserve mitochondrial genomic stability [234].

Considering the mutagenic potential of AP sites, our results strongly suggest that Ogg1 competes for binding to AP sites and protect a fraction of the lesions from

spurious cleavage by the uncontrolled action of the overexpressed Apn1. One could also consider the possibility that the repair of AP sites mediated by Ogg1 follows a pathway that is less mutagenic than the pathway that is initiated by Apn1 operating at 8-oxo-dGuo lesions. To date, no reports favor this hypothesis. On the contrary, a recent report by Ischenko *et al.* found Apn1 to be involved in an Ogg1-independent DNA repair pathway for 8-oxo-dGuo residues, in addition to the BER pathway. The authors revealed that this alternative repair requires the 3'-5'-exonuclease activity of Apn1, which they showed to be as efficient as its AP endonuclease activity [86]. Notably, during our structure-function analysis of Apn1 (Chapter 2) we also observed that Apn1 displays the ability to remove additional nucleotides in a 3' to 5' direction following cleavage of an AP site [177]. However, the elucidation of the biological significance of this 3'-5'-exonuclease activity was beyond the scope of our study. Together, our findings further support the idea that uncontrolled Apn1 activity generates excessive DNA strand breaks, which are cytotoxic DNA repair intermediates as they could induce DNA double strand breaks.

In a context, where proteins involved in DNA repair and replication co-exist in the vicinity of DNA damage, the cell may preferably chose to protect AP sites from further cleavage by an AP endonuclease. In agreement with this hypothesis, we showed that *APN1* deletion leads to a 2-fold decreased in the rate of poly(GT) tract instablity in *ogg1Δ* cells (Chapter 3) [212]. We propose that Ogg1 competes with Apn1 for binding to AP sites such that these mutagenic lesions are protected from undesirable repair. Indeed, it was previously estimated that human homolog of yeast Ogg1 (hOGG1) is tightly bound to an AP site with the calculated half-life of the complex being greater that 2 h [119,184]. Thus, to further support the functional interaction between Ogg1 and Apn1, the binding affinity of Ogg1 and Apn1 for AP sites needs to be clearly assessed. Using surface plasmon resonance (SPR) as described by Hedge *et al.*, we could propose to monitor in real time the interaction between either Ogg1 or Apn1 and DNA substrate containing an AP site [235]. The sensorgrams generated by the SPR analysis can provide information on the binding affinity of the protein for the DNA substrate. With this approach, Hedge *et al.* found that hOGG1 has a higher affinity for AP sites than APE1 [235]. As such, we predict

similar behavior for yeast Ogg1 and Apn1. In addition, competition binding assays with various damaged DNA substrates, including AP site-containing oligonucleotides could also be performed to compare the binding affinities and specificities of Ogg1 and Apn1.

Moreover, using an innovative covalent trapping strategy, which consists of inducing a disulfide crosslink between a protein and DNA to prevent the dissociation of the protein-DNA interaction, Banerjee *et al.* established that hOGG1 is capable of discriminating G from 8-oxo-dGuo due to the presence of two distinct pockets, the G-specific pocket and the 8-oxo-dGuo recognition pocket, respectively [236]. The unique structure of hOGG1 allows access to the normal G base to the G-specific pocket and excluding it completely from the subsequent binding to the 8-oxo-dGuo pocket. This active site of hOGG1 only binds to DNA where it encounters 8-oxodGuo lesions [236]. Following cleavage of 8-oxo-dGuo, hOGG1 is likely to use its refined structure to bind very tightly to the AP site repair intermediate and protect it from uncontrolled cleavage by the AP endonuclease APE1. The disulfide trapping strategy could certainly be used to test whether AP sites can be 'trapped' in the active site pocket of yeast Ogg1 [236].

Interestingly, we demonstrated that anaerobic growth conditions prevented destabilization of mitochondrial poly(GT) tract, suggesting that oxidative DNA damages, particularly, 8-oxo-dGuo, are most likely the cause of poly(GT) tract instability. However, we were unsuccessful at detecting a significant increase in the levels of 8-oxo-dGuo lesions in the mtDNA derived from the *ogg1Δ* mutant, as compared to the parent strain. In fact, the analysis by HPLC of mitochondrial DNA revealed a comparable level of 8-oxo-dGuo in the *ogg1Δ* mutant (198 ± 12 lesions/10^6 G) and the parent (184 ± 10 lesions/10^6 G). In general, the assessements of the precise amounts of 8-oxo-dGuo lesions in both nuclear and mitochondrial DNA can be a challenging task due to the formation of artifacts by oxidation of dGuo during sample preparation [237]. To circumvent this problem, Brink *et al.* developed a highly sensitive quantitative method consisting of on-line sample preparation by HPLC column switching combined with tandem mass spectrometry (ESI-MS/MS) [238]. This technique may prove to be a useful tool to study the biological importance

of DNA repair proteins in the removal of both endogenous and exogenous DNA damage.

Besides the BER pathway, mismatch repair (MMR) is the only pathway reported to play an important role in the maintenance of the poly(GT) tract stability as well as in the repair of oxidative damage in mtDNA [170,239]. The *MSH1* gene encodes for the yeast homologue of the bacterial MMR protein MutS, which possesses a critical function in mtDNA stability [170]. One study reported that the high frequency of mitochondrial mutations in an *ogg1Δ* mutant was significantly suppressed by overexpresssion of the *MSH1* gene [239]. Thus, it would be interesting to confirm this observation by overproducing Msh1 in our *ogg1Δ* mutant. Although the detailed mechanism by which Msh1 prevents genomic instability remains to be elucidated, Chang *et al.* recently provided evidence that APE1 increased microsatellite instability (MSI) by decreasing the levels of MSH6 protein, which is a key player in the MMR pathway [240]. This suggested mechanism could also be linked to the mitochondrial poly(GT) tract instability observed in our yeast strains overexpressing Apn1 since it was previously reported that Msh6 participates in the removal of 8-oxo-dGuo lesions through the mismatch repair pathway [241] Thus, it remains to be investigated whether the poly(GT) tract instability is caused by yeast Apn1-mediated reduction of Msh6 expression in the mitochondria.

In BER, the enzymatic mechanism of the incision step accomplished by AP endonucleases is well understood. However, knowledge of the molecular mechanisms responsible for the regulation of the AP endonuclease activity is still scanty. This situation is further complicated by the multifunctional nature of mammalian AP endonucleases. Indeed, APE1 is not only responsible for repair of AP sites, but it also plays a crucial role as a redox factor (thus the acronym Ref-1) that maintains important transcription factors (e.g. AP-1, NF-κB, and p53) in an active reduced state. These two activities of APE1/Ref-1 are encoded by two distinct functionally independent protein domains: the non-conserved N-terminal domain is required for the redox activity, whereas the conserved C-terminal domain contains the DNA repair activity [112]. Thus, for a coordinated and proper functioning of APE1/Ref-1 in the cellular context, it is necessary that its diverse functions are well regulated.

Previously, the studies on the regulation of APE1/Ref-1 functions mainly focused on the gene expression and subcellular localization of the protein. The reports showed that APE1/Ref-1 is a ubiquitous protein whose expression can be induced at the transcriptional level by alleviating APE1/Ref-1 repression on its own promoter activity [111]. While most studies have localized APE1/Ref-1 in the nucleus, it has been reported that APE1/Ref-1 is also present in the cytoplasm, mitochondria, and the endoplasmic reticulum [111]. More recent studies have shifted their focus towards other aspects of APE1/Ref-1 regulation, namely, protein-protein interactions and posttranslational modifications [115]. Evidence from reconstituted systems and cell biology suggests that APE1/Ref-1 activities are regulated by both physical and functional interactions with BER enzymes and proteins participating in other biological processes, such as DNA transcription and replication. Moreover, recent data have emerged showing that APE1/Ref-1 is modified posttranslationally by phosphorylation, acetylation, and redox modification [115]. Importantly, these three kinds of posttranslational modifications were reported to affect APE1/Ref-1 activities.

Our study in Chapter 4 supports the notion that APE1/Ref-1 activities are modulated via redox modification. We provided strong evidence that GAPDH, a well established glycolytic enzyme, reduces APE1/Ref-1 through direct complex formation. The redox reaction involves Cys152 and Cys156 in the putative redox center of GAPDH, and although the target residues on APE1/Ref-1 were not determined, one residue is likely to be Cys310. This residue, which is immediately adjacent to the crucial His309 residue in the DNA repair active site, was previously found to be involved in the redox control of DNA repair function [118]. Functionally, the interaction of APE1/Ref-1 and GAPDH stimulates the AP endonuclease activity of oxidized APE/Ref-1. As the DNA glycosylase activity of OGG1 was recently demonstrated to be completely inhibited under oxidizing conditions, it is tempting to speculate that GAPDH may serve as a general redox factor for other BER enzymes [213]. Thus, mammalian cells may have found an efficient way to increased BER efficiency by utilizing GAPDH, one of the most abundant cellular proteins, to reactivate oxidatively damaged DNA repair enzymes. Thus, future studies may reveal other biologically relevant protein interactions of GAPDH with BER enzymes.

The mere association of GAPDH with the DNA repair enzyme APE1/Ref-1 implicates that the glycolytic enzyme is also a nuclear protein, although it does not contain a NLS like APE1/Ref-1 [242]. Recent studies demonstrated that GAPDH nuclear localization is governed by both nuclear export and import, which are mediated by its CRM1-dependent nuclear export signal and its binding to the NLS of Siah1 (seven in absentia homolog 1), a ubiquitin-E3 ligase, respectively [211,216]. Furthermore, GAPDH was shown to translocate from the cytoplasm to the nucleus following various oxidative stresses such as treatment with H_2O_2, FeCN, and 1-methyl-4-phenylpyridinium (MPP^+) [200]. The importance of GAPDH nuclear translocation is becoming more apparent as new nuclear functions for the enzyme emerge. These include the transcriptional regulation of histone H2B gene expression, the maintenance of telomere structure, the induction of apoptosis, and the binding of incorrect nucleotides in DNA arising from cancer chemotherapy [242]. The role of GAPDH in DNA repair was initially reported by Baxi and Vishwanata who demonstrated that the enzyme has uracil DNA glycosylase activity [194]. More recently, Krynetski *et al.* showed that GAPDH is part of protein complex, distinct from MMR, that binds to DNA containing thiopurines, such as mercaptopurine [202].

The cell survival assays that we performed following treatment of two human colon carcinoma cell lines with various genotoxic agents clearly demonstrated the importance of GAPDH in the protection against genomic threats. Our data clearly showed that DLD-1 cells overexpressing GAPDH have an increased survival rate following exposure to MMS and H_2O_2, two DNA damaging agents known to induce APE1-repairable lesions, as compared to cells with basal levels of GAPDH. Moreover, knockdown of GAPDH causes HCT116 cells to be sensitive to MMS. However, neither overexpression nor GAPDH knockdown altered the sensitivity of the cells to UVC (254 nm) irradiation. Although these results strongly suggest that GAPDH actively participate in BER by stimulating APE1/Ref-1 activity, additional *in vivo* experiments are needed to support this hypothesis. First, we can monitor the AP endonuclease activity of total cell extracts derived from cells that either overexpress GAPDH or that are knockdown for GAPDH, following exposure to the various genotoxic agents. According to our assumption, cell extracts with

overexpressed GAPDH should display higher AP endonuclease activity than cell extracts containing endogenous levels of GAPDH, whereas cell extracts with reduced amount of GAPDH should exhibit decreased AP endonuclease activity, as compared to the control cell extracts. In the case of GAPDH knockdown, we also need to verify that the decreased AP endonuclease activity is not resulting from a reduction in APE1/Ref-1 protein levels. Second, we can compare the levels of total AP site damage in chromosomal DNA of GAPDH-deficient and control HCT116 cells. Based on our hypothesis, knockdown of GAPDH should contain higher levels of AP sites than control cells.

Our study attributes a novel nuclear role to GAPDH as a redox factor for APE1/Ref-1 enzyme (manuscript in preparation). More importantly, this study has contributed to the understanding the redox modification as an important regulatory switch between the DNA repair and redox function of Ape1/Ref-1. Previously, several groups have demonstrated that thioredoxin (TRX), a dithiol-reducing enzyme, reduces APE1/Ref-1 to potentiate the DNA binding of transcription factors AP-1 and p53 mediated by APE1/Ref-1 [116,117]. Although the specific residues of APE1/Ref-1 involved in the interaction with TRX are not known, they may include Cys65 and Cys93 as they have been shown to be redox-sensitive [116,117]. On the other hand, Kelley and Parsons demonstrated that the DNA repair activity of APE1/Ref-1 is also redox-regulated with the specific involvement of Cys310 [118]. Together, these observations suggest that redox modification by TRX and GAPDH, two abundant cellular proteins, of different sites in APE1/Ref-1 provides a flexible and powerful means for fine-switching between the different functions of APE1/Ref-1.

Concluding remarks

AP endonucleases appear to be crucial enzymes of BER. Indeed, unrepaired AP sites can result in a block to DNA replication and in cytotoxicity, mutations, as well as genomic instability. The biological importance of AP endonucleases is underscored by the findings that knockout of APE1/Ref-1 in mice cause embryonic lethality as well as by the lack of stable APE1/Ref-1 cell lines. Until the recent report by Fung and Demple (2005), it was unclear whether the lethality in APE1/Ref1

knockout mice was due to the loss of the DNA repair function or the redox activity of APE1/Ref-1 [103]. In fact, these authors clearly showed that the AP endonuclease activity is essential for cellular viability by using RNAi [103]. However, their results do not completely rule out the possible relevance of APE1/Ref-1 redox function in the maintenance of cellular viability. Still, our group and others have shown that overexpression of AP endonucleases in either yeast or human cells is not clearly protective against cytotoxic and mutagenic lesions [212] [233]. In some cancers, including ovarian, cervical and prostate cancer, increased levels of APE1/Ref-1 has been observed which strongly correlates with enhanced resistance to radiotherapy and chemotherapy [111]. These features make APE1/Ref-1 an attractive target for anticancer drug development. Furthermore, growing evidence for posttranslational modification of APE1/Ref-1, including the one provided by our group, which demonstrated that APE1/Ref-1 AP endonuclease activity is regulated through a GAPDH-dependent redox mechanism, confirm a future investigative direction toward a better comprehension of the role of APE1/Ref-1 in cancer. More importantly, the challenge will be to integrate these findings in a biological context considering the many proteins interactions involving APE1/Ref-1. These future studies will certainly provide valuable insights for exploiting APE1/Ref-1 as a therapeutic target for several pathologies, including cancer.

REFERENCES

REFERENCES

1. Demple, B. and Harrison, L. (1994) Repair of oxidative damage to DNA: enzymology and biology. *Annu Rev Biochem*, **63**, 915-48.
2. Gilchrest, B.A. and Bohr, V.A. (1997) Aging processes, DNA damage, and repair. *Faseb J*, **11**, 322-30.
3. Hutchinson, F. (1985) Chemical changes induced in DNA by ionizing radiation. *Prog Nucleic Acid Res Mol Biol*, **32**, 115-54.
4. von Sonntag, C. (1987) New aspects in the free-radical chemistry of pyrimidine nucleobases. *Free Radic Res Commun*, **2**, 217-24.
5. Ames, B.N., Shigenaga, M.K. and Hagen, T.M. (1993) Oxidants, antioxidants, and the degenerative diseases of aging. *Proc Natl Acad Sci U S A*, **90**, 7915-22.
6. Jaruga, P. and Dizdaroglu, M. (1996) Repair of products of oxidative DNA base damage in human cells. *Nucleic Acids Res*, **24**, 1389-94.
7. Evans, M.D., Dizdaroglu, M. and Cooke, M.S. (2004) Oxidative DNA damage and disease: induction, repair and significance. *Mutat Res*, **567**, 1-61.
8. Fridovich, I. (1997) Superoxide anion radical (O2-.), superoxide dismutases, and related matters. *J Biol Chem*, **272**, 18515-7.
9. Jackson, R.L. (1993) Anti-oxidants for the treatment and the prevention of atherosclerosis. *Biochem Soc Trans*, **21**, 650-1.
10. Gutteridge, J.M. and Halliwell, B. (1989) Iron toxicity and oxygen radicals. *Baillieres Clin Haematol*, **2**, 195-256.
11. Teoule, R. (1987) Radiation-induced DNA damage and its repair. *Int J Radiat Biol Relat Stud Phys Chem Med*, **51**, 573-89.
12. Dizdaroglu, M. (1992) Oxidative damage to DNA in mammalian chromatin. *Mutat Res*, **275**, 331-42.
13. Laspia, M.F. and Wallace, S.S. (1988) Excision repair of thymine glycols, urea residues, and apurinic sites in Escherichia coli. *J Bacteriol*, **170**, 3359-66.

14. Dizdaroglu, M. (1985) Formation of an 8-hydroxyguanine moiety in deoxyribonucleic acid on gamma-irradiation in aqueous solution. *Biochemistry*, **24**, 4476-81.

15. Grollman, A.P. and Moriya, M. (1993) Mutagenesis by 8-oxoguanine: an enemy within. *Trends Genet*, **9**, 246-9.

16. Boiteux, S. (1993) Properties and biological functions of the NTH and FPG proteins of Escherichia coli: two DNA glycosylases that repair oxidative damage in DNA. *J Photochem Photobiol B*, **19**, 87-96.

17. Moriya, M. and Grollman, A.P. (1993) Mutations in the mutY gene of Escherichia coli enhance the frequency of targeted G:C-->T:a transversions induced by a single 8-oxoguanine residue in single-stranded DNA. *Mol Gen Genet*, **239**, 72-6.

18. Shibutani, S., Takeshita, M. and Grollman, A.P. (1991) Insertion of specific bases during DNA synthesis past the oxidation-damaged base 8-oxodG. *Nature*, **349**, 431-4.

19. Lindahl, T. and Nyberg, B. (1972) Rate of depurination of native deoxyribonucleic acid. *Biochemistry*, **11**, 3610-8.

20. Lindahl, T. (1990) Repair of intrinsic DNA lesions. *Mutat Res*, **238**, 305-11.

21. Lindahl, T. (1993) Instability and decay of the primary structure of DNA [see comments]. *Nature*, **362**, 709-15.

22. Dianov, G. and Lindahl, T. (1994) Reconstitution of the DNA base excision-repair pathway. *Curr Biol*, **4**, 1069-76.

23. Nicholl, I.D., Nealon, K. and Kenny, M.K. (1997) Reconstitution of human base excision repair with purified proteins. *Biochemistry*, **36**, 7557-66.

24. Cunningham, R.P. (1997) DNA glycosylases. *Mutat Res*, **383**, 189-96.

25. Sakumi, K. and Sekiguchi, M. (1990) Structures and functions of DNA glycosylases. *Mutat Res*, **236**, 161-72.

26. Krokan, H.E., Standal, R. and Slupphaug, G. (1997) DNA glycosylases in the base excision repair of DNA. *Biochem J*, **325**, 1-16.

27. Kim, J. and Linn, S. (1988) The mechanisms of action of E. coli endonuclease III and T4 UV endonuclease (endonuclease V) at AP sites. *Nucleic Acids Res*, **16**, 1135-41.

28. Friedberg, E.C., Walker, G.C. and Siede, W. (eds.) (1995) *DNA Repair and Mutagenesis*. ASM Press, Washington, D.C.

29. Matsumoto, Y., Kim, K. and Bogenhagen, D.F. (1994) Proliferating cell nuclear antigen-dependent abasic site repair in Xenopus laevis oocytes: an alternative pathway of base excision DNA repair. *Mol Cell Biol*, **14**, 6187-97.

30. Wu, X., Li, J., Li, X., Hsieh, C.L., Burgers, P.M. and Lieber, M.R. (1996) Processing of branched DNA intermediates by a complex of human FEN-1 and PCNA. *Nucleic Acids Res*, **24**, 2036-43.

31. Kubota, Y., Nash, R.A., Klungland, A., Schar, P., Barnes, D.E. and Lindahl, T. (1996) Reconstitution of DNA base excision-repair with purified human proteins: interaction between DNA polymerase beta and the XRCC1 protein. *Embo J*, **15**, 6662-70.

32. Alseth, I., Osman, F., Korvald, H., Tsaneva, I., Whitby, M.C., Seeberg, E. and Bjoras, M. (2005) Biochemical characterization and DNA repair pathway interactions of Mag1-mediated base excision repair in Schizosaccharomyces pombe. *Nucleic Acids Res*, **33**, 1123-31.

33. Akbari, M., Otterlei, M., Pena-Diaz, J., Aas, P.A., Kavli, B., Liabakk, N.B., Hagen, L., Imai, K., Durandy, A., Slupphaug, G. and Krokan, H.E. (2004) Repair of U/G and U/A in DNA by UNG2-associated repair complexes takes place predominantly by short-patch repair both in proliferating and growth-arrested cells. *Nucleic Acids Res*, **32**, 5486-98.

34. Pascucci, B., Maga, G., Hubscher, U., Bjoras, M., Seeberg, E., Hickson, I.D., Villani, G., Giordano, C., Cellai, L. and Dogliotti, E. (2002) Reconstitution of the base excision repair pathway for 7,8-dihydro-8-oxoguanine with purified human proteins. *Nucleic Acids Res*, **30**, 2124-30.

35. Fortini, P., Parlanti, E., Sidorkina, O.M., Laval, J. and Dogliotti, E. (1999) The type of DNA glycosylase determines the base excision repair pathway in mammalian cells. *J Biol Chem*, **274**, 15230-6.

36. Petermann, E., Keil, C. and Oei, S.L. (2006) Roles of DNA ligase III and XRCC1 in regulating the switch between short patch and long patch BER. *DNA Repair (Amst)*.

37. Hung, R.J., Hall, J., Brennan, P. and Boffetta, P. (2005) Genetic polymorphisms in the base excision repair pathway and cancer risk: a HuGE review. *Am J Epidemiol*, **162**, 925-42.

38. Al-Tassan, N., Chmiel, N.H., Maynard, J., Fleming, N., Livingston, A.L., Williams, G.T., Hodges, A.K., Davies, D.R., David, S.S., Sampson, J.R. and Cheadle, J.P. (2002) Inherited variants of MYH associated with somatic G:C-->T:A mutations in colorectal tumors. *Nat Genet*, **30**, 227-32.

39. Larsen, E., Meza, T.J., Kleppa, L. and Klungland, A. (2006) Organ and cell specificity of base excision repair mutants in mice. *Mutat Res*.

40. Ramotar, D., Popoff, S.C., Gralla, E.B. and Demple, B. (1991) Cellular role of yeast Apn1 apurinic endonuclease/3'-diesterase: repair of oxidative and alkylation DNA damage and control of spontaneous mutation. *Mol Cell Biol*, **11**, 4537-44.

41. Loeb, L.A. (1985) Apurinic sites as mutagenic intermediates. *Cell*, **40**, 483-4.

42. Klungland, A., Rosewell, I., Hollenbach, S., Larsen, E., Daly, G., Epe, B., Seeberg, E., Lindahl, T. and Barnes, D.E. (1999) Accumulation of premutagenic DNA lesions in mice defective in removal of oxidative base damage. *Proc Natl Acad Sci U S A*, **96**, 13300-5.

43. Hirano, S., Tominaga, Y., Ichinoe, A., Ushijima, Y., Tsuchimoto, D., Honda-Ohnishi, Y., Ohtsubo, T., Sakumi, K. and Nakabeppu, Y. (2003) Mutator phenotype of MUTYH-null mouse embryonic stem cells. *J Biol Chem*, **278**, 38121-4.

44. Xie, Y., Yang, H., Cunanan, C., Okamoto, K., Shibata, D., Pan, J., Barnes, D.E., Lindahl, T., McIlhatton, M., Fishel, R. and Miller, J.H. (2004) Deficiencies in mouse Myh and Ogg1 result in tumor predisposition and G to T mutations in codon 12 of the K-ras oncogene in lung tumors. *Cancer Res*, **64**, 3096-102.

45. Takao, M., Kanno, S., Shiromoto, T., Hasegawa, R., Ide, H., Ikeda, S., Sarker, A.H., Seki, S., Xing, J.Z., Le, X.C., Weinfeld, M., Kobayashi, K., Miyazaki, J., Muijtjens, M., Hoeijmakers, J.H., van der Horst, G. and Yasui, A. (2002) Novel nuclear and mitochondrial glycosylases revealed by disruption of the mouse Nth1 gene encoding an endonuclease III homolog for repair of thymine glycols. *Embo J*, **21**, 3486-93.

46. Karahalil, B., de Souza-Pinto, N.C., Parsons, J.L., Elder, R.H. and Bohr, V.A. (2003) Compromised incision of oxidized pyrimidines in liver mitochondria of mice deficient in NTH1 and OGG1 glycosylases. *J Biol Chem*, **278**, 33701-7.

47. Nilsen, H., Rosewell, I., Robins, P., Skjelbred, C.F., Andersen, S., Slupphaug, G., Daly, G., Krokan, H.E., Lindahl, T. and Barnes, D.E. (2000) Uracil-DNA glycosylase (UNG)-deficient mice reveal a primary role of the enzyme during DNA replication. *Mol Cell*, **5**, 1059-65.

48. Elder, R.H., Jansen, J.G., Weeks, R.J., Willington, M.A., Deans, B., Watson, A.J., Mynett, K.J., Bailey, J.A., Cooper, D.P., Rafferty, J.A., Heeran, M.C., Wijnhoven, S.W., van Zeeland, A.A. and Margison, G.P. (1998) Alkylpurine-DNA-N-glycosylase knockout mice show increased susceptibility to induction of mutations by methyl methanesulfonate. *Mol Cell Biol*, **18**, 5828-37.

49. Hang, B., Singer, B., Margison, G.P. and Elder, R.H. (1997) Targeted deletion of alkylpurine-DNA-N-glycosylase in mice eliminates repair of 1,N6-ethenoadenine and hypoxanthine but not of 3,N4-ethenocytosine or 8-oxoguanine. *Proc Natl Acad Sci U S A*, **94**, 12869-74.

50. Ludwig, D.L., MacInnes, M.A., Takiguchi, Y., Purtymun, P.E., Henrie, M., Flannery, M., Meneses, J., Pedersen, R.A. and Chen, D.J. (1998) A murine AP-endonuclease gene-targeted deficiency with post-implantation embryonic progression and ionizing radiation sensitivity. *Mutat Res*, **409**, 17-29.

51. Meira, L.B., Devaraj, S., Kisby, G.E., Burns, D.K., Daniel, R.L., Hammer, R.E., Grundy, S., Jialal, I. and Friedberg, E.C. (2001) Heterozygosity for the mouse Apex gene results in phenotypes associated with oxidative stress. *Cancer Res*, **61**, 5552-7.

52. Sugo, N., Aratani, Y., Nagashima, Y., Kubota, Y. and Koyama, H. (2000) Neonatal lethality with abnormal neurogenesis in mice deficient in DNA polymerase beta. *Embo J*, **19**, 1397-404.

53. Kucherlapati, M., Yang, K., Kuraguchi, M., Zhao, J., Lia, M., Heyer, J., Kane, M.F., Fan, K., Russell, R., Brown, A.M., Kneitz, B., Edelmann, W., Kolodner, R.D., Lipkin, M. and Kucherlapati, R. (2002) Haploinsufficiency of Flap endonuclease (Fen1) leads to rapid tumor progression. *Proc Natl Acad Sci U S A*, **99**, 9924-9.

54. Larsen, E., Gran, C., Saether, B.E., Seeberg, E. and Klungland, A. (2003) Proliferation failure and gamma radiation sensitivity of Fen1 null mutant mice at the blastocyst stage. *Mol Cell Biol*, **23**, 5346-53.

55. Tebbs, R.S., Flannery, M.L., Meneses, J.J., Hartmann, A., Tucker, J.D., Thompson, L.H., Cleaver, J.E. and Pedersen, R.A. (1999) Requirement for the Xrcc1 DNA base excision repair gene during early mouse development. *Dev Biol*, **208**, 513-29.

56. Bentley, D., Selfridge, J., Millar, J.K., Samuel, K., Hole, N., Ansell, J.D. and Melton, D.W. (1996) DNA ligase I is required for fetal liver erythropoiesis but is not essential for mammalian cell viability. *Nat Genet*, **13**, 489-91.

57. Barzilay, G. and Hickson, I.D. (1995) Structure and function of apurinic/apyrimidinic endonucleases. *Bioessays*, **17**, 713-9.

58. Saporito, S.M. and Cunningham, R.P. (1988) Nucleotide sequence of the nfo gene of Escherichia coli K-12. *J Bacteriol*, **170**, 5141-5.

59. Saporito, S.M., Smith-White, B.J. and Cunningham, R.P. (1988) Nucleotide sequence of the xth gene of Escherichia coli K-12. *J Bacteriol*, **170**, 4542-7.

60. Mol, C.D., Hosfield, D.J. and Tainer, J.A. (2000) Abasic site recognition by two apurinic/apyrimidinic endonuclease families in DNA base excision repair: the 3' ends justify the means. *Mutat Res*, **460**, 211-29.

61. Unk, I., Haracska, L., Johnson, R.E., Prakash, S. and Prakash, L. (2000) Apurinic endonuclease activity of yeast Apn2 protein. *J Biol Chem*, **275**, 22427-34.

62. Shatilla, A., Ishchenko, A.A., Saparbaev, M. and Ramotar, D. (2005) Characterization of Caenorhabditis elegans exonuclease-3 and evidence that a Mg2+-dependent variant exhibits a distinct mode of action on damaged DNA. *Biochemistry*, **44**, 12835-48.

63. Shatilla, A., Leduc, A., Yang, X. and Ramotar, D. (2005) Identification of two apurinic/apyrimidinic endonucleases from Caenorhabditis elegans by cross-species complementation. *DNA Repair (Amst)*, **4**, 655-70.

64. Mol, C.D., Kuo, C.F., Thayer, M.M., Cunningham, R.P. and Tainer, J.A. (1995) Structure and function of the multifunctional DNA-repair enzyme exonuclease III. *Nature*, **374**, 381-6.

65. Gorman, M.A., Morera, S., Rothwell, D.G., de La Fortelle, E., Mol, C.D., Tainer, J.A., Hickson, I.D. and Freemont, P.S. (1997) The crystal structure of the human DNA repair endonuclease HAP1 suggests the recognition of extra-helical deoxyribose at DNA abasic sites. *Embo J*, **16**, 6548-58.

66. Kaneda, K., Sekiguchi, J. and Shida, T. (2006) Role of the tryptophan residue in the vicinity of the catalytic center of exonuclease III family AP endonucleases: AP site recognition mechanism. *Nucleic Acids Res*, **34**, 1552-63.

67. Hosfield, D.J., Guan, Y., Haas, B.J., Cunningham, R.P. and Tainer, J.A. (1999) Structure of the DNA repair enzyme endonuclease IV and its DNA complex: double-nucleotide flipping at abasic sites and three-metal-ion catalysis. *Cell*, **98**, 397-408.

68. Richardson, C.C. and Kornberg, A. (1964) A Deoxyribonucleic Acid Phosphatase-Exonuclease from Escherichia Coli. I. Purification of the Enzyme and Characterization of the Phosphatase Activity. *J Biol Chem*, **239**, 242-50.

69. Ljungquist, S., Lindahl, T. and Howard-Flanders, P. (1976) Methyl methane sulfonate-sensitive mutant of Escherichia coli deficient in an endonuclease specific for apurinic sites in deoxyribonucleic acid. *J Bacteriol*, **126**, 646-53.

70. Kow, Y.W. and Wallace, S.S. (1985) Exonuclease III recognizes urea residues in oxidized DNA. *Proc Natl Acad Sci U S A*, **82**, 8354-8.

71. Demple, B., Halbrook, J. and Linn, S. (1983) Escherichia coli xth mutants are hypersensitive to hydrogen peroxide. *J Bacteriol*, **153**, 1079-82.

72. Saporito, S.M., Gedenk, M. and Cunningham, R.P. (1989) Role of exonuclease III and endonuclease IV in repair of pyrimidine dimers initiated by bacteriophage T4 pyrimidine dimer-DNA glycosylase. *J Bacteriol*, **171**, 2542-6.

73. Demple, B., Johnson, A. and Fung, D. (1986) Exonuclease III and endonuclease IV remove 3' blocks from DNA synthesis primers in H2O2-damaged Escherichia coli. *Proc Natl Acad Sci U S A*, **83**, 7731-5.

74. Souza, L.L., Eduardo, I.R., Padula, M. and Leitao, A.C. (2006) Endonuclease IV and exonuclease III are involved in the repair and mutagenesis of DNA lesions induced by UVB in Escherichia coli. *Mutagenesis*, **21**, 125-30.

75. Cunningham, R.P., Saporito, S.M., Spitzer, S.G. and Weiss, B. (1986) Endonuclease IV (nfo) mutant of Escherichia coli. *J Bacteriol*, **168**, 1120-7.

76. Levin, J.D. and Demple, B. (1996) In vitro detection of endonuclease IV-specific DNA damage formed by bleomycin in vivo. *Nucleic Acids Res*, **24**, 885-9.

77. Johnson, A.W. and Demple, B. (1988) Yeast DNA diesterase for 3'-fragments of deoxyribose: purification and physical properties of a repair enzyme for oxidative DNA damage. *J Biol Chem*, **263**, 18009-16.

78. Johnson, A.W. and Demple, B. (1988) Yeast DNA 3'-repair diesterase is the major cellular apurinic/apyrimidinic endonuclease: substrate specificity and kinetics. *J Biol Chem*, **263**, 18017-22.

79. Levin, J.D., Johnson, A.W. and Demple, B. (1988) Homogeneous Escherichia coli endonuclease IV. Characterization of an enzyme that recognizes oxidative damage in DNA. *J Biol Chem*, **263**, 8066-71.

80. Popoff, S.C., Spira, A.I., Johnson, A.W. and Demple, B. (1990) Yeast structural gene (APN1) for the major apurinic endonuclease: homology to Escherichia coli endonuclease IV. *Proc Natl Acad Sci U S A*, **87**, 4193-7.

81. Ramotar, D., Kim, C., Lillis, R. and Demple, B. (1993) Intracellular localization of the Apn1 DNA repair enzyme of Saccharomyces cerevisiae. Nuclear transport signals and biological role. *J Biol Chem*, **268**, 20533-9.

82. Vongsamphanh, R., Fortier, P.K. and Ramotar, D. (2001) Pir1p mediates translocation of the yeast Apn1p endonuclease into the mitochondria to maintain genomic stability. *Mol Cell Biol*, **21**, 1647-55.

83. Liu, C., Pouliot, J.J. and Nash, H.A. (2002) Repair of topoisomerase I covalent complexes in the absence of the tyrosyl-DNA phosphodiesterase Tdp1. *Proc Natl Acad Sci U S A*, **99**, 14970-5.

84. Ischenko, A.A. and Saparbaev, M.K. (2002) Alternative nucleotide incision repair pathway for oxidative DNA damage. *Nature*, **415**, 183-7.

85. Vance, J.R. and Wilson, T.E. (2001) Repair of dna strand breaks by the overlapping functions of lesion-specific and non-lesion-specific dna 3' phosphatases. *Mol Cell Biol*, **21**, 7191-8.

86. Ishchenko, A.A., Yang, X., Ramotar, D. and Saparbaev, M. (2005) The 3'-5' exonuclease of Apn1 provides an alternative pathway to repair 7,8-dihydro-8-oxodeoxyguanosine in Saccharomyces cerevisiae. *Mol Cell Biol*, in press.

87. Kunz, B.A., Henson, E.S., Roche, H., Ramotar, D., Nunoshiba, T. and Demple, B. (1994) Specificity of the mutator caused by deletion of the yeast structural gene (APN1) for the major apurinic endonuclease. *Proc Natl Acad Sci U S A*, **91**, 8165-9.

88. Masson, J.Y. and Ramotar, D. (1997) Normal processing of AP sites in Apn1-deficient Saccharomyces cerevisiae is restored by Escherichia coli genes expressing either exonuclease III or endonuclease III. *Mol Microbiol*, **24**, 711-21.

89. Johnson, R.E., Torres-Ramos, C.A., Izumi, T., Mitra, S., Prakash, S. and Prakash, L. (1998) Identification of APN2, the saccharomyces cerevisiae homolog of the major human AP endonuclease HAP1, and its role in the repair of abasic sites [In Process Citation]. *Genes Dev*, **12**, 3137-43.

90. Sander, M. and Ramotar, D. (1997) Partial purification of Pde1 from Saccharomyces cerevisiae: enzymatic redundancy for the repair of 3'-terminal DNA lesions and abasic sites in yeast. *Biochemistry*, **36**, 6100-6.

91. Bennett, R.A. (1999) The Saccharomyces cerevisiae ETH1 gene, an inducible homolog of exonuclease III that provides resistance to DNA-damaging agents and limits spontaneous mutagenesis. *Mol Cell Biol*, **19**, 1800-9.

92. Unk, I., Haracska, L., Prakash, S. and Prakash, L. (2001) 3'-phosphodiesterase and 3'-->5' exonuclease activities of yeast Apn2 protein and requirement of these activities for repair of oxidative DNA damage. *Mol Cell Biol*, **21**, 1656-61.

93. Unk, I., Haracska, L., Gomes, X.V., Burgers, P.M., Prakash, L. and Prakash, S. (2002) Stimulation of 3'-->5' exonuclease and 3'-phosphodiesterase activities of yeast apn2 by proliferating cell nuclear antigen. *Mol Cell Biol*, **22**, 6480-6.

94. Guillet, M. and Boiteux, S. (2002) Endogenous DNA abasic sites cause cell death in the absence of Apn1, Apn2 and Rad1/Rad10 in Saccharomyces cerevisiae. *Embo J*, **21**, 2833-41.

95. Demple, B., Herman, T. and Chen, D.S. (1991) Cloning and expression of APE, the cDNA encoding the major human apurinic endonuclease: definition of a family of DNA repair enzymes. *Proc Natl Acad Sci U S A*, **88**, 11450-4.

96. Robson, C.N., Hochhauser, D., Craig, R., Rack, K., Buckle, V.J. and Hickson, I.D. (1992) Structure of the human DNA repair gene HAP1 and its localisation to chromosome 14q 11.2-12. *Nucleic Acids Res*, **20**, 4417-21.

97. Xanthoudakis, S., Miao, G., Wang, F., Pan, Y.C. and Curran, T. (1992) Redox activation of Fos-Jun DNA binding activity is mediated by a DNA repair enzyme. *Embo J*, **11**, 3323-35.

98. Seki, S., Ikeda, S., Watanabe, S., Hatsushika, M., Tsutsui, K., Akiyama, K. and Zhang, B. (1991) A mouse DNA repair enzyme (APEX nuclease) having exonuclease and apurinic/apyrimidinic endonuclease activities: purification and characterization. *Biochim Biophys Acta*, **1079**, 57-64.

99. Jackson, E.B., Theriot, C.A., Chattopadhyay, R., Mitra, S. and Izumi, T. (2005) Analysis of nuclear transport signals in the human apurinic/apyrimidinic endonuclease (APE1/Ref1). *Nucleic Acids Res*, **33**, 3303-12.

100. Chattopadhyay, R., Wiederhold, L., Szczesny, B., Boldogh, I., Hazra, T.K., Izumi, T. and Mitra, S. (2006) Identification and characterization of mitochondrial abasic (AP)-endonuclease in mammalian cells. *Nucleic Acids Res*, **34**, 2067-76.

101. Gros, L., Ishchenko, A.A., Ide, H., Elder, R.H. and Saparbaev, M.K. (2004) The major human AP endonuclease (Ape1) is involved in the nucleotide incision repair pathway. *Nucleic Acids Res*, **32**, 73-81.

102. Xanthoudakis, S., Smeyne, R.J., Wallace, J.D. and Curran, T. (1996) The redox/DNA repair protein, Ref-1, is essential for early embryonic development in mice. *Proc Natl Acad Sci U S A*, **93**, 8919-23.

103. Fung, H. and Demple, B. (2005) A vital role for Ape1/Ref1 protein in repairing spontaneous DNA damage in human cells. *Mol Cell*, **17**, 463-70.

104. Wilson, D.M., 3rd and Barsky, D. (2001) The major human abasic endonuclease: formation, consequences and repair of abasic lesions in DNA. *Mutat Res*, **485**, 283-307.

105. Hadi, M.Z. and Wilson, D.M., 3rd (2000) Second human protein with homology to the Escherichia coli abasic endonuclease exonuclease III. *Environ Mol Mutagen*, **36**, 312-24.

106. Hadi, M.Z., Ginalski, K., Nguyen, L.H. and Wilson, D.M., 3rd (2002) Determinants in nuclease specificity of Ape1 and Ape2, human homologues of Escherichia coli exonuclease III. *J Mol Biol*, **316**, 853-66.

107. Ide, Y., Tsuchimoto, D., Tominaga, Y., Nakashima, M., Watanabe, T., Sakumi, K., Ohno, M. and Nakabeppu, Y. (2004) Growth retardation and dyslymphopoiesis accompanied by G2/M arrest in APEX2-null mice. *Blood*, **104**, 4097-103.

108. Burkovics, P., Szukacsov, V., Unk, I. and Haracska, L. (2006) Human Ape2 protein has a 3'-5' exonuclease activity that acts preferentially on mismatched base pairs. *Nucleic Acids Res*, **34**, 2508-15.

109. Xanthoudakis, S. and Curran, T. (1992) Identification and characterization of Ref-1, a nuclear protein that facilitates AP-1 DNA-binding activity. *Embo J*, **11**, 653-65.

110. Abate, C., Patel, L., Rauscher, F.J., 3rd and Curran, T. (1990) Redox regulation of fos and jun DNA-binding activity in vitro. *Science*, **249**, 1157-61.

111. Evans, A.R., Limp-Foster, M. and Kelley, M.R. (2000) Going APE over ref-1. *Mutat Res*, **461**, 83-108.

112. Xanthoudakis, S., Miao, G.G. and Curran, T. (1994) The redox and DNA-repair activities of Ref-1 are encoded by nonoverlapping domains. *Proc Natl Acad Sci U S A*, **91**, 23-7.

113. Izumi, T., Brown, D.B., Naidu, C.V., Bhakat, K.K., Macinnes, M.A., Saito, H., Chen, D.J. and Mitra, S. (2005) Two essential but distinct functions of the mammalian abasic endonuclease. *Proc Natl Acad Sci U S A*, **102**, 5739-43.

114. Grosch, S., Fritz, G. and Kaina, B. (1998) Apurinic endonuclease (Ref-1) is induced in mammalian cells by oxidative stress and involved in clastogenic adaptation. *Cancer Res*, **58**, 4410-6.

115. Fan, J. and Wilson, D.M., 3rd (2005) Protein-protein interactions and posttranslational modifications in mammalian base excision repair. *Free Radic Biol Med*, **38**, 1121-38.

116. Hirota, K., Matsui, M., Iwata, S., Nishiyama, A., Mori, K. and Yodoi, J. (1997) AP-1 transcriptional activity is regulated by a direct association between thioredoxin and Ref-1. *Proc Natl Acad Sci U S A*, **94**, 3633-8.

117. Seemann, S. and Hainaut, P. (2005) Roles of thioredoxin reductase 1 and APE/Ref-1 in the control of basal p53 stability and activity. *Oncogene*, **24**, 3853-63.

118. Kelley, M.R. and Parsons, S.H. (2001) Redox regulation of the DNA repair function of the human AP endonuclease Ape1/ref-1. *Antioxid Redox Signal*, **3**, 671-83.

119. Vidal, A.E., Hickson, I.D., Boiteux, S. and Radicella, J.P. (2001) Mechanism of stimulation of the DNA glycosylase activity of hOGG1 by the major human AP endonuclease: bypass of the AP lyase activity step. *Nucleic Acids Res*, **29**, 1285-92.

120. Parikh, S.S., Mol, C.D., Slupphaug, G., Bharati, S., Krokan, H.E. and Tainer, J.A. (1998) Base excision repair initiation revealed by crystal structures and binding kinetics of human uracil-DNA glycosylase with DNA. *Embo J*, **17**, 5214-26.

121. Waters, T.R., Gallinari, P., Jiricny, J. and Swann, P.F. (1999) Human thymine DNA glycosylase binds to apurinic sites in DNA but is displaced by human apurinic endonuclease 1. *J Biol Chem*, **274**, 67-74.

122. Marenstein, D.R., Chan, M.K., Altamirano, A., Basu, A.K., Boorstein, R.J., Cunningham, R.P. and Teebor, G.W. (2003) Substrate specificity of human endonuclease III (hNTH1). Effect of human APE1 on hNTH1 activity. *J Biol Chem*, **278**, 9005-12.

123. Parker, A., Gu, Y., Mahoney, W., Lee, S.H., Singh, K.K. and Lu, A.L. (2001) Human homolog of the MutY repair protein (hMYH) physically interacts with proteins involved in long patch DNA base excision repair. *J Biol Chem*, **276**, 5547-55.

124. Dianova, II, Bohr, V.A. and Dianov, G.L. (2001) Interaction of human AP endonuclease 1 with flap endonuclease 1 and proliferating cell nuclear antigen involved in long-patch base excision repair. *Biochemistry*, **40**, 12639-44.

125. Bennett, R.A., Wilson, D.M., 3rd, Wong, D. and Demple, B. (1997) Interaction of human apurinic endonuclease and DNA polymerase beta in the base excision repair pathway. *Proc Natl Acad Sci U S A*, **94**, 7166-9.

126. Vidal, A.E., Boiteux, S., Hickson, I.D. and Radicella, J.P. (2001) XRCC1 coordinates the initial and late stages of DNA abasic site repair through protein-protein interactions. *Embo J*, **20**, 6530-6539.

127. Ranalli, T.A., Tom, S. and Bambara, R.A. (2002) AP endonuclease 1 coordinates flap endonuclease 1 and DNA ligase I activity in long patch base excision repair. *J Biol Chem*, **277**, 41715-24.

128. Ahn, B., Harrigan, J.A., Indig, F.E., Wilson, D.M., 3rd and Bohr, V.A. (2004) Regulation of WRN helicase activity in human base excision repair. *J Biol Chem*, **279**, 53465-74.

129. Sukhanova, M.V., Khodyreva, S.N., Lebedeva, N.A., Prasad, R., Wilson, S.H. and Lavrik, O.I. (2005) Human base excision repair enzymes apurinic/apyrimidinic endonuclease1 (APE1), DNA polymerase beta and poly(ADP-ribose) polymerase 1: interplay between strand-displacement DNA synthesis and proofreading exonuclease activity. *Nucleic Acids Res*, **33**, 1222-9.

130. Kenny, M.K., Mendez, F., Sandigursky, M., Kureekattil, R.P., Goldman, J.D., Franklin, W.A. and Bases, R. (2001) Heat shock protein 70 binds to human apurinic/apyrimidinic endonuclease and stimulates endonuclease activity at abasic sites. *J Biol Chem*, **276**, 9532-6.

131. Gaiddon, C., Moorthy, N.C. and Prives, C. (1999) Ref-1 regulates the transactivation and pro-apoptotic functions of p53 in vivo. *Embo J*, **18**, 5609-21.

132. Hanson, S., Kim, E. and Deppert, W. (2005) Redox factor 1 (Ref-1) enhances specific DNA binding of p53 by promoting p53 tetramerization. *Oncogene*, **24**, 1641-7.

133. Ramotar, D. (1997) The apurinic-apyrimidinic endonuclease IV family of DNA repair enzymes. *Biochem Cell Biol*, **75**, 327-36.

134. Singhal, R.K., Prasad, R. and Wilson, S.H. (1995) DNA polymerase beta conducts the gap-filling step in uracil-initiated base excision repair in a bovine testis nuclear extract. *J Biol Chem*, **270**, 949-57.

135. Matsumoto, Y. and Kim, K. (1995) Excision of deoxyribose phosphate residues by DNA polymerase beta during DNA repair. *Science*, **269**, 699-702.

136. Ramotar, D., Popoff, S.C. and Demple, B. (1991) Complementation of DNA repair-deficient Escherichia coli by the yeast Apn1 apurinic/apyrimidinic endonuclease gene. *Mol Microbiol*, **5**, 149-55.

137. Gibbs, P.E., and Lawrence, C. W. (1995) Novel mutagenic properties of abasic sites in *Saccharomyces cerevisiae. J Mol. Biol.*, **251**, 229-236.

138. Ramotar, D. and Demple, B. (1996) Functional expression of Escherichia coli endonuclease IV in apurinic endonuclease-deficient yeast. *J Biol Chem*, **271**, 7368-74.

139. Yang, X., Tellier, P., Masson, J.Y., Vu, T. and Ramotar, D. (1999) Characterization of amino acid substitutions that severely alter the DNA repair functions of Escherichia coli endonuclease IV. *Biochemistry*, **38**, 3615-23.

140. Sherman, F., Fink, G. and Hicks, J. (eds.) (1983) *Methods in yeast genetics*. Cold Spring Harbor, New York.

141. Jilani, A., Ramotar, D., Slack, C., Ong, C., Yang, X.M., Scherer, S.W. and Lasko, D.D. (1999) Molecular cloning of the human gene, PNKP, encoding a polynucleotide kinase 3'-phosphatase and evidence for its role in repair of DNA strand breaks caused by oxidative damage. *J Biol Chem*, **274**, 24176-86.

142. Bradford, M.M. (1976) A rapid and sensitive method for the quantitation of microgram quantities of protein utilizing the principle of protein-dye binding. *Anal Biochem*, **72**, 248-54.

143. Shatilla, A. and Ramotar, D. (2002) Embryonic extracts derived from the nematode Caenorhabditis elegans remove uracil from DNA by the sequential action of uracil-DNA glycosylase and AP (apurinic/apyrimidinic) endonuclease. *Biochem J*, **365**, 547-53.

144. Jurado, J., Saparbaev, M., Matray, T.J., Greenberg, M.M. and Laval, J. (1998) The ring fragmentation product of thymidine C5-hydrate when present in DNA is repaired by the Escherichia coli Fpg and Nth proteins. *Biochemistry*, **37**, 7757-63.

145. Saparbaev, M. and Laval, J. (1994) Excision of hypoxanthine from DNA containing dIMP residues by the Escherichia coli, yeast, rat, and human alkylpurine DNA glycosylases. *Proc Natl Acad Sci U S A*, **91**, 5873-7.

146. Audet, J.F., Masson, J.Y., Rosen, G.D., Salesse, C. and Guerin, S.L. (1994) Multiple regulatory elements control the basal promoter activity of the human alpha 4 integrin gene. *DNA Cell Biol*, **13**, 1071-85.

147. Shatilla, A. and Ramotar, D. (2002) Embryonic extracts derived from the nematode Caenorhabditis elegans remove uracil from DNA by the sequential action of uracil-DNA glycosylase and AP (apurinic/apyrimidinic) endonuclease. *Biochem J*, **365**, 547-53.

148. Ide, H., Tedzuka, K., Shimzu, H., Kimura, Y., Purmal, A.A., Wallace, S.S. and Kow, Y.W. (1994) Alpha-deoxyadenosine, a major anoxic radiolysis product of adenine in DNA, is a substrate for Escherichia coli endonuclease IV. *Biochemistry*, **33**, 7842-7.

149. Levin, J.D., Shapiro, R. and Demple, B. (1991) Metalloenzymes in DNA repair. Escherichia coli endonuclease IV and Saccharomyces cerevisiae Apn1. *J Biol Chem*, **266**, 22893-8.

150. Kerins, S.M., Collins, R. and McCarthy, T.V. (2003) Characterization of an endonuclease IV 3'-5' exonuclease activity. *J Biol Chem*, **278**, 3048-54.

151. Grimes, G.W., Mahler, H.R. and Perlman, R.S. (1974) Nuclear gene dosage effects on mitochondrial mass and DNA. *J Cell Biol*, **61**, 565-74.

152. Foury, F., Roganti, T., Lecrenier, N. and Purnelle, B. (1998) The complete sequence of the mitochondrial genome of Saccharomyces cerevisiae. *FEBS Lett*, **440**, 325-31.

153. Richter, C. (1992) Reactive oxygen and DNA damage in mitochondria. *Mutat Res*, **275**, 249-55.

154. Shigenaga, M.K., Hagen, T.M. and Ames, B.N. (1994) Oxidative damage and mitochondrial decay in aging. *Proc Natl Acad Sci U S A*, **91**, 10771-8.

155. Shigenaga, M.K., Aboujaoude, E.N., Chen, Q. and Ames, B.N. (1994) Assays of oxidative DNA damage biomarkers 8-oxo-2'-deoxyguanosine and 8-oxoguanine in nuclear DNA and biological fluids by high-performance liquid chromatography with electrochemical detection. *Methods Enzymol*, **234**, 16-33.

156. Grossman, L.I. and Shoubridge, E.A. (1996) Mitochondrial genetics and human disease. *Bioessays*, **18**, 983-91.

157. Beckman, K.B. and Ames, B.N. (1996) Detection and quantification of oxidative adducts of mitochondrial DNA. *Methods Enzymol*, **264**, 442-53.

158. Kang, D. and Hamasaki, N. (2002) Maintenance of mitochondrial DNA integrity: repair and degradation. *Curr Genet*, **41**, 311-22.

159. Hayakawa, M., Katsumata, K., Yoneda, M., Tanaka, M., Sugiyama, S. and Ozawa, T. (1996) Age-related extensive fragmentation of mitochondrial DNA into minicircles. *Biochem Biophys Res Commun*, **226**, 369-77.

160. Singh, K.K. (2004) Mitochondrial dysfunction is a common phenotype in aging and cancer. *Ann N Y Acad Sci*, **1019**, 260-4.

161. Luft, R. and Landau, B.R. (1995) Mitochondrial medicine. *J Intern Med*, **238**, 405-21.

162. Kajander, O.A., Rovio, A.T., Majamaa, K., Poulton, J., Spelbrink, J.N., Holt, I.J., Karhunen, P.J. and Jacobs, H.T. (2000) Human mtDNA sublimons resemble rearranged mitochondrial genoms found in pathological states. *Hum Mol Genet*, **9**, 2821-35.

163. Takao, M., Aburatani, H., Kobayashi, K. and Yasui, A. (1998) Mitochondrial targeting of human DNA glycosylases for repair of oxidative DNA damage. *Nucleic Acids Res*, **26**, 2917-22.

164. Bohr, V.A. and Dianov, G.L. (1999) Oxidative DNA damage processing in nuclear and mitochondrial DNA. *Biochimie*, **81**, 155-60.

165. O'Rourke, T.W., Doudican, N.A., Mackereth, M.D., Doetsch, P.W. and Shadel, G.S. (2002) Mitochondrial dysfunction due to oxidative mitochondrial DNA damage is reduced through cooperative actions of diverse proteins. *Mol Cell Biol*, **22**, 4086-93.

166. Singh, K.K., Sigala, B., Sikder, H.A. and Schwimmer, C. (2001) Inactivation of Saccharomyces cerevisiae OGG1 DNA repair gene leads to an increased frequency of mitochondrial mutants. *Nucleic Acids Res*, **29**, 1381-8.

167. Cui, Z. and Mason, T.L. (1989) A single nucleotide substitution at the rib2 locus of the yeast mitochondrial gene for 21S rRNA confers resistance to erythromycin and cold-sensitive ribosome assembly. *Curr Genet*, **16**, 273-9.

168. Heimberg, H., Boyen, A., Crabeel, M. and Glansdorff, N. (1990) Escherichia coli and Saccharomyces cerevisiae acetylornithine aminotransferase: evolutionary relationship with ornithine aminotransferase. *Gene*, **90**, 69-78.

169. Jauniaux, J.C., Urrestarazu, L.A. and Wiame, J.M. (1978) Arginine metabolism in Saccharomyces cerevisiae: subcellular localization of the enzymes. *J Bacteriol*, **133**, 1096-1107.

170. Sia, E.A., Butler, C.A., Dominska, M., Greenwell, P., Fox, T.D. and Petes, T.D. (2000) Analysis of microsatellite mutations in the mitochondrial DNA of Saccharomyces cerevisiae. *Proc Natl Acad Sci U S A*, **97**, 250-5.

171. Brachmann, C.B., Davies, A., Cost, G.J., Caputo, E., Li, J., Hieter, P. and Boeke, J.D. (1998) Designer deletion strains derived from Saccharomyces cerevisiae S288C: a useful set of strains and plasmids for PCR-mediated gene disruption and other applications. *Yeast*, **14**, 115-32.

172. Guthrie, C. and Fink, G.R. (1991) Guide to yeast genetics and molecular biology. *Meth Enzymol*, **194**, 3-37.

173. Gietz, D., St. Jean, A., Woods, R.A. and Schiestl, R.H. (1992) Improved method for high efficiency transformation of intact yeast cells. *Nucleic Acids Res*, **20**, 1425.

174. Lea, D.E.a.C., C.A. (1949) The distribution of the numbers of mutants in bacterial populations. *J. Genet.*, **49**, 264-285.

175. Guthrie, C. and Fink, G.R. (1991) Guide to yeast genetics and molecular biology. *Meth Enzymol*, **194**, 160-162.

176. van der Kemp, P.A., Thomas, D., Barbey, R., de Oliveira, R. and Boiteux, S. (1996) Cloning and expression in Escherichia coli of the OGG1 gene of Saccharomyces cerevisiae, which codes for a DNA glycosylase that excises 7,8-dihydro-8-oxoguanine and 2,6-diamino-4-hydroxy-5-N-methylformamidopyrimidine. *Proc Natl Acad Sci U S A*, **93**, 5197-202.

177. Jilani, A., Vongsamphanh, R., Leduc, A., Gros, L., Saparbaev, M. and Ramotar, D. (2003) Characterization of two independent amino acid substitutions that disrupt the DNA repair functions of the yeast Apn1. *Biochemistry*, **42**, 6436-45.

178. You, H.J., Swanson, R.L. and Doetsch, P.W. (1998) Saccharomyces cerevisiae possesses two functional homologues of Escherichia coli endonuclease III. *Biochemistry*, **37**, 6033-40.

179. Bruner, S.D., Nash, H.M., Lane, W.S. and Verdine, G.L. (1998) Repair of oxidatively damaged guanine in Saccharomyces cerevisiae by an alternative pathway. *Curr Biol*, **8**, 393-403.

180. Leipold, M.D., Workman, H., Muller, J.G., Burrows, C.J. and David, S.S. (2003) Recognition and removal of oxidized guanines in duplex DNA by the base excision repair enzymes hOGG1, yOGG1, and yOGG2. *Biochemistry*, **42**, 11373-81.

181. Hamilton, M.L., Van Remmen, H., Drake, J.A., Yang, H., Guo, Z.M., Kewitt, K., Walter, C.A. and Richardson, A. (2001) Does oxidative damage to DNA increase with age? *Proc Natl Acad Sci U S A*, **98**, 10469-74.

182. de Souza-Pinto, N.C., Eide, L., Hogue, B.A., Thybo, T., Stevnsner, T., Seeberg, E., Klungland, A. and Bohr, V.A. (2001) Repair of 8-oxodeoxyguanosine lesions in mitochondrial dna depends on the oxoguanine dna glycosylase (OGG1) gene and 8-oxoguanine accumulates in the mitochondrial dna of OGG1-defective mice. *Cancer Res*, **61**, 5378-81.

183. Dirmeier, R., O'Brien, K.M., Engle, M., Dodd, A., Spears, E. and Poyton, R.O. (2002) Exposure of yeast cells to anoxia induces transient oxidative stress. Implications for the induction of hypoxic genes. *J Biol Chem*, **277**, 34773-84.

184. Hill, J.W., Hazra, T.K., Izumi, T. and Mitra, S. (2001) Stimulation of human 8-oxoguanine-DNA glycosylase by AP-endonuclease: potential coordination of the initial steps in base excision repair. *Nucleic Acids Res*, **29**, 430-8.

185. You, H.J., Swanson, R.L., Harrington, C., Corbett, A.H., Jinks-Robertson, S., Senturker, S., Wallace, S.S., Boiteux, S., Dizdaroglu, M. and Doetsch, P.W.

(1999) Saccharomyces cerevisiae Ntg1p and Ntg2p: broad specificity N-glycosylases for the repair of oxidative DNA damage in the nucleus and mitochondria. *Biochemistry*, **38**, 11298-306.

186. Xiao, W. and Samson, L. (1993) In vivo evidence for endogenous DNA alkylation damage as a source of spontaneous mutation in eukaryotic cells. *Proc Natl Acad Sci U S A*, **90**, 2117-21.

187. Xiao, W., Chow, B.L., Hanna, M. and Doetsch, P.W. (2001) Deletion of the MAG1 DNA glycosylase gene suppresses alkylation-induced killing and mutagenesis in yeast cells lacking AP endonucleases. *Mutat Res*, **487**, 137-47.

188. Reenan, R.A. and Kolodner, R.D. (1992) Characterization of insertion mutations in the Saccharomyces cerevisiae MSH1 and MSH2 genes: evidence for separate mitochondrial and nuclear functions. *Genetics*, **132**, 975-85.

189. Ni, T.T., Marsischky, G.T. and Kolodner, R.D. (1999) MSH2 and MSH6 are required for removal of adenine misincorporated opposite 8-oxo-guanine in S. cerevisiae. *Mol Cell*, **4**, 439-44.

190. Haracska, L., Yu, S.L., Johnson, R.E., Prakash, L. and Prakash, S. (2000) Efficient and accurate replication in the presence of 7,8-dihydro-8-oxoguanine by DNA polymerase eta. *Nat Genet*, **25**, 458-61.

191. Modrich, P. and Lahue, R. (1996) Mismatch repair in replication fidelity, genetic recombination, and cancer biology. *Annu Rev Biochem*, **65**, 101-33.

192. Schapira, A.H. (1998) Mitochondrial dysfunction in neurodegenerative disorders. *Biochim Biophys Acta*, **1366**, 225-33.

193. Stone, E.M., Rothblum, K.N., Alevy, M.C., Kuo, T.M. and Schwartz, R.J. (1985) Complete sequence of the chicken glyceraldehyde-3-phosphate dehydrogenase gene. *Proc Natl Acad Sci U S A*, **82**, 1628-32.

194. Baxi, M.D. and Vishwanatha, J.K. (1995) Uracil DNA-glycosylase/glyceraldehyde-3-phosphate dehydrogenase is an Ap4A binding protein. *Biochemistry*, **34**, 9700-7.

195. Meyer-Siegler, K., Mauro, D.J., Seal, G., Wurzer, J., deRiel, J.K. and Sirover, M.A. (1991) A human nuclear uracil DNA glycosylase is the 37-kDa subunit

of glyceraldehyde-3-phosphate dehydrogenase. *Proc Natl Acad Sci U S A*, **88**, 8460-4.

196. Singh, R. and Green, M.R. (1993) Sequence-specific binding of transfer RNA by glyceraldehyde-3-phosphate dehydrogenase. *Science*, **259**, 365-8.

197. Zang, W.Q., Fieno, A.M., Grant, R.A. and Yen, T.S. (1998) Identification of glyceraldehyde-3-phosphate dehydrogenase as a cellular protein that binds to the hepatitis B virus posttranscriptional regulatory element. *Virology*, **248**, 46-52.

198. Saunders, P.A., Chen, R.W. and Chuang, D.M. (1999) Nuclear translocation of glyceraldehyde-3-phosphate dehydrogenase isoforms during neuronal apoptosis. *J Neurochem*, **72**, 925-32.

199. Zheng, L., Roeder, R.G. and Luo, Y. (2003) S phase activation of the histone H2B promoter by OCA-S, a coactivator complex that contains GAPDH as a key component. *Cell*, **114**, 255-66.

200. Dastoor, Z. and Dreyer, J.L. (2001) Potential role of nuclear translocation of glyceraldehyde-3-phosphate dehydrogenase in apoptosis and oxidative stress. *J Cell Sci*, **114**, 1643-53.

201. Kim, J.H., Lee, S., Park, J.B., Lee, S.D., Ha, S.H., Hasumi, K., Endo, A., Suh, P.G. and Ryu, S.H. (2003) Hydrogen peroxide induces association between glyceraldehyde 3-phosphate dehydrogenase and phospholipase D2 to facilitate phospholipase D2 activation in PC12 cells. *J Neurochem*, **85**, 1228-36.

202. Krynetski, E.Y., Krynetskaia, N.F., Gallo, A.E., Murti, K.G. and Evans, W.E. (2001) A novel protein complex distinct from mismatch repair binds thioguanylated DNA. *Mol Pharmacol*, **59**, 367-74.

203. Jayaraman, L., Murthy, K.G., Zhu, C., Curran, T., Xanthoudakis, S. and Prives, C. (1997) Identification of redox/repair protein Ref-1 as a potent activator of p53. *Genes Dev*, **11**, 558-70.

204. Walker, L.J., Robson, C.N., Black, E., Gillespie, D. and Hickson, I.D. (1993) Identification of residues in the human DNA repair enzyme HAP1 (Ref-1) that are essential for redox regulation of Jun DNA binding. *Mol Cell Biol*, **13**, 5370-6.

205. Huang, L.E., Arany, Z., Livingston, D.M. and Bunn, H.F. (1996) Activation of hypoxia-inducible transcription factor depends primarily upon redox-sensitive stabilization of its alpha subunit. *J Biol Chem*, **271**, 32253-9.

206. Gershoni, J.M. and Palade, G.E. (1983) Protein blotting: principles and applications. *Anal Biochem*, **131**, 1-15.

207. Motwani, M., Jung, C., Sirotnak, F.M., She, Y., Shah, M.A., Gonen, M. and Schwartz, G.K. (2001) Augmentation of apoptosis and tumor regression by flavopiridol in the presence of CPT-11 in Hct116 colon cancer monolayers and xenografts. *Clin Cancer Res*, **7**, 4209-19.

208. Mathonnet, G., Leger, C., Desnoyers, J., Drouin, R., Therrien, J.P. and Drobetsky, E.A. (2003) UV wavelength-dependent regulation of transcription-coupled nucleotide excision repair in p53-deficient human cells. *Proc Natl Acad Sci U S A*, **100**, 7219-24.

209. Chittum, H.S., Lane, W.S., Carlson, B.A., Roller, P.P., Lung, F.D., Lee, B.J. and Hatfield, D.L. (1998) Rabbit beta-globin is extended beyond its UGA stop codon by multiple suppressions and translational reading gaps. *Biochemistry*, **37**, 10866-70.

210. Xing, C., LaPorte, J.R., Barbay, J.K. and Myers, A.G. (2004) Identification of GAPDH as a protein target of the saframycin antiproliferative agents. *Proc Natl Acad Sci U S A*, **101**, 5862-6.

211. Brown, V.M., Krynetski, E.Y., Krynetskaia, N.F., Grieger, D., Mukatira, S.T., Murti, K.G., Slaughter, C.A., Park, H.W. and Evans, W.E. (2004) A novel CRM1-mediated nuclear export signal governs nuclear accumulation of glyceraldehyde-3-phosphate dehydrogenase following genotoxic stress. *J Biol Chem*, **279**, 5984-92.

212. Vongsamphanh, R., Wagner, J.R. and Ramotar, D. (2006) Saccharomyces cerevisiae Ogg1 prevents poly(GT) tract instability in the mitochondrial genome. *DNA Repair (Amst)*, **5**, 235-42.

213. Bravard, A., Vacher, M., Gouget, B., Coutant, A., de Boisferon, F.H., Marsin, S., Chevillard, S. and Radicella, J.P. (2006) Redox regulation of human

OGG1 activity in response to cellular oxidative stress. *Mol Cell Biol*, **26**, 7430-6.

214. Erzberger, J.P. and Wilson, D.M., 3rd (1999) The role of Mg2+ and specific amino acid residues in the catalytic reaction of the major human abasic endonuclease: new insights from EDTA-resistant incision of acyclic abasic site analogs and site-directed mutagenesis. *J Mol Biol*, **290**, 447-57.

215. Sirover, M.A. (1999) New insights into an old protein: the functional diversity of mammalian glyceraldehyde-3-phosphate dehydrogenase. *Biochim Biophys Acta*, **1432**, 159-84.

216. Hara, M.R. and Snyder, S.H. (2006) Nitric Oxide-GAPDH-Siah: A Novel Cell Death Cascade. *Cell Mol Neurobiol*.

217. Sundararaj, K.P., Wood, R.E., Ponnusamy, S., Salas, A.M., Szulc, Z., Bielawska, A., Obeid, L.M., Hannun, Y.A. and Ogretmen, B. (2004) Rapid shortening of telomere length in response to ceramide involves the inhibition of telomere binding activity of nuclear glyceraldehyde-3-phosphate dehydrogenase. *J Biol Chem*, **279**, 6152-62.

218. Nakagawa, T., Hirano, Y., Inomata, A., Yokota, S., Miyachi, K., Kaneda, M., Umeda, M., Furukawa, K., Omata, S. and Horigome, T. (2003) Participation of a fusogenic protein, glyceraldehyde-3-phosphate dehydrogenase, in nuclear membrane assembly. *J Biol Chem*, **278**, 20395-404.

219. Krynetski, E.Y., Krynetskaia, N.F., Bianchi, M.E. and Evans, W.E. (2003) A nuclear protein complex containing high mobility group proteins B1 and B2, heat shock cognate protein 70, ERp60, and glyceraldehyde-3-phosphate dehydrogenase is involved in the cytotoxic response to DNA modified by incorporation of anticancer nucleoside analogues. *Cancer Res*, **63**, 100-6.

220. Chuang, D.M., Hough, C. and Senatorov, V.V. (2005) Glyceraldehyde-3-phosphate dehydrogenase, apoptosis, and neurodegenerative diseases. *Annu Rev Pharmacol Toxicol*, **45**, 269-90.

221. Nakamura, H. (2005) Thioredoxin and its related molecules: update 2005. *Antioxid Redox Signal*, **7**, 823-8.

222. Biteau, B., Labarre, J. and Toledano, M.B. (2003) ATP-dependent reduction of cysteine-sulphinic acid by S. cerevisiae sulphiredoxin. *Nature*, **425**, 980-4.

223. Burke, J.R., Enghild, J.J., Martin, M.E., Jou, Y.S., Myers, R.M., Roses, A.D., Vance, J.M. and Strittmatter, W.J. (1996) Huntingtin and DRPLA proteins selectively interact with the enzyme GAPDH. *Nat Med*, **2**, 347-50.

224. Schulze, H., Schuler, A., Stuber, D., Dobeli, H., Langen, H. and Huber, G. (1993) Rat brain glyceraldehyde-3-phosphate dehydrogenase interacts with the recombinant cytoplasmic domain of Alzheimer's beta-amyloid precursor protein. *J Neurochem*, **60**, 1915-22.

225. Kragten, E., Lalande, I., Zimmermann, K., Roggo, S., Schindler, P., Muller, D., van Oostrum, J., Waldmeier, P. and Furst, P. (1998) Glyceraldehyde-3-phosphate dehydrogenase, the putative target of the antiapoptotic compounds CGP 3466 and R-(-)-deprenyl. *J Biol Chem*, **273**, 5821-8.

226. Koshy, B., Matilla, T., Burright, E.N., Merry, D.E., Fischbeck, K.H., Orr, H.T. and Zoghbi, H.Y. (1996) Spinocerebellar ataxia type-1 and spinobulbar muscular atrophy gene products interact with glyceraldehyde-3-phosphate dehydrogenase. *Hum Mol Genet*, **5**, 1311-8.

227. Barnes, D.E. and Lindahl, T. (2004) Repair and genetic consequences of endogenous DNA base damage in mammalian cells. *Annu Rev Genet*, **38**, 445-76.

228. Nakamura, J. and Swenberg, J.A. (1999) Endogenous apurinic/apyrimidinic sites in genomic DNA of mammalian tissues. *Cancer Res*, **59**, 2522-6.

229. Ishchenko, A.A., Sanz, G., Privezentzev, C.V., Maksimenko, A.V. and Saparbaev, M. (2003) Characterisation of new substrate specificities of Escherichia coli and Saccharomyces cerevisiae AP endonucleases. *Nucleic Acids Res*, **31**, 6344-53.

230. Ishchenko, A.A., Ide, H., Ramotar, D., Nevinsky, G. and Saparbaev, M. (2004) Alpha-anomeric deoxynucleotides, anoxic products of ionizing radiation, are substrates for the endonuclease IV-type AP endonucleases. *Biochemistry*, **43**, 15210-6.

231. Taladriz, S., Gonzalez-Aseguinolaza, G., Marquet, A. and Larraga, V. (1999) Cloning, molecular analysis and differential cell localisation of the p36 RACK analogue antigen from the parasite protozoon Crithidia fasciculata. *FEBS Lett*, **443**, 375-80.

232. Simonelli, V., Narciso, L., Dogliotti, E. and Fortini, P. (2005) Base excision repair intermediates are mutagenic in mammalian cells. *Nucleic Acids Res*, **33**, 4404-11.

233. Phadnis, N., Mehta, R., Meednu, N. and Sia, E.A. (2006) Ntg1p, the base excision repair protein, generates mutagenic intermediates in yeast mitochondrial DNA. *DNA Repair (Amst)*, **5**, 829-39.

234. Doudican, N.A., Song, B., Shadel, G.S. and Doetsch, P.W. (2005) Oxidative DNA damage causes mitochondrial genomic instability in Saccharomyces cerevisiae. *Mol Cell Biol*, **25**, 5196-204.

235. Hegde, V., Wang, M. and Deutsch, W.A. (2004) Characterization of human ribosomal protein S3 binding to 7,8-dihydro-8-oxoguanine and abasic sites by surface plasmon resonance. *DNA Repair (Amst)*, **3**, 121-6.

236. Banerjee, A., Yang, W., Karplus, M. and Verdine, G.L. (2005) Structure of a repair enzyme interrogating undamaged DNA elucidates recognition of damaged DNA. *Nature*, **434**, 612-8.

237. Cadet, J., Douki, T., Frelon, S., Sauvaigo, S., Pouget, J.P. and Ravanat, J.L. (2002) Assessment of oxidative base damage to isolated and cellular DNA by HPLC-MS/MS measurement. *Free Radic Biol Med*, **33**, 441-9.

238. Brink, A., Lutz, U., Volkel, W. and Lutz, W.K. (2006) Simultaneous determination of O6-methyl-2'-deoxyguanosine, 8-oxo-7,8-dihydro-2'-deoxyguanosine, and 1,N6-etheno-2'-deoxyadenosine in DNA using on-line sample preparation by HPLC column switching coupled to ESI-MS/MS. *J Chromatogr B Analyt Technol Biomed Life Sci*, **830**, 255-61.

239. Dzierzbicki, P., Koprowski, P., Fikus, M.U., Malc, E. and Ciesla, Z. (2004) Repair of oxidative damage in mitochondrial DNA of Saccharomyces cerevisiae: involvement of the MSH1-dependent pathway. *DNA Repair (Amst)*, **3**, 403-11.

240. Chang, I.Y., Kim, S.H., Cho, H.J., Lee, D.Y., Kim, M.H., Chung, M.H. and You, H.J. (2005) Human AP endonuclease suppresses DNA mismatch repair activity leading to microsatellite instability. *Nucleic Acids Res*, **33**, 5073-81.

241. Mazurek, A., Berardini, M. and Fishel, R. (2002) Activation of human MutS homologs by 8-oxo-guanine DNA damage. *J Biol Chem*, **277**, 8260-6.

242. Sirover, M.A. (2005) New nuclear functions of the glycolytic protein, glyceraldehyde-3-phosphate dehydrogenase, in mammalian cells. *J Cell Biochem*, **95**, 45-52.